DAMPING SUBSYNCHRONOUS FREQUENCY OSCILLATIONS IN POWER SYSTEMS USING A STATIC PHASE-SHIFTER

by

Mohammad Reza Iravani

A thesis
presented to the University of Manitoba
in partial fulfillment of the
requirements for the degree of
Doctor of Philosophy
in
Department of Electrical Engineering

Winnipeg, Manitoba

DAMPING SUBSYNCHRONOUS FREQUENCY OSCILLATIONS IN POWER SYSTEMS USING A STATIC PHASE-SHIFTER

BY

MOHAMMAD REZA IRAVANI

A thesis submitted to the Faculty of Graduate Studies of the University of Manitoba in partial fulfillment of the requirements of the degree of

DOCTOR OF PHILOSOPHY

ABSTRACT

A new method for damping the Subsynchronous frequency Oscillations (SSO) in power systems is suggested. The supplementary damping is achieved based on the active power modulation characteristics of the static phase-shifters, using the rotor speed deviation from the synchronous speed as the control signal. The complex torque coefficient method and an eigenvalue analysis technique are used for small signal analysis and optimization of the parameters of the control system. The analytical results are verified by a detailed digital time simulation study on the first IEEE benchmark model for SSO, using the Electro-Magnetic Transients Program (EMTP) developed by the Bonneville Power Administration (BPA).

The results from the analytical and the digital computer studies reveal the technical feasibility of using a static phase-shifter for damping the shaft torsional stresses of a turbine-generator, as a result of small signal perturbations and large disturbances.

ACKNOWLEDGEMENT

The author wishes to express his gratitude to Professor R.M.Mathur, for suggesting the research topic and his invaluable guidance, support and encouragement.

CONTENTS

LIST OF FIGURES

Chapter I

INTRODUCTION

1.1 BACKGROUND

The phenomenon of Subsynchronous frequency Oscillations (SSO) in power systems was first discussed in the literature in 1937 [1], and until 1970 it was treated as an electrical phenomenon. The theory of interaction between electrical resonance in a series compensated network and torsional resonance in a turbine-generator mechanical system was understood and developed after two shaft failures in the Mohave Generating Station in southern Nevada.

Since the second failure of the Mohave generating unit in 1971, as a result of SSO, several other projects in North America have been identified as potential SSO problems. Considerable effort has recently been devoted to its study and suppression. The IEEE Bibliography on SSO [2,3] identifies more than 80 technical papers presented on this subject. These reports discuss the theory, the methods of analysis, the methods of prevention, the phenomena leading to shaft failure and the test results. Since 1978 more than 40 papers have been published on SSO, most of which discuss new methods for damping SSO.

Subsynchronous oscillation is an electric power system condition where the electic network exchanges energy with a turbine-generator at one or more of the natural frequencies of the combined system below the synchronous frequency of the electrical system [4]. The SSO phenomenon is a result of interaction between a turbine-generator unit and a series compensated network, or HVDC converter controllers [5], or power system stabilizers [6]. The possibility of mechanical resonance, due to SSO, exists for the steam turbine-generators and not for the hydraulic units [7].

The main concerns with the torsional oscillations of a turbine-generator are:

1. Possibility of shaft damage as a result of torsional stresses [8]. There are two categories of shaft failure. One is a result of low amplitude oscillatory torsional torques in which shaft fails in fatigue. The other relates to high torque levels where the stress at some locations increases above the endurance limit of the shaft material.
2. Possibility of turbine blade fracture as a result of interaction between double frequency electrical torques and higher torsional natural frequencies of the mechanical system of a turbine-generator unit [9].

In the technical literature the SSO phenomenon is addressed under three titles, namely:

1. self-excited torsional interaction,
2. induction generator effect, and
3. transient torque problems.

The self-excited torsional interaction is stimulated as a result of small amplitude perturbations in power systems. The transient torque problems are associated with the oscillations of a turbine-generator due to large disturbances in a power system. It should be noted that in all cases there is one single phenomenon responsible for SSO. Separation of the problem into three foregoing aspects is either a result of emphasis on a certain method of analysis or importance of particular system parameters [10].

The self-excited torsional interaction is the interplay between the mechanical system of a turbine-generator unit and the electrical system. Small amplitude oscillations in a power system can cause simultaneous self-excitation of the electrical and the mechanical systems at subsynchronous frequencies. If the subsynchronous torque component is equal to or more than the mechanical damping torque of the rotating system; the system is electromechanically self-excited. The exchange of energy between the electrical and the mechanical sections of a power system is referred as the torsional interaction [11,12]. The induction generator effect is the

self-excitation of the electrical system alone [13,14,15,16].

As a result of large disturbances in a power system, high amplitude electrical torques are imposed on the generator rotor. Such excessive torques may result in a catastrophic shaft failure or a drastic life-time reduction as a result of fatigue process. In the technical literature this is referred as the transient torque problem.

1.2 MOTIVATION AND OBJECTIVE

Detailed investigations of the SSO phenomenon during the last 12 years have resulted in the proposed methods to mitigate or eliminate the SSO damage to turbine-generator units. In spite of the efforts that have been involved, and the diversity of concepts and methods, none of the proposed countermeasures can be considered to be the best possible solution for the SSO problem. Moreover, some of the solutions are rather special and suitable only for a certain system configuration or condition.

The objective of this study is to present the technical feasibility of a dynamically-controlled static phase-shifter as a new, alternative approach for suppressing the shaft torsional stresses of a turbine-generator, as a result of small signal perturbations and large disturbances.

1.3 OUTLINE OF THE THESIS

The available methods of analysis and suppression of SSO are briefly explained in Chapter II.

The effect of injecting a dynamically-controlled quadrature phase voltage on the electrical damping of a power system, during small signal perturbations, is discussed in Chapter III.

In Chapter IV, two practical schemes for quadrature phase voltage injection in power systems by use of static phase-shifters are explained, and their control algorithms are developed.

Chapter V covers the results obtained form a detailed digital time simulation study, in order to verify the analytical results of Chapter III. The simulation study is performed on the first IEEE benchmark model [18], using the Bonneville Power Administration (BPA) Electro-Magnetic Transients Program (EMTP) [19].

In Chapter VI, the feasibility of the static phase-shifters for suppressing the shaft torsional torques, due to large disturbances, is examined.

Final conclusions, major contributions and suggestions for further research are stated in Chapter VII.

Chapter II

KNOWN METHODS OF ANALYSIS AND COUNTERMEASURES FOR SSO

2.1 INTRODUCTION

In this chapter the available methods for the analysis of SSO are reviewed. The theory of operation, merits, drawbacks and the operating experiences pertaining to each countermeasure technique are briefly discussed.

2.2 MATHEMATICAL MODEL FOR SSO ANALYSIS

Analysis of the torsional interaction requires the mathematical model of the power system under consideration. Fig.2.1 illustrates the mechanical system of a turbine-generator unit consisting of six masses: high-pressure turbine (HP), intermediate-pressure turbine (IP), low-pressure turbines A and B (LPA, LPB), generator rotor (G) and exciter (EXC). Assuming the shaft system as a continuous mass, an exact mathematical representation requires the solution of the elastic behaviour of the whole rotating body. However, depending on the objective and the required accuracy, certain simplifications can be made to reduce the complexity of the mathematical model of the mechanical system.

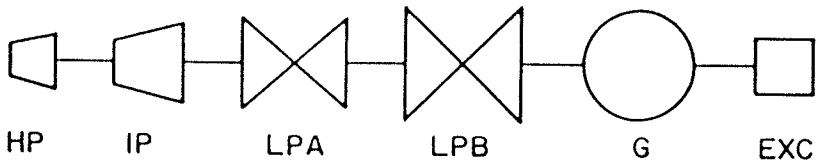

Figure 2.1: Shaft system of a steam turbine-generator

For the study of the shaft torsional stresses of a turbine-generator unit, a spring-mass model [20] based on discrete mass representation allows the computation of the system variables within the required accuracy. Other shaft vibrational analysis, i.e., study of the effect of double frequency torque component on the turbine blades, requires more detailed mathematical modelling of the shaft system, through the application of finite element techniques [21,22]. Such a detailed study was considered to be outside the scope of the results presented in this thesis, therefore, is not discussed any further.

Fig.2.2 shows the spring-mass representation of the turbine-generator unit of Fig.2.1. Applying the Newton's second law, the equation of motion for each mass is obtained. The equations of motion for a mechanical system consisting of N masses, constitute a system of N simultaneous, second order differential equations with constant coefficients.

The mathematical model of the electrical system of a generator is obtained from the voltage equations of the generator circuits in the d-q-0 reference frame [23,24]. For this

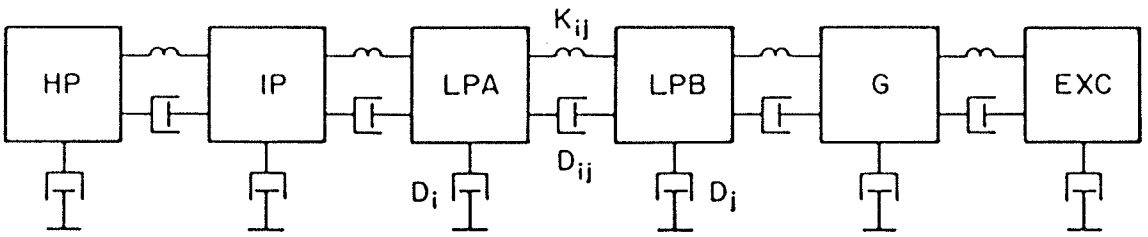

Figure 2.2: Spring-mass model of the shaft system of a turbine-generator

purpose, the generator is represented with three identical and symmetrically placed, lumped armature windings, and lumped rotor windings. The rotor circuits represent the field winding and the damper windings in the d-q frame.

combination of the electrical and the mechanical equations constitute a system of nonlinear, second order, constant coefficient differential equations which describes the complete behaviour of the turbine-generator.

2.3 METHODS OF ANALYSIS FOR SSO

The available methods for SSO analysis are:

1. eigenvalue method,
2. frequency scan method,
3. complex torque coefficient method, and
4. digital time simulation techniques.

The first three of the above are analytical methods which utilize numerical techniques for practical system configurations. Digital computer methods utilize a step-by-step nu-

merical integration technique to solve the system of nonlinear differential equations.

2.3.1 Eigenvalue Method

The modal data [4,25] of a turbine-generator is deduced by performing a modal analysis [20] on the mathematical model of the mechanical system.

For simple power system configurations, the voltage equations of the line components are obtained in the d-q reference frame [26] and combined with the generator mathematical model. Then an eigenvalue method is applied to obtain the eigenvalues of the linearized equations. This mathematically laborious method is not feasible in the following cases:

1. when the system has more than one turbine-generator unit,
2. when the effect of several controllers are to considered, and
3. when the generator is supplying power to a mesh connected network.

However, an eigenvalue analysis can be applied to the foregoing cases, provided considerable simplifications are made.

2.3.2 Frequency Scan Method

The frequency scan method [27] determines the system impedance viewed from the terminals of the generator under study. The frequency scan method is an approximation method which is used to screen out those system conditions which are potentially dangerous with regard to SSO [28]. Also it is used to identify those parts of the system which do not influence the SSO phenomenon.

The frequency scan method can be used to study the electrical self-excitation of one machine at a time. The generator under study is represented by its induction generator equivalent circuit, and other machines are approximated as voltage sources behind reactances [29]. The transmission lines and loads are represented by equivalent impedances at the given stator frequency. The electrical self-excitation is predicted from the plots of the system resistance and reactance as functions of frequency. Since the frequency scan method neglects the effect of mechanical oscillations, it cannot identify the self-excitation as a result of torsional interaction.

2.3.3 Complex Torque Coefficient Method

The torsional oscillations of a turbine-generator can be predicted by comparing the electrical damping with the mechanical damping at the shaft modal frequencies. This is

achieved by calculating the net damping, using the complex torque coefficient method [30,31]. The complex torque coefficient method can be used to investigate the effect of important system parameters on SSO. Another advantage of this method is that it can be used for the analysis of meshed power systems [32]. This method is applicable only for the analysis of power system dynamics due to small signal disturbances.

2.3.4 Digital Time Simulation Techniques

For the prediction of the behaviour of a power system, subsequent to severe electrical disturbances or small signal perturbations, a digital computer program can be used to solve the system equations in the time domain. The behaviour of a power system during small signal perturbations can also be obtained by solving the linearized mathematical model of the system around the operating point. The solutions which are obtained from the linearized equations have the following limitations:

1. The linearization method is an approximation approach, therefore, the results are valid only for small amplitude oscillations and not for large disturbances.
2. The linearized mathematical model can be obtained if the physical system is fairly simple. When the system consists of more than one generator, several control-

lers, and/or meshed networks, the linearization method is not feasible.

3. The mathematical model of the thyristor-controlled devices are approximated by linear transfer functions which neglect the switching effects of such devices.
4. The physical nonlinearities can not be easily included in a linearized mathematical model.

The above mentioned difficulties are overcome by using digital computer programs which are applicable to a broad range of machine-network problems.

The Electro-Magnetic Transients Program [33] is a widely used state-of-the-art program for the digital time simulation study of the machine-network problems. The EMTP solves the differential equations of the turbine-generator by a numerical integration [34,35] and interfaces the results with the solution of the rest of the system [36,37]. Furthermore, in the EMTP provisions are made to incorporate the physical nonlinearities of power systems.

2.4 COUNTERMEASURES FOR SSO PROBLEMS

A back-up relaying scheme is necessary to detect and remove the unit from service in the case of an unforeseen failure of the countermeasure used for SSO [39,39]. Countermeasures for SSO are classified as:

1. countermeasures for transient torques, and
2. countermeasures for sustained oscillations.

2.4.1 Control of Transient Torques

High amplitude transient torques resulting from large disturbances in power systems, are more difficult to control as compared with the problem of sustained SSO. In a series compensated system, the magnitude of the transient torques are limited by using a lower level of over-voltage protection devices across the series capacitor [41,42]. Also, the adverse effect of severe torsional torques can be reduced by installing damping devices in the control circuitry of the series capacitor [42,43].

2.4.2 Control of Sustained SSO

The available methods for mitigating the SSO problems, as a result of small perturbations, are base on the utilization of: (1) static blocking filters, (2) dynamic filters, (3) dynamic stabilizers, (4) HVDC converter controllers, (5) series capacitor control, (6) excitation control and, (7) static var systems.

2.4.2.1 Static Blocking Filters

The purpose of the application of the blocking filters is to prevent SSO currents from entering the generator unit.

This is accomplished by introducing sections of high Q parallel resonant circuits, tuned to block the electrical currents at frequencies corresponding to the torsional modes [44,45,46,47]. The filters are installed on the neutral ends of the high-voltage winding of the step-up transformer. The static blocking filters have been under service in the Navajo Generating Station since 1976 [48,49]. Application of the blocking filters result in a higher BIL. Also, they have not been recommended for meshed systems.

2.4.2.2 Dynamic Filters

A dynamic filter is used to generate a voltage in series, with equal magnitude, and in phase opposition with the voltage produced by SSO [50,51,52]. A solid-state cycloconverter can be used to generate the required voltage. The cycloconverter is energized by a synchronous generator and controlled by a signal from the rotor speed to provide the required damping. In contrast to the blocking filters, the performance of the dynamic filters is independent of the electrical system parameters. The technical feasibility of the dynamic filters have been demonstrated by laboratory tests and digital computer studies, however, there is no system which uses this method as a countermeasure for SSO.

2.4.2.3 Dynamic Stabilizers

The principle of operation of a dynamic stabilizer is to modulate one or more of the system variables in order to provide positive damping for SSO.

The modulated inductance stabilizer which principally uses static var generator hardware with modified controller, is the first suggested dynamic stabilizer [53,54]. A modulated inductance stabilizer consists of three delta connected reactors each one in series with an anti-parallel thyristor switch. This device is in service in the San Juan Plant [55,56].

Thyristor-controlled resistors can be used to damp the shaft torsional oscillations, as a result of small signal perturbations and large disturbances in power systems [57]. A thyristor-controlled resistor bank consists of three delta connected resistors, each one in series with an anti-parallel thyristor switch. Another configuration utilizes a twelve-pulse converter as the interface between a resistor bank and the low voltage side of the generator step-up transformer [58].

The idea of application of superconductive energy storage inductor-converter unit has been suggested for damping the low frequency oscillations (hunting) [59]. An ambient temperature inductor-converter unit may be used to damp SSO [60,61], which can also be employed as a controlled var compensator, provided additional controllers are installed.

2.4.2.4 Damping SSO by HVDC Converter Controller

The current and the voltage generated due to HVDC converter controllers have frequencies in the range of 5-50 Hz, which can excite the shaft torsional oscillations [62,63]. Torsional damping from HVDC links is obtained by modifying their current controllers [64,65]. The design procedures of a supplementary subsynchronous damping control (SSDC) have been reported in [66,67]. In the systems where SSO is excited by series compensated lines and if in such systems HVDC links exist, modifications to the HVDC controls do not provide significant damping for SSO.

2.4.2.5 Series Capacitor Control

The methods of damping SSO by controlling the series capacitor are: (a) application of a line filters, (b) application of a bypass damping filters and (c) application of the thyristor-controlled series capacitor, which is referred as the NGH Scheme (N.G.Hingorani's Scheme). A line filter is a reactor connected in parallel with the series capacitor to block the flow of subsynchronous current at the specified frequency. In principle, this approach is similar to the application of the blocking filters. There is no project utilizing this technique.

A bypass damping filter is connected in parallel across the series capacitor to act as an inductive-resistive bypass

path for the subsynchronous current [discussion of 47]. This method has been employed in a number of installations.

The basic circuit for one phase of the NGH scheme [68,69] consists of a resistor in series with an anti-parallel thyristor switch, connected across the series capacitor. When the half cycle of the capacitor voltage exceeds the set time, the thyristors are fired in order to discharge the excess energy through the resistors and to prevent the line participation in SSO.

2.4.2.6 Damping SSO by Excitation Control

Power system stabilizers (PSS) have been used to damp the low frequency power system oscillations by modulating the generator excitation [70]. The damping provided by PSS is used for: intertie (inter-area) oscillations [71] and local oscillations [72]. PSS may exhibit destabilizing effect on the shaft torsional oscillations [73]. Because of the destabilizing effect of PSS at some frequencies, torsional filters [74] are provided in the stabilizer loop. The destabilizing effect is more pronounced when the rotor speed is used as the feedback signal. On this account an active search for alternative [75,76,77] or complementary signals [78,79,80,81] is to be noticed in the literature. The damping effect of PSS has been employed at the Navajo Plant to augment the damping provided by the static blocking filters [48,49].

2.4.2.7 Damping SSO by Static var Systems

Enhancement of transient stability, voltage control and damping low frequency oscillations by means of static var systems have been extensively reported. A recent study demonstrates the feasibility of static var compensators for damping torsional oscillations [82], through modification of the controls of the existing compensators.

Chapter III

NEW TECHNIQUE FOR DAMPING SSO BY USING STATIC PHASE-SHIFTERS

3.1 INTRODUCTION

In this chapter the effect of thyristor controlled phase-shifters on the electrical damping of power systems is studied. Based on the results obtained, a new method for suppressing the shaft torsional torques of turbine-generators is suggested. The comples torque coefficient method and an eigenvalue analysis method are used to examine the effect of quadrature phase voltage injection on the unstable modes of torsional oscillations of the turbine-generator units. The studies are performed on the first IEEE benchmark model for subsynchronous oscillation studies.

The analytical results show that the injection of a dynamically controlled quadrature phase voltage, proportional to the rotor speed deviation from the synchronous speed, can stabilize the torsional oscillations of the first IEEE benchmark model.

3.2 THE STUDY SYSTEM

In order to compare the static phase-shifters with those methods used by other investigators for damping SSO, the analytical studies in this chapter and also further detailed investigations by a digital time simulation study, are conducted for the first IEEE benchmark system [18]. Furthermore, a comprehensive data on the torsional modes and zones of instability of the IEEE benchmark is available [83].

The first IEEE benchmark model consists of a two-pole 892.4 MVA turbine-generator, connected through a 500 kV series compensated transmission line to an infinite bus. The shaft system of the turbine-generator comprises six masses: high pressure-turbine (HP), intermediate-pressure turbine (IP), two low-pressure turbines (LPA, LPB), generator rotor (G) and exciter (EXC). A spring-mass model representation of the mechanical system is utilized for the torsional studies. The mechanical data of the turbine-generator is given in Appendix A.

The electrical data for the generator is presented for a two axes model, with one damper winding on the d-axis and two damper windings on the q-axis. The electrical data for the generator, in perunit values based on the generator MVA, is given in Appendix B.

The transmission system of the benchmark model consists of a three-phase 26/520 kV step-up transformer, a three-

phase 500 kV series compensated transmission line which is divided into two sections by the series capacitor. The infinite bus is represented by a three-phase voltage source with zero impedance at all frequencies. The electical data of the transmission system, in perunit values, is also provided in Appendix B. The first IEEE benchmark model is characterized by four unstable torsional oscillatory modes at 15.7, 20.2, 25.5 and 32.3 Hz.

3.3 DAMPING SHAFT TORSIONAL OSCILLATIONS BY ACTIVE POWER MODULATION

The generator rotor oscillations due to a disturbance in a power system, result in the generation of an oscillatory electric torque of the rotor oscillation frequency. The phase and the amplitude of the oscillatory torque are determined by the system parameters. When the frequency of the rotor oscillations is equal to the synchronous frequency minus the electrical system natural frequency, the oscillatory electrical torque is in-phase with the rotor speed deviation and causes negative damping [29,53]. This negative damping, introduced as a consequence of the interaction between the electrical and the mechanical systems, is the cause for the torsional torques instability.

Intuitively, production of an additional oscillatory electrical torque in phase opposition to the electrical torque produced by the rotor oscillations, should cause po-

sitive damping for the generator rotor. One method to implement this technique is to modulate the generator output power. The generator shaft speed can be measured accurately. It contains all the modal frequencies, and during torsional oscillations is in-phase with the oscillatory electrical torque. Thus, the shaft speed can be used as the required feedback control signal. Modulation of the generator power, proportional to the rotor speed deviation, generates an electrical torque which provides a positive damping at the corresponding mode of the torsional oscillations [57]. Modulation of the generator power by means of inductor converter units and dynamic resistors have been reported in the literature.

3.3.1 New Technique Employing Static Phase-Shifters

An alternative approach to modulate the output power of a generator is to introduce a phase shift in the generator terminal voltages, proportional to the rotor speed deviation. A three-phase thyristor-controlled phase-shifter unit can be used for the purpose. Injection of a lead-lag quadrature phase voltage at the generator terminals, changes the effective phase angle between the generator and the system voltage. This results in the power modulation, which provides positive damping for the shaft oscillations during both half-cycles of the torsional oscillation [84,85].

The thyristor-controlled phase-shifters proposed for the injection of the quadrature phase voltage are described in Chapter 4.

3.4 COMPLEX TORQUE COEFFICIENT METHOD

The complex torque coefficient method [31] is used to reveal the positive damping effect of the quadrature phase voltage injection on the torsional oscillations of the IEEE turbine-generator. Fig.3.1 shows the single line diagram of the first IEEE benchmark model, which is used for this study. In Fig.3.1, the quadrature phase voltage injection is represented as an ideal controlled voltage source.

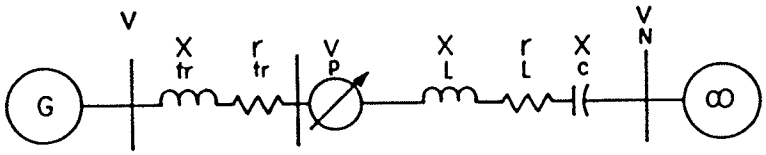

Figure 3.1: Single line diagram of the system studied

In Fig.3.1, r_{tr} and x_{tr} are the step-up transformer resistance and reactance, r_L and x_L are the line resistance and reactance, and x_c is the capacitive reactance of the series capacitor.

Assuming sustained small signal oscillations of the generator in the system as a result of a disturbance, the network currents and voltages oscillate about their constant

values, determined by the system operating point. The rotor oscillations with the amplitude $\Delta\hat{\delta}$ and the frequency f_r Hz in the d-q axes appear as a pulsation around the steady-state value δ_o between $\delta_o - \Delta\hat{\delta}$ and $\delta_o + \Delta\hat{\delta}$.

$$\Delta\delta = \text{Re}\,[\Delta\underline{\delta}] \tag{3.1}$$

where $\Delta\underline{\delta} = \Delta\hat{\delta}\, e^{j\lambda t}$

$$\lambda = f_r/60 \quad \text{pu}$$

For the sake of simplicity, in this study, time is normalized such that, $1s = 2\Pi f = 377$ pu. In the d-q reference frame, the system variables are represented by two components: a constant term corresponding to the fixed operating point plus a term with prefix Δ which indicates small changes.

The complex torque coefficient $K_e(j\lambda)$ is defined by Eqn.3.2 [31].

$$\Delta\underline{T}_e = K_e(j\lambda)\ \Delta\underline{\delta} = [K_e + j\lambda D_e]\ \Delta\underline{\delta} \tag{3.2}$$

where $\Delta T_e = \text{Re}[\Delta\underline{T}_e]$

In Eqn.3.2 $\Delta\underline{T}_e$ is the complex phasor of the oscillatory electrical torque and is obtained by linearizing the torque expression, Eqn.3.3, around the system operating point as follows:

$$T_e = \psi_d i_q - \psi_q i_d \tag{3.3}$$

where i_d is the direct axis current,

i_q is the quadrature axis current,

ψ_d is the direct axis air-gap flux, and

ψ_q is the quadrature axis air-gap flux.

The relationships of the air-gap fluxes, the generator parameters and the stator currents are given by

$$\psi_d = G(p)v_f - x_d(p)\, i_d$$

$$\psi_q = - X_q(p)\, i_q \qquad (3.4)$$

where $X_d(p)$, $X_q(p)$ and $G(p)$ are the operational impedances (Appendix B), v_f is the excitation voltage, and

p is the Laplace operator.

From the linearization of Eqn.3.3, one obtaines the small signal torque component

$$\Delta T_e = \psi_{do}\, \Delta i_q + i_{qo}\, \Delta\psi_d - \psi_{qo}\, \Delta i_d - i_{do}\, \Delta\psi_q \qquad (3.5)$$

The oscillatory components of the air-gap flux are deduced from Eqns.3.4 as given by Eqns.3.6.

$$\psi_{do} = -x_d\, i_{do} + v_{fo}$$

$$\psi_{qo} = - x_q\, i_{qo}$$

$$\Delta\psi_d = G(p)\, \Delta v_f - X_d(p)\, \Delta i_d \qquad (3.6)$$

$$\Delta\psi_q = - X_q(p)\, \Delta i_q$$

The oscillatory electrical torque component in the Laplace domain as a function of the generator parameters, the operating point and the stator currents are deduced from Eqns.3.5 and Eqn.3.6, as given by Eqn.3.7.

$$\Delta T_e = \phi_d \Delta i_d + \phi_q \Delta i_q + G(p)\, i_{qo}\, \Delta v_f \qquad (3.7)$$

where $\phi_d = [x_q - X_d(p)]\, i_{qo}$

$$\phi_q = v_{fo} - [x_d - X_q(p)]\, i_{do}$$

Small signal changes in the field voltage, Δv_f, due to the rotor oscillations, is determined from the transfer function of the excitation control. Thus, by calculating Δi_d and Δi_q as functions of the rotor small amplitude oscillations, and substituting the Laplace operator p by $j\lambda$ in Eqn.3.7, the complex torque coefficient in the general form of Eqn.3.2 is obtained.

The oscillatory stator current components are obtained by developing two sets of small signal voltage equations for the generator and the transmission system in the d-q frame, as functions of the stator currents, and eliminating the voltage components in favour of the current components. For this purpose the small signal voltage components of all the system elements in the d-q reference frame must be developed.

3.4.1 Generator Voltage Components

The generator terminal voltage in the in the d-q frame is expressed by

$$v_d = - r_a i_d - \omega \psi_q + \frac{d}{dt} \psi_d$$

$$v_q = - r_a i_q + \omega \psi_d + \frac{d}{dt} \psi_q \qquad (3.8)$$

where r_a is the stator resistance, and

ω is the rotor speed.

The oscillatory components of the generator voltage, as a result of the rotor oscillations, are obtained by linearizing Eqns.3.8, as given below:

$$\Delta v_d = - r_a \Delta i_d - \psi_{qo} \frac{d}{dt} (\Delta\delta) - \Delta\psi_q + \frac{d}{dt} (\Delta\psi_d)$$

$$\Delta v_q = - r_a \Delta i_q + \psi_{do} \frac{d}{dt} (\Delta\delta) + \Delta\psi_d + \frac{d}{dt} (\Delta\psi_q) \qquad (3.9)$$

Small signal voltage components of the generator in the Laplace domain are obtained from Eqns.3.9, by substituting the flux components from Eqns.3.6.

$$\begin{vmatrix} \Delta v_d \\ \Delta v_q \end{vmatrix} = - \begin{vmatrix} Z_{g11} & Z_{g12} \\ Z_{g21} & Z_{g22} \end{vmatrix} \begin{vmatrix} \Delta i_d \\ \Delta i_q \end{vmatrix} + \begin{vmatrix} p \\ 1 \end{vmatrix} G(p) \Delta v_f + \begin{vmatrix} \psi_{qo} \\ -\psi_{do} \end{vmatrix} p \, \Delta\delta \qquad (3.10)$$

where $Z_{g11} = r_a + p \, X_d(p)$

$$Z_{g12} = - X_q(p)$$

$$Z_{g21} = X_d(p)$$

$$Z_{g22} = r_a + p\, X_q(p)$$

The voltage equation of the transmission system, (Fig.3.1), is given as:

$$\underline{v} - \underline{v}_N = r_t \underline{i} + x_t \frac{d}{dt} \underline{i} + \underline{v}_c - \underline{v}_p \qquad (3.11)$$

where $r_t = r_{tr} + r_L$

$$x_t = x_{tr} + x_L$$

where $\underline{v}$ is the complex phasor of the generator voltage,

$\underline{v}_N$ is the complex phasor of the infinite bus voltage,

$\underline{i}$ is the complex phasor of the stator current,

$\underline{v}_c$ is the complex phasor of the series capacitor voltage, and

$\underline{v}_p$ is the complex phasor of the injected voltage.

$$\underline{v} = (v_d + j\, v_q)\, e^{j(t+\Delta\delta)}$$

$$\underline{v}_N = (v_{Nd} + j\, v_{Nq})\, e^{j(t+\Delta\delta)}$$

$$\underline{i} = (i_d + j\, i_q)\, e^{j(t+\Delta\delta)} \qquad (3.12)$$

$$\underline{v}_c = (v_{cd} + j\, v_{cq})\, e^{j(t+\Delta\delta)}$$

$$\underline{v}_p = (v_{pd} + j\, v_{pq})\, e^{j(t+\Delta\delta)}$$

The voltage components of the transmission system in the d-q axes, are obtained by substituting the phasors of the current and voltages from Eqns.3.12 in Eqn.3.11, and linearizing the deduced equations around the system operating point.

$$\Delta v_d - \Delta v_{Nd} = r_t \Delta i_d - x_t \Delta i_q - x_t i_{qo} \frac{d}{dt}(\Delta\delta) + x_t \frac{d}{dt}(\Delta i_d) + \Delta v_{cd} - \Delta v_{pd}$$

$$\Delta v_q - \Delta v_{Nq} = r_t \Delta i_q - x_t \Delta i_d + x_t i_{do} \frac{d}{dt}(\Delta\delta) + x_t \frac{d}{dt}(\Delta i_q) + \Delta v_{cq} - \Delta v_{pq} \qquad (3.13)$$

3.4.2 Oscillatory Components of Network Voltage

For the analysis of the machine-network problems, the variables of each machine must be transformed to the system global rotating frame by the linear transformation:

$$T = \begin{vmatrix} \cos\theta_i & -\sin\theta_i \\ \sin\theta_i & \cos\theta_i \end{vmatrix} \qquad (3.14)$$

In Eqn.3.14, θ_i is the angle between the quadrature axis of the machine i and the system reference axis. However in the case of a single machine system, as in Fig.3.1, the system equations will have a simpler form if all the variables are defined in the generator reference frame.

Fig.3.2 illustrates the infinite bus voltage phasor in the d-q reference frame of the generator. During the rotor oscillations, the small signal voltage components of the infinite bus, viewed from the generator rotating frame are obtained from Fig.3.2, as given by Eqns.3.15 and 3.16.

$$\Delta v_{Nd} = \Delta\hat{\delta}\ |\underline{v}_N|\ \sin(\alpha_o - \Delta\delta/2) = v_{Nqo}\ \Delta\hat{\delta} \qquad (3.15)$$

$$\Delta v_{Nq} = -\ \Delta\hat{\delta}\ |\underline{v}_N|\ \cos(\alpha_o - \Delta\delta/2) = -\ v_{Ndo}\ \Delta\hat{\delta} \qquad (3.16)$$

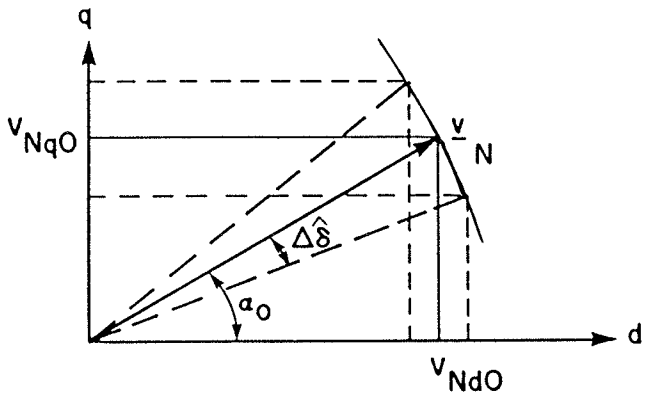

Figure 3.2: Network voltage components in generator d-q axis

3.4.3 Components of Injected Quadrature Voltage

Fig.3.3 shows the generator voltage phasor, $\underline{v}$, and the injected quadrature phase voltage, $\underline{v}_p$, in the generator d-q frame. Assuming that the magnitude of the injected voltage is a fraction of the generator terminal voltage, the components of the injected quadrature phase voltage are expressed by Eqn.3.17.

$$\begin{vmatrix} v_{pd} \\ v_{pq} \end{vmatrix} = K \begin{vmatrix} v_q \\ -v_d \end{vmatrix} \qquad (3.17)$$

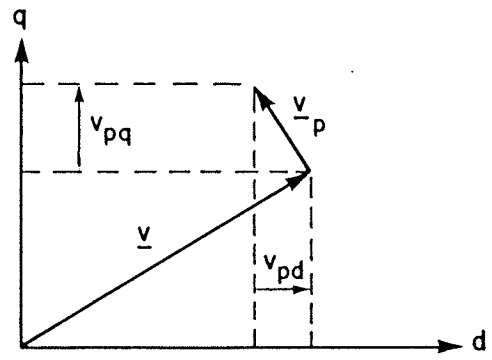

Figure 3.3: Components of quadrature phase voltage in generator d-q axis

In Eqn.3.17, K is a factor which determines the fraction of the generator voltage which is injected into the system as the quadrature phase voltage. Positive and negative values of K indicate lagging and leading voltages respectively. The components of the injected quadrature phase voltage, during small signal perturbations, are deduced by linearizing Eqn.3.17.

$$\begin{vmatrix} \Delta v_{pd} + v_{pdo} \\ \Delta v_{pq} + v_{pqo} \end{vmatrix} = (K_o + \Delta K) \begin{vmatrix} v_{qo} + \Delta v_q \\ -v_{do} - \Delta v_d \end{vmatrix} \qquad (3.18)$$

When the objective is only to inject a quadrature phase voltage, during the system disturbances, the initial value K_o is set equal to zero. Thus, the components of the dynamically injected voltage are:

$$\begin{vmatrix} \Delta v_{pd} \\ \Delta v_{pq} \end{vmatrix} = \Delta K \begin{vmatrix} v_{qo} \\ -v_{do} \end{vmatrix} \qquad (3.19)$$

When the injected voltage is proportional to the rotor speed deviation, from Eqn.3.1

$$\Delta K = g \frac{d}{dt} [\Delta\hat{\delta} \cos(\lambda t - \gamma)] \tag{3.20}$$

where g is the controller gain, and

γ is the controller phase shift.

3.4.4 Voltage Components of Series Capacitors

The voltage drop, $\underline{v}_c$, across the series capacitor is calculated from

$$\frac{d}{dt} \underline{v}_c = x_c \underline{i} \tag{3.21}$$

The quadrature components of the voltage drop across the series capacitor are given by Eqns.3.22, which are obtained by substituting $\underline{v}_c$ and $\underline{i}$ in Eqn.3.21, and linearizing around the system operating point.

$$\Delta v_{cd} = \frac{p^2}{p^2+1} v_{cqo} \Delta\delta + \frac{p}{p^2+1} x_c \Delta i_d - \frac{p}{p^2+1} v_{cdo} \Delta\delta + \frac{1}{p^2+1} x_c \Delta i_q$$

$$\Delta v_{cq} = -\frac{p}{p^2+1} v_{cqo} \Delta\delta - \frac{1}{p^2+1} x_c \Delta i_d - \frac{p^2}{p^2+1} v_{cdo} \Delta\delta + \frac{p}{p^2+1} x_c \Delta i_q \tag{3.22}$$

where $v_{cqo} = -x_c i_{do}$

$$v_{cdo} = + x_c \, i_{qo}$$

3.4.5 Oscillatory Components of Stator Currents

The small signal voltage components of the generator in the Laplace domain are given by Eqns.3.23, which are obtained by substituting the voltage components from Eqn.3.15, Eqn.3.16, Eqn.3.19 and Eqn.3.22 in Eqns.3.13.

$$\begin{vmatrix} \Delta v_d \\ \Delta v_q \end{vmatrix} = \begin{vmatrix} v_{qo} \\ -v_{do} \end{vmatrix} \Delta\delta + \begin{vmatrix} Z_{t11} & Z_{t12} \\ Z_{t21} & Z_{t22} \end{vmatrix} \begin{vmatrix} \Delta i_d - i_{qo} \, \Delta\delta \\ \Delta i_q + i_{do} \, \Delta\delta \end{vmatrix}$$

$$- \Delta K \begin{vmatrix} v_{qo} \\ -v_{do} \end{vmatrix} \qquad (3.23)$$

where $$Z_{t11} = r_t + p\, x_t + \frac{p}{p^2+1} x_c$$

$$Z_{t12} = - x_t + \frac{1}{p^2+1} x_c$$

$$Z_{t21} = x_t - \frac{1}{p^2+1} x_c$$

$$Z_{t22} = r_t + p\, x_t + \frac{p}{p^2+1} x_c$$

The components of the stator current in the d-q axes, as functions of the generator rotor oscillation angle and the system controller parameters, are obtained by substituting the generator terminal voltage, Eqn.3.10, in Eqn.3.23.

$$\begin{vmatrix} \Delta i_d \\ \Delta i_q \end{vmatrix} = \begin{vmatrix} i_{qo} \\ -i_{do} \end{vmatrix} \Delta\delta + \underline{Z}^{-1} \begin{vmatrix} p & -1 \\ 1 & p \end{vmatrix} \begin{vmatrix} \phi_d \\ \phi_q \end{vmatrix} \Delta\delta$$

$$+ \underline{Z}^{-1} \begin{vmatrix} p \\ 1 \end{vmatrix} G(p)\Delta v_f - \underline{Z}^{-1} \begin{vmatrix} v_{qo} \\ -v_{do} \end{vmatrix} \Delta K \qquad (3.24)$$

where $$\underline{Z} = \begin{vmatrix} Z_{g11} + Z_{t11} & Z_{g12} + Z_{t12} \\ Z_{g21} + Z_{t21} & Z_{g22} + Z_{t22} \end{vmatrix}$$

The real and the imaginary parts of the complex torque coefficient are deduced by substituting the current components from Eqns.3.24 and $p=j\lambda$ in Eqn.3.7.

3.5 ELECTRICAL DAMPING CONSTANT

The magnitudes of the electrical spring constant K_e and the electrical damping D_e are dependent upon the operating point and the parameters of the system. The mechanical damping of the rotating masses is also dependent upon the system operating point. Under all operating conditions, the mechanical damping of the shaft system has a positive value. However, the electrical damping can exhibit negative values,

depending on the system operating point, the parameters and the frequency of perturbation. When the magnitude of the negative electrical damping exceeds the positive mechanical damping value, the system will experience an unstable mode of operation. A plot of the electrical damping as a function of frequency, can reveal the regions of unstability, corresponding to the system operating point.

Fig.3.4 and Fig.3.5 show the variation of D_e and K_e of the first IEEE benchmark model, as functions of the rotor oscillation frequency. The curves shown in Fig.3.4 and Fig.3.5 were obtained under the conditions discussed below.

1. The excitation voltage is held constant, $\Delta v_f = 0.0$.
2. The controller of the quadrature phase voltage source is inactive, g=0.0 .
3. For all different values of the series capacitor, the operating point corresponds to the rated MVA.

The unstable torsional oscillatory modes of the first IEEE benchmark, were stimulated at series compensation levels 30%, 50% and 80% respectively.

Fig.3.4 indicates that even when the series capacitor is not in service, the system exhibits a negative electrical damping in the frequency range of $f_r > 28$ Hz. The negative magnitude of the electrical damping at the shaft torsional frequencies increases as the series compensation level

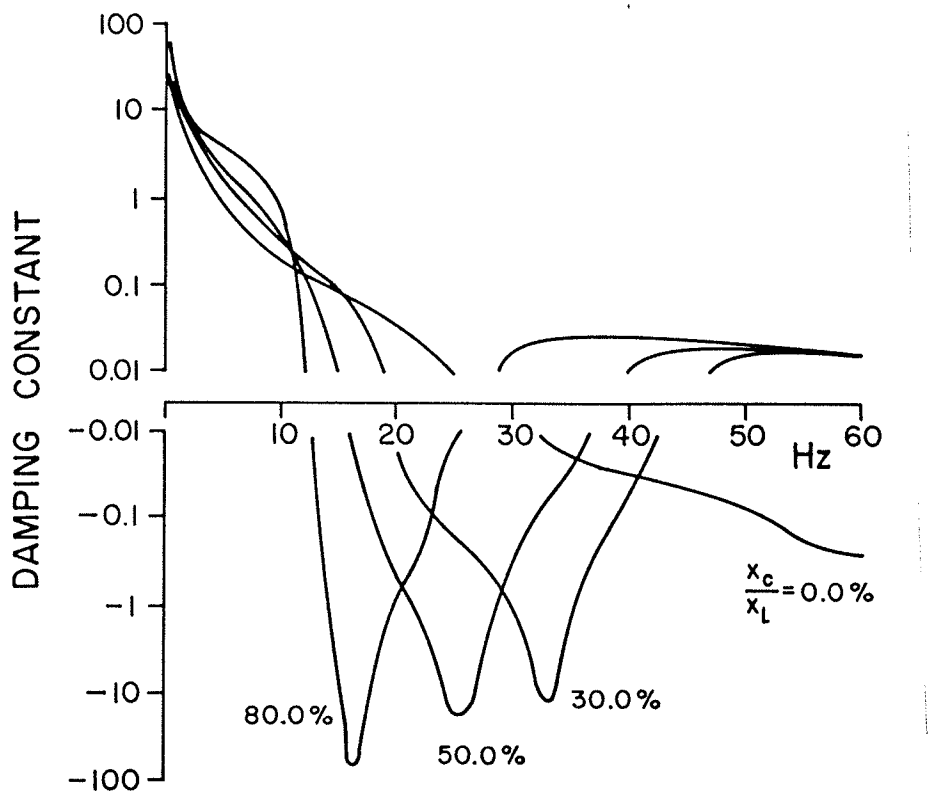

Figure 3.4: Damping constant of the first IEEE benchmark, phase-shifter out of service

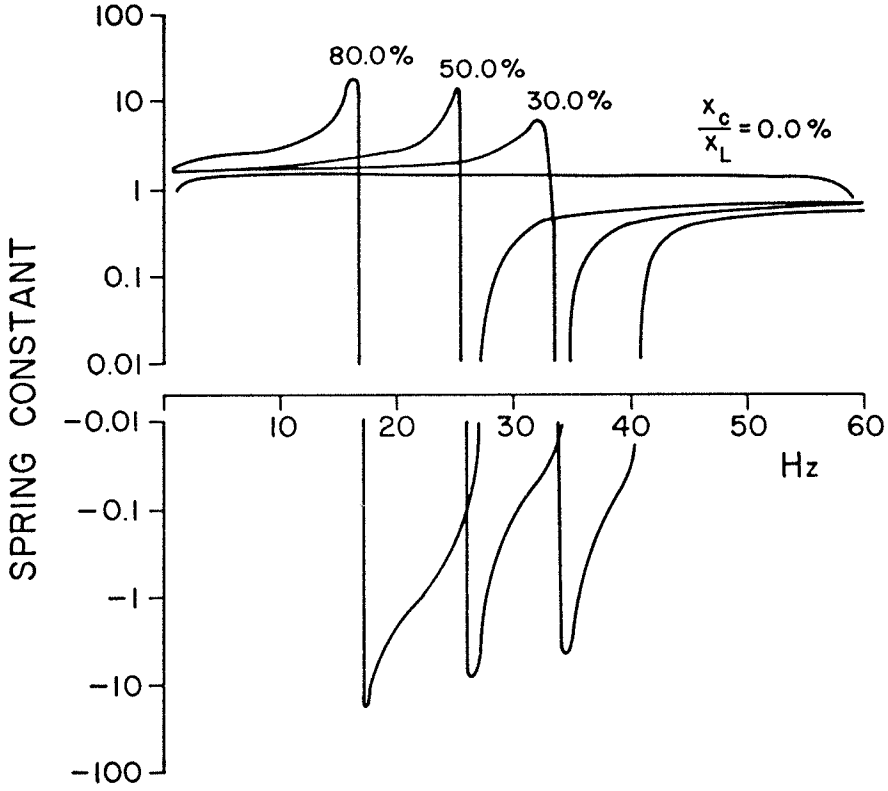

Figure 3.5: Spring constant of the first IEEE benchmark, phase-shifter out of service

approaches those values which cause electrical oscillations at the complementary frequency of the mechanical natural frequencies. With increase in the level of series compensation, the range of negative electrical damping shifts towards lower frequencies. For the first IEEE benchmark model, the maximum negative electrical damping occurs at a narrow range of frequency, corresponding to the first mode of torsional oscillations (f=15.7 Hz).

Fig.3.6 shows the electrical damping of the system, when a dynamically controlled quadrature phase voltage proportional to the rotor speed deviation is injected in the system. The generator delivers the rated MVA and the series compensation level is set at 80.0%. The electrical damping constants for different values of the controller gain and the phase-shift, over the subsynchronous frequency range were calculated. The results indicate that for the first mode of torsional oscillations (15.5 Hz), the positive electrical damping with smooth variation over the subsynchronous frequency range is obtained when the controller injects a quadrature phase voltage proportional to the rotor speed deviation and introduces a phase lag in the range of 5-17 degrees. Fig.3.6 shows the electrical damping for three different values of the controller gain, when the controller phase lag is adjusted at 10 degrees.

Fig.3.7 and Fig.3.8 depict the system electrical damping constants when the series compensation levels are set at

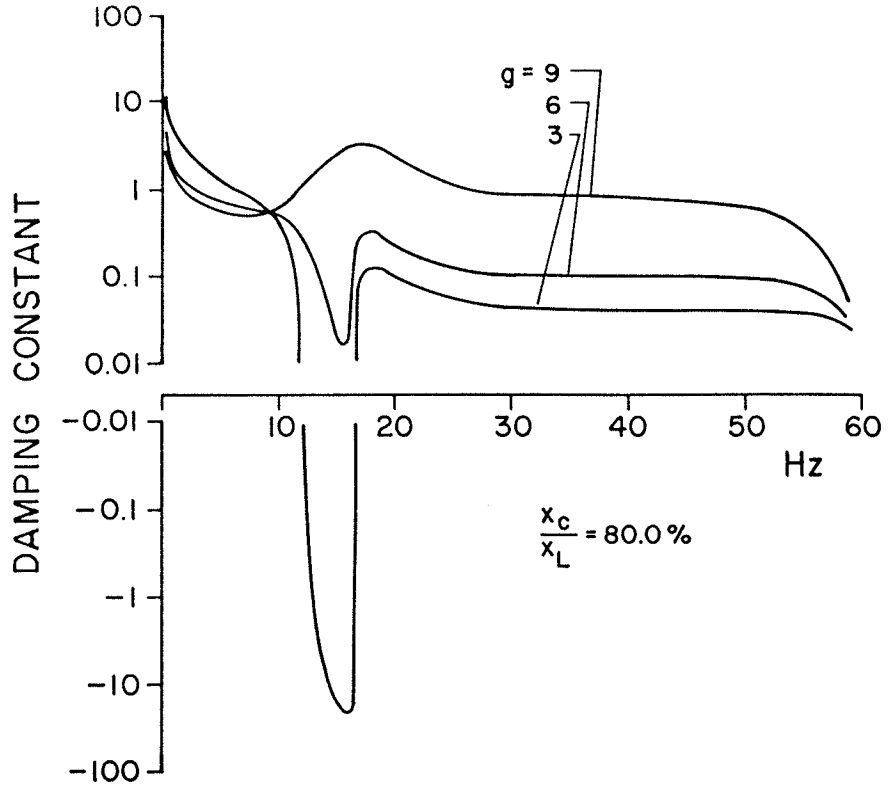

Figure 3.6: Damping constant of the first IEEE benchmark, phase-shifter in service

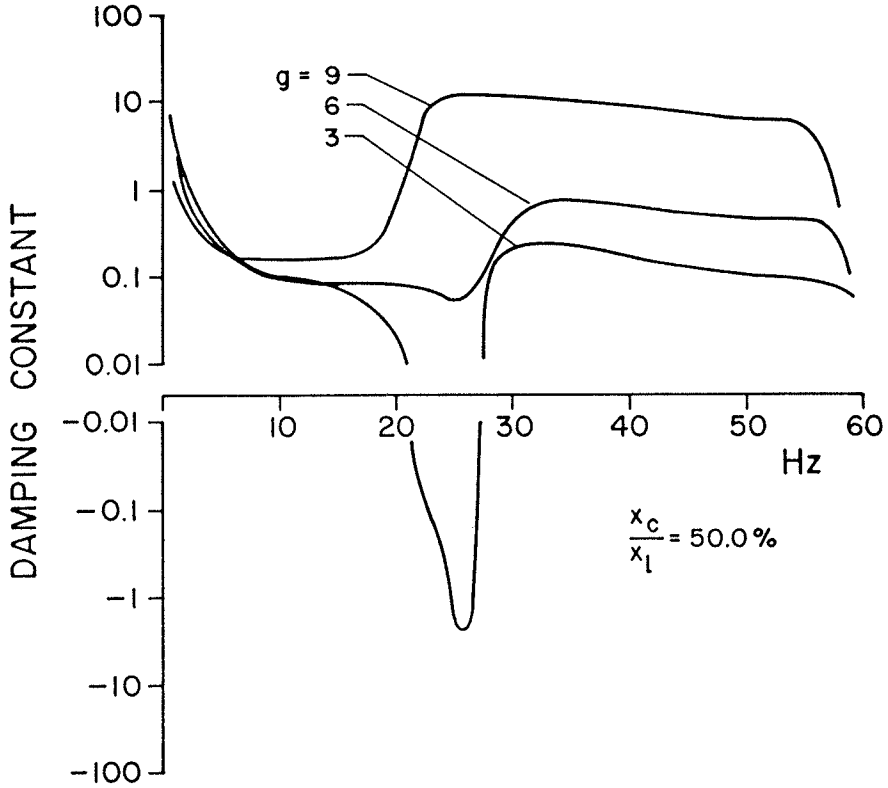

Figure 3.7: Damping constant of the first IEEE benchmark, phase-shifter in service

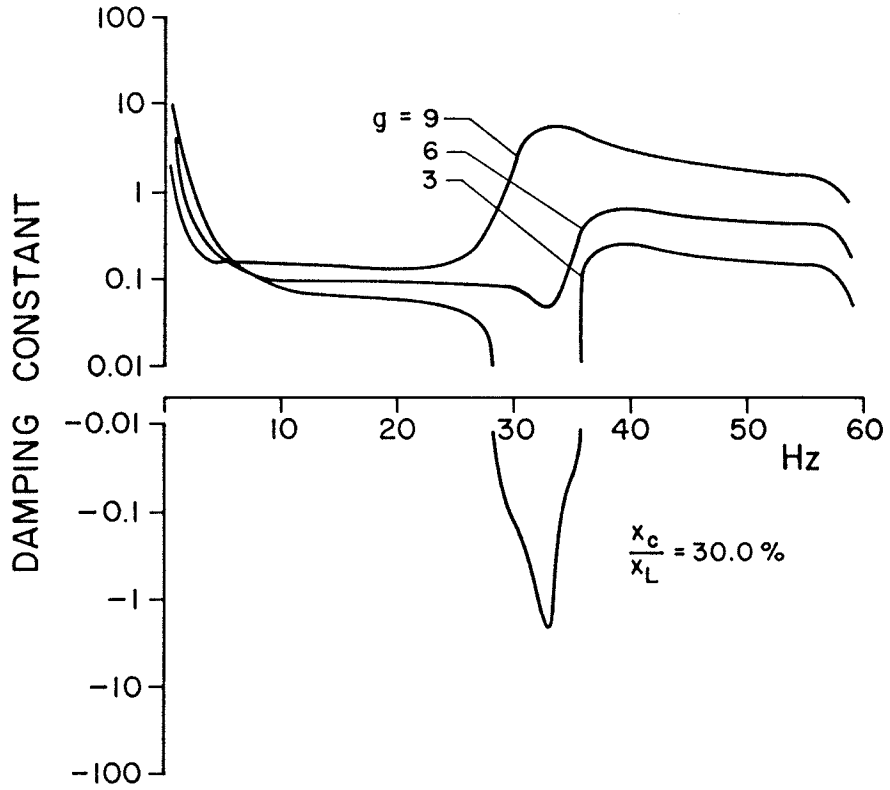

Figure 3.8: Damping constant of the first IEEE benchmark, phase-shifter in service

50% and 30% respectively. The generator delivers the rated MVA and the controller phase lag is 10 degrees. The effect of the controller phase-shift on the electrical damping, for different magnitudes of the controller gain was examined. The results show that at 50.0% and 30.0% compensation levels, positive electrical damping over the subsynchronous frequency range can be obtained, when the controller phase-lag is between three to 21 degrees.

Figs.3.6-8 reveal that injection of the quadrature phase voltage, proportional to the rotor speed deviation with proper phase and gain can provide positive electrical damping for all the torsional modes. Assuming under torsional instability the generator speed can rise up to 0.01 pu, Eqn.3.25 indicates that injection of 6.0% of the system line-to-ground voltage, in quadrature phase, can suppress the unstable oscillatory modes.

$$|\Delta v| = |g \cdot \Delta\omega| = 6.0 \times 0.01 = 0.06 \text{ pu} \qquad (3.25)$$

In practice a higher magnitude of the quadrature voltage might be needed to provide the required damping effect. This is due to the non-continuous operating nature of the devices used to inject the voltage. However, the shaft torsional oscillations can be suppressed even with a smaller magnitude of the injected voltage, provided that the oscillations are detected before the shaft speed deviation reaches 0.01 per-unit.

3.6 EIGENVALUE ANALYSIS

An eigenvalue analysis is performed on the first IEEE benchmark model to investigate the effect of the proposed damping method on the unstable modes of the torsional oscillations, and to determine the decrement factors of the oscillatory modes. For this purpose, the system of nonlinear equations, representing the electromechanical system of the first IEEE benchmark, is developed and linearized around the system operating point. The small signal behaviour of the system is determined from the characteristic matrix of the linearized equations.

3.6.1 System Equations

3.6.1.1 Dynamics of Mechanical System

The equations of motion of the six-mass mechanical system of the first IEEE benchmark model are given by Eqn.3.26.

$$\underline{M}\,\ddot{\underline{\delta}} + \underline{D}\,\dot{\underline{\delta}} + \underline{K}\,\underline{\delta} = \underline{T}_m - \underline{T}_e \qquad (3.26)$$

where $\ddot{\underline{\delta}} = [\ddot{\delta}_{HP} \quad \ddot{\delta}_{IP} \quad \ddot{\delta}_{LPA} \quad \ddot{\delta}_{LPB} \quad \ddot{\delta}_{G} \quad \ddot{\delta}_{EXC}]^t$

$\dot{\underline{\delta}} = [\dot{\delta}_{HP} \quad \dot{\delta}_{IP} \quad \dot{\delta}_{LPA} \quad \dot{\delta}_{LPB} \quad \dot{\delta}_{G} \quad \dot{\delta}_{EXC}]^t$

$\underline{\delta} = [\delta_{HP} \quad \delta_{IP} \quad \delta_{LPA} \quad \delta_{LPB} \quad \delta_{G} \quad \delta_{EXC}]^t$

$\underline{T}_m = [T_{HP} \quad T_{IP} \quad T_{LPA} \quad T_{LPB} \quad 0 \quad 0]^t$

$$T = [0 \quad 0 \quad 0 \quad 0 \quad T_{ELE} \; 0 \;]^t$$

$\ddot{\underline{\delta}}$ is the vector of acceleration,

$\dot{\underline{\delta}}$ is the vector of speed,

$\underline{\delta}$ is the vector of position,

$\underline{T}_m$ is the vector of input mechanical torques,

$\underline{T}_e$ is the vector of electrical torque,

$\underline{M}$ is the matrix of moment of inertia (Appendix C),

$\underline{D}$ is the matrix of mechanical damping, and

$\underline{K}$ is the matrix of stiffness (Appendix C).

In a state space form, Eqn.3.26 is represented as:

$$\begin{vmatrix} \dot{\underline{\delta}} \\ \ddot{\underline{\delta}} \end{vmatrix} = \underline{U} \begin{vmatrix} \underline{\delta} \\ \dot{\underline{\delta}} \end{vmatrix} + \begin{vmatrix} \underline{0} \\ \underline{M}^{-1} \end{vmatrix} \begin{vmatrix} \underline{0} \\ \underline{T}_m - \underline{T}_e \end{vmatrix} \tag{3.27}$$

where $$\underline{U} = \begin{vmatrix} \underline{0} & \underline{I} \\ -\underline{M}^{-1}\underline{K} & -\underline{M}^{-1}\underline{D} \end{vmatrix}$$

The numerical values of the elements of the matrices $\underline{M}$ and $\underline{K}$ in perunit, based on the generator MVA rating, are given in Appendix A.

3.6.1.2 Synchronous Machine Electrical Dynamics

Under balanced operating conditions, the voltage equations in the d-q axes, for the IEEE benchmark generator are:

$$v_d = \dot{\psi}_d - \psi_q \dot{\delta}_G - r_a i_d$$

$$v_f = \dot{\psi}_f + r_f i_f$$

$$0 = \dot{\psi}_{kd} + r_{kd}\, i_{kd}$$

$$v_q = \dot{\psi}_q + \psi_d\, \dot{\delta}_G - r_a\, i_q \qquad (3.28)$$

$$0 = \dot{\psi}_{kq} + r_{kq}\, i_{kq}$$

$$0 = \dot{\psi}_g + r_g\, i_g$$

Eqn.3.29 is the matrix representation of Eqns.3.28.

$$\underline{v} = \dot{\underline{\psi}} + \underline{R}\,\underline{i} + \dot{\delta}_G\,\underline{N}\,\underline{\psi} \qquad (3.29)$$

where $\underline{v} = [v_d \;\; v_f \;\; 0 \;\; v_q \;\; 0 \;\; 0]^t$

$\dot{\underline{\psi}} = [\dot{\psi}_d \;\; \dot{\psi}_f \;\; \dot{\psi}_{kd} \;\; \dot{\psi}_q \;\; \dot{\psi}_{kq} \;\; \dot{\psi}_g]^t$

$\underline{R} = \text{diag}[-r_a \;\; r_f \;\; r_{kd} \;\; -r_a \;\; r_{kq} \;\; r_g]$

$\underline{i} = [i_d \;\; i_f \;\; i_{kd} \;\; i_q \;\; i_{kq} \;\; i_g]^t$

$\underline{\psi} = [\psi_d \;\; \psi_f \;\; \psi_{kd} \;\; \psi_q \;\; \psi_{kq} \;\; \psi_g]^t$

$\underline{N}$ is a 6x6 matrix with all the elements equal to zero, except $n_{1,4}=-1$ and $n_{4,1}=1$.

The linkage flux has a linear relationship with the current $\underline{i}$, as given by Eqn.3.30.

$$\underline{\psi} = \underline{L}\,\underline{i} \qquad (3.30)$$

where $\underline{L}$ is the matrix of the generator inductances (Appendix C).

A state space representation of the generator electrical model is obtained by substituting $\underline{\psi}$ from Eqn.3.30 in Eqn.3.29

$$\dot{\underline{i}} = -\left[+ \underline{L}^{-1} \underline{R} + \dot{\delta}_G \underline{L}^{-1} \underline{N} \underline{L}\right] \underline{i} + \underline{L}^{-1} \underline{v} \qquad (3.31)$$

The generator electrical torque as a function of the stator and rotor currents is obtained from the general torque expression

$$T_{ELE} = \psi_d i_q - \psi_q i_d = \underline{i}^t \underline{L}^t \underline{N}^t \underline{i} \qquad (3.32)$$

3.6.1.3 Transmission System Dynamics

The voltage equations in the generator d-q axes for the transmission system (Fig.3.1) are obtained from Eqn.3.11.

$$\begin{aligned} v_d - v_{Nd} &= r_t i_d - x_t i_q \dot{\delta}_G + x_t i_d + v_{cd} - v_{pd} \\ v_q - v_{Nq} &= r_t i_q + x_t i_d \dot{\delta}_G + x_t i_q + v_{cq} - v_{pq} \end{aligned} \qquad (3.33)$$

where r_t is the transmission system resistance, and

x_t is the transmission system reactance.

The voltage drop across the series capacitor is deduced from Eqn.3.21 as:

$$\begin{aligned} \dot{v}_{cd} - v_{cq} \dot{\delta}_G &= x_c i_d \\ \dot{v}_{cq} + v_{cd} \dot{\delta}_G &= x_c i_q \end{aligned} \qquad (3.34)$$

The controller is represented by a gain and a time constant, as shown by Eqn.3.35.

$$\Delta K = \frac{g}{1 + pT} \Delta\dot{\delta}_G \tag{3.35}$$

3.7 CONSTRUCTION OF SYSTEM MATRIX

The mathematical model of the shaft dynamics is related to the electrical equations by the rotor speed and the electrical torque. The behaviour of the electromechanical system in the general form is described by Eqn.3.36, which is obtained by substituting the generator voltage components from Eqn.3.33 in Eqn.3.31, and the air-gap torque from Eqn.3.32 in Eqn.3.27, and combining Eqns.3.27, 3.31, 3.34 and 3.35.

$$\dot{\underline{x}} = f(\underline{x}) \tag{3.36}$$

The small signal behaviour of the system is obtained by linearizing Eqn.3.36 around the system operating point.

$$\Delta\dot{\underline{x}} = \underline{A}\ \Delta\underline{x} \tag{3.37}$$

where $\Delta\dot{\underline{x}} = [\Delta\dot{\delta}_{HP}\ \ \Delta\dot{\delta}_{IP}\ \ \Delta\dot{\delta}_{LPA}\ \ \Delta\dot{\delta}_{LPB}\ \ \Delta\dot{\delta}_{G}\ \ \Delta\dot{\delta}_{EXC}$

$\Delta\ddot{\delta}_{HP}\ \ \Delta\ddot{\delta}_{IP}\ \ \Delta\ddot{\delta}_{LPA}\ \ \Delta\ddot{\delta}_{LPB}\ \ \Delta\ddot{\delta}_{G}\ \ \Delta\ddot{\delta}_{EXC}$

$\Delta\dot{i}_{d}\ \ \Delta\dot{i}_{f}\ \ \Delta\dot{i}_{kd}\ \ \Delta\dot{i}_{q}\ \ \Delta\dot{i}_{kq}\ \ \Delta\dot{i}_{g}$

$$\Delta\dot{v}_{cd} \quad \Delta\dot{v}_{cq} \quad \Delta\dot{K}\rfloor^{t}$$

$$\underline{\Delta x} = \lfloor \Delta\delta_{HP} \quad \Delta\delta_{IP} \quad \Delta\delta_{LPA} \quad \Delta\delta_{LPB} \quad \Delta\delta_{G} \quad \Delta\delta_{EXC}$$

$$\Delta\dot{\delta}_{HP} \quad \Delta\dot{\delta}_{IP} \quad \Delta\dot{\delta}_{LPA} \quad \Delta\dot{\delta}_{LPB} \quad \Delta\dot{\delta}_{G} \quad \Delta\dot{\delta}_{EXC}$$

$$\Delta i_{d} \quad \Delta i_{f} \quad \Delta i_{kd} \quad \Delta i_{q} \quad \Delta i_{kq} \quad \Delta i_{g}$$

$$\Delta v_{cd} \quad \Delta v_{cq} \quad \Delta K\rfloor^{t}$$

The elements of $\underline{A}$ are functions of the system parameters and the operating point (Appendix C). The elements of the system matrix $\underline{A}$ were obtained by making the following three assumptions.

1. The effect of mechanical damping is neglected.
2. The governor system is disabled.
3. The excitation voltage during the system torsional oscillations is considered to be constant.

The eigenvalues of the system matrix $\underline{A}$ determine the small signal behaviour of the power system. The eigenvalues with positive real parts, indicate growing oscillations, and consequently an unstable operating condition. The maximum positive decrement factor for each mode of oscillation occurs at a specific series compensation level, corresponding to the complementary electrical natural frequency of the tor-

sional mode. The magnitude of the decrement factor for each mode of oscillation at a fixed level of series compensation depends upon the system operating point.

Fig.3.9 shows the real part of the eigenvalues corresponding to the unstable modes of the shaft torsional oscillations of the IEEE benchmark, as functions of the series compensations level. The numerical value of the decrement factors (Fig.3.9) were obtained when the generator delivered the rated MVA at the lagging power factor 0.90, and the phase-shifter was out of service. Fig.3.9 indicates that the highest value for the decrement factors occur at the series compensation level corresponding to the mode one, f=15.7 Hz. This indicates that the mode one is the most unstable mode of torsional oscillations for the IEEE benchmark. The numerical values of the decrement factors illustrated in Fig.3.9, are in agreement with the numerical values of the electrical damping constant shown in Fig.3.6.

Fig.3.10 shows the eigenvalues of the system matrix $\underline{A}$, corresponding to the unstable shaft torsional modes, when a dynamically controlled quadrature voltage, proportional to the rotor speed deviation is injected in the power system. Under all different compensation levels, the generator de-

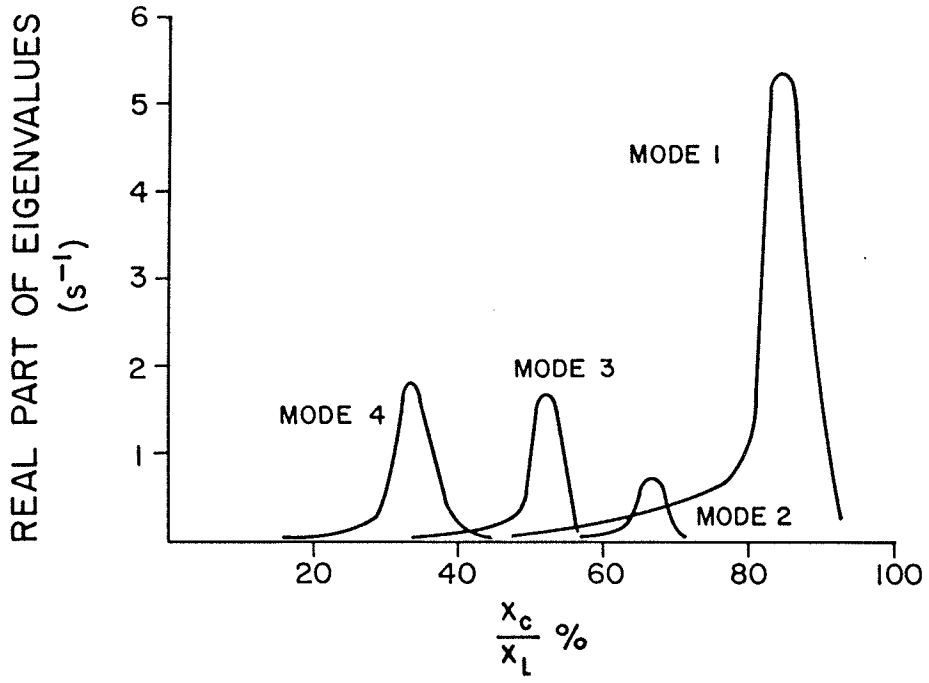

Figure 3.9: Decrement factors of unstable oscillatory modes of the first IEEE benchmark system, phase-shifter out of service

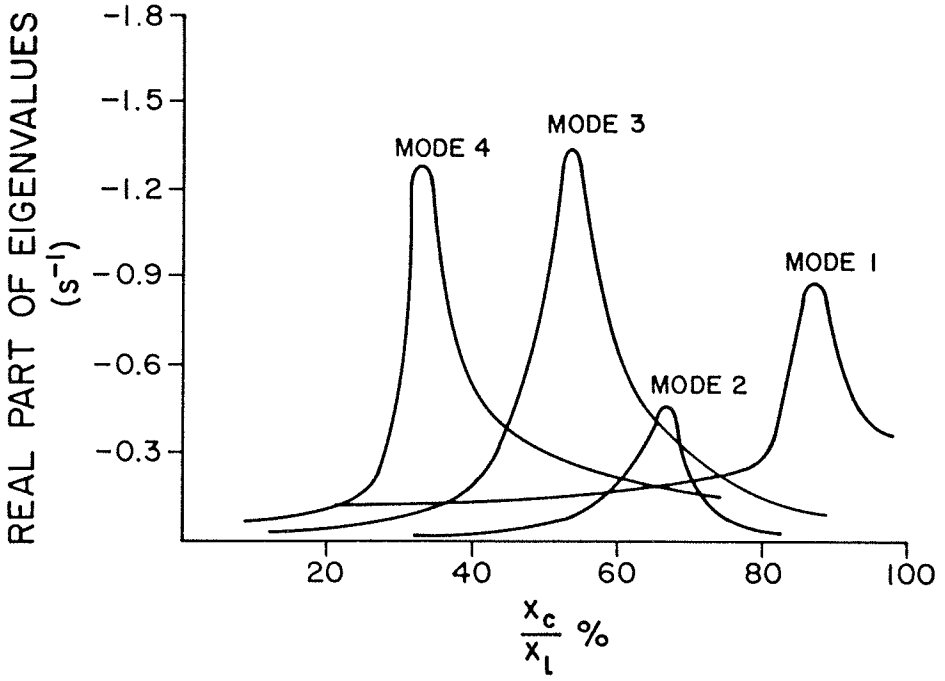

Figure 3.10: Decrement factors of unstable oscillatory modes of the first IEEE benchmark system, phase-shifter in service

livers the rated MVA at the lagging power factor 0.90, and the controller gain and time constant are set at g=9.0 and T=0.0015. Fig.3.10 shows that the real part of the eigenvalues corresponding to the shaft unstable torsional modes have negative values, as a result of the injected quadrature phase voltage. This reveals the technical feasibility of a static phase-shifter for stabilizing the torsional modes of the first IEEE benchmark model.

3.8 CONCLUSIONS

A new method for damping the shaft torsional oscillations, based on injecting a dynamically controlled quadrature phase voltage, was presented. the proposed countermeasure for SSO, provides the required positive damping by modulating the generator active power, using the shaft speed deviation as the feedback signal.

The complex torque coefficient method and an eigenvalue analysis technique were utilized to investigate the effect of quadrature phase voltage injection on the electrical damping and the decrement factors of the unstable modes of oscillations of a power system, during small signal disturbances. The results from the analytical studies reveal that the injection of 6.0% of the system line-to-ground voltage, in quadrature phase, proportional to the rotor speed deviation, provides the required positives electrical damping for the unstable torsional modes of the first IEEE benchmark.

Chapter IV

METHODS OF QUADRATURE PHASE VOLTAGE INJECTION

4.1 BACKGROUND

The emergence of power semiconductor devices during the last two decades and the replacement of mechanical switches by fast acting thyristor valves, indicate a wider range of application of the phase-shifting and on-load tap changing transformers in power systems. The steady-state power flow regulation of power systems by means of conventional phase-shifters is a common practice [86]. The operation of a conventional phase-shifter is characterized by a high response time as a result of the inertia of the moving parts, and high level of maintenance due to mechanical contacts and oil deterioration. If the speed and the controlability is improved, the phase-shifters may be used for the enhancement of transient stability and damping the shaft torsional oscillations due to small signal perturbations and large disturbances.

The technical drawbacks of the conventional phase-shifters can be overcome by the use of thyristor valves instead of mechanical switches [87]. However, utilization of the static switches with the principle of operation of the con-

ventional phase-shifters requires that the static valves to withstand all the system abnormal conditions, and a large number of thyristors are necessary to provide a desirable range of phase shifting. To avoid the foregoing difficulty, phase shifting can be achieved by using either the point-on-wave control method [88] or the discrete step method [89].

Transient stability enhancement by introducing a rapid phase-shift in the system voltage was first suggested in 1973 [90], without indicating the method to realize a fast changing phase-shift. Based on quadrature phase voltage injection, by means of the thyristor-controlled phase-shifters, a method of transient stability enhancement in power systems has been suggested in [91,92,93].

There are two practical schemes for the thyristor-controlled phase-shifters. In the literature they are referred as the point-on-wave controlled phase-shifter and the discrete step controlled phase-shifter.

4.2 POINT-ON-WAVE CONTROL METHOD FOR PHASE SHIFTING

Fig.4.1 shows the schematic diagram of one phase of a static phase-shifter which injects a continuously adjustable voltage in a system by controlling the firing pulses of the thyristor switches [92,94]. The excitation transformer ET provides the quadrature phase voltage, and the series boosting transformer BT injects the required quadrature phase voltage

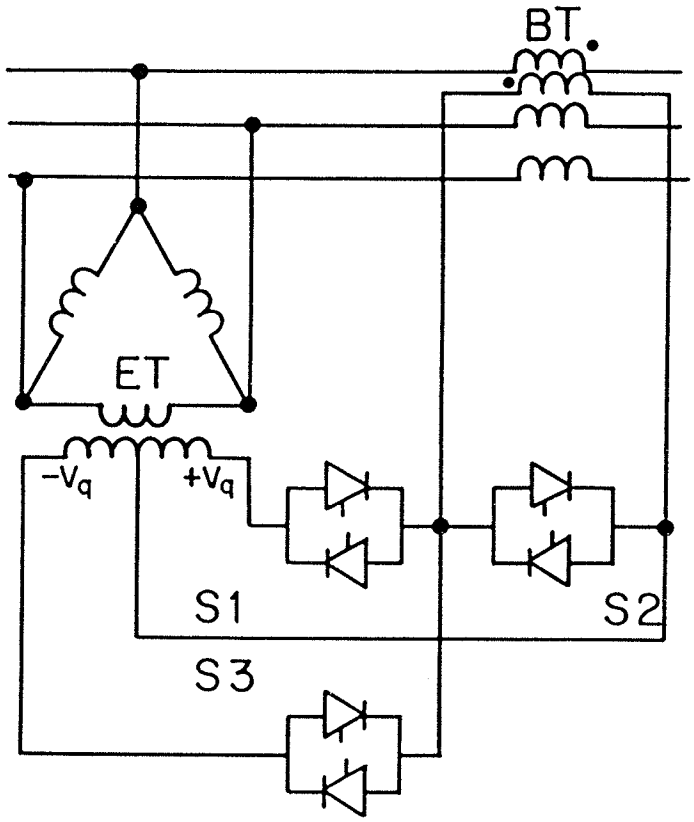

Figure 4.1: Single line diagram of one phase of a point-on-wave control phase-shifter

in the system. Thyristor switches S1 and S3 are referred as the boosting and the bucking switches respectively. The current path for the boosting transformer, during the time intervals when the phase-shifter is inactive, is provided by the thyristor switch S2. The magnitude of the injected voltage is adjusted by controlling the firing angles of the thyristor switches S1, S2, and S3. If only the boosting or the bucking mode of operation is required, the phase-shifter is equipped with either switches S1-S2 or S3-S2 respectively. The principle of operation of the point-on-wave controlled phase-shifters is described in Appendix D.

4.3 DISCRETE STEP CONTROL METHOD FOR PHASE SHIFTING

Fig.4.2 shows the schematic diagram of one phase of a static phase shifter which introduces a phase shift in the voltage of a power system, in discrete steps. The maximum number of the steps is equal to the number of sub-converters. Each sub-converter consists of a bridge circuit with antiparallel connected thyristors in each arm of the bridge. In contrast to the switches S1, S2 and S3 in Fig.4.1, the sub-converters are not phase controlled, but the magnitude of the injected voltage is determined by those sub-converters which are not shorted. The output voltages of the sub-converters can be of equal or different magnitudes, depending upon the turns ratio of the partial windings of the excitation transformer ET. The principle of operation of the discrete step phase-shifters is described in Appendix D.

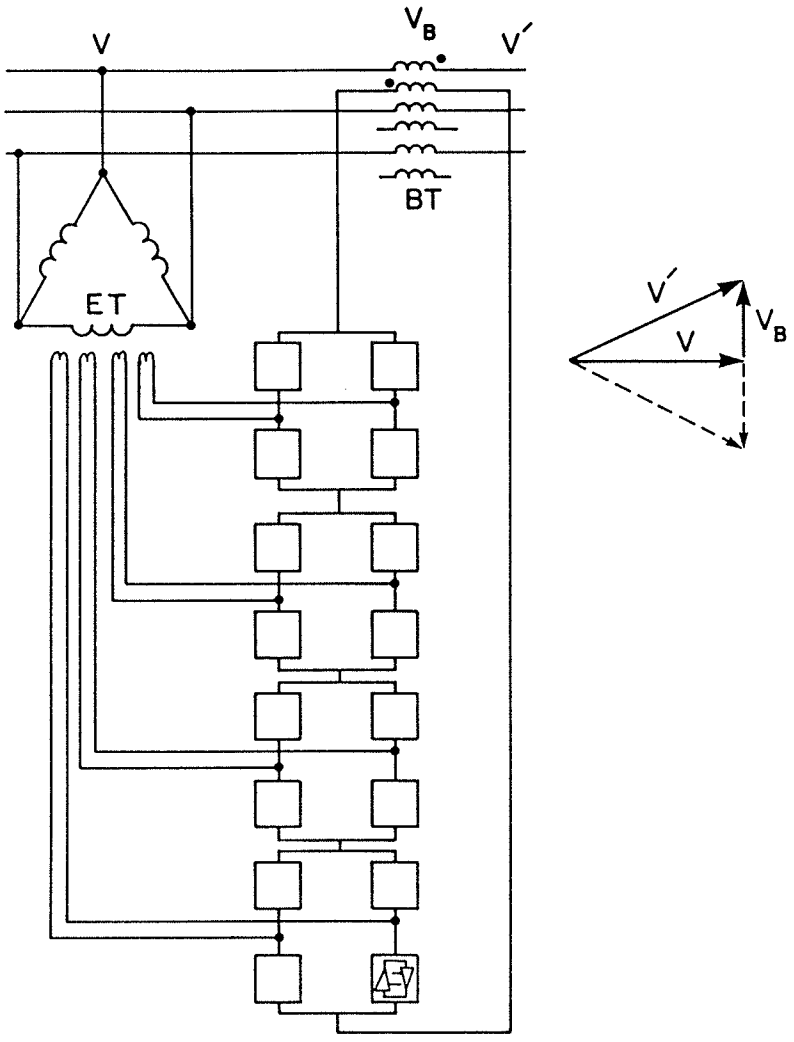

Figure 4.2: Single line diagram of one phase of a discrete step control phase shifter

4.4 CONTROL SYSTEM FOR STATIC PHASE-SHIFTERS

The simplified block diagram of the control system for one phase of the phase-shifters which were discussed in sections 4.2 and 4.3 is given in Fig.4.3. The required signals for the control system are:

1. the shaft speed deviation from the synchronous speed,
2. the line current,
3. the quadrature phase voltage, and
4. the phase angle between the line current and the phase voltage.

Based on the magnitude and the sign of the generator rotor speed deviation from the synchronous speed, the controller block determines the magnitude and the lead/lag of the quadrature phase voltage to be injected in the system. For the static phase-shifter which operates based on the point-on-wave control method, the output of the controller block determines the conduction angles of the boosting and the bucking switches S1 and S3. In the case of the discrete step controlled phase-shifter, the controller block determines the number of steps that voltage must be injected and the mode of operation of the thyristor bridges.

After a disturbance in a power system, the rotor speed signal contains a low frequency (0.5-2.0 Hz) component, associated with the hunting mode, as well as high frequency speed components as a result of the shaft torsional

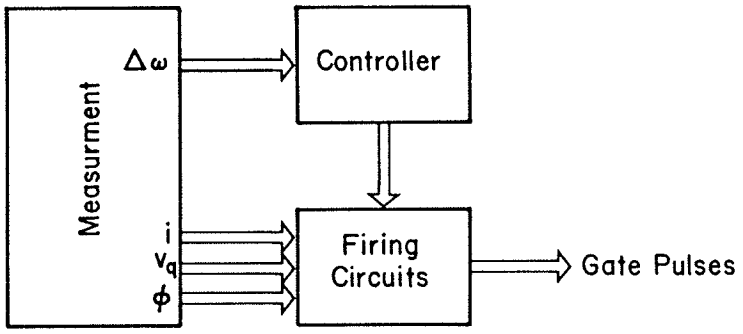

Figure 4.3: Simplified representation of the control system of one phase of a phase-shifter

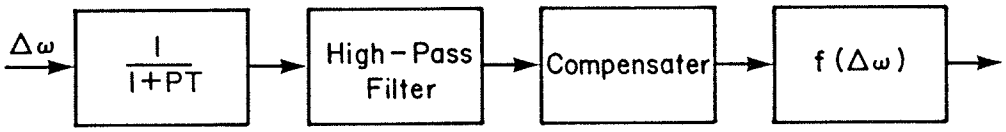

Figure 4.4: Block diagram of the controller section

oscillations. Depending upon the level of series compensation, the system operating point and the severity of the disturbance, the slower component may dominate the speed signal. Thus, it is necessary to eliminate the low frequency from the generator speed signal. This is accomplished by passing the generator speed through a high-pass filter. For the turbine-generators with the torsional frequencies in the range of 12-60 Hz, a high-pass filter with the transfer function

$$H_1(p) = \frac{0.0177p(1 + 0.0088p)}{1 + 0.0177p + 0.0002p^2} \qquad (4.1)$$

can be used to eliminate the effect of low frequency oscillations on the control system [60].

Fig.4.4 shows the block diagram of the controller section. In Fig.4.4 the transfer function with a single time constant represents the effect of speed transducer on the control system. The high-pass filter is used to eliminate the hunting effect on the control system. The compensator block with the transfer function

$$H_2(p) = \frac{1 + 0.01p}{(1 + 0.0125p)(1 + 0.002p)} \qquad (4.2)$$

is used to optimize the phase of the control signal and to compensate the effect of the high-pass filter.

Function $f(\Delta\omega)$, (Fig.4.4), determines the conduction angles of the thyristor switches S1 and S3 (Fig.4.1). Function

$f(\Delta\omega)$ is obtained based on the required magnitude of the quadrature voltage to be injected as a function of the generator speed deviation. The rms magnitude of the fundamental 60 Hz quadrature phase voltage, injected by the point-on-wave phase-shifter, during the boosting and the bucking modes of operation are plotted as functions of conduction angle in Fig.4.5 and Fig.4.6, respectively. The magnitude of the injected voltage is limited depending on the system power factor. As compared with Fig.4.5, Fig.4.6 shows that for the same magnitude of the excitation voltage, in the bucking mode of operation, a higher magnitude of voltage can be injected. However, the phase-shift of the fundamental component of the injected voltage in the bucking mode, increases as the firing angles of the thyristors increase. Therefore, full conduction angle of of the thyristor switches can not be utilized and the magnitude of the injected voltage in the bucking mode cannot reach to the highest values of Fig.4.6. AT 0.90 lagging power factor, changes in the conduction angle from 0 to 60 degrees causes a phase shift in the injected voltage between 0 to 14.2 degrees respectively.

Graphical representation of $f(\Delta\omega)$ during the boosting and bucking modes of operation are given in Fig.4.7 and Fig.4.8. The numerical values for Fig.4.7 and Fig.4.8 are for the cases when the power factor is 0.90 lagging, the excitation voltage of the static phase-shifter is 6.0% of the system phase voltage and the controller gain is set at g=9.0. When the quadrature voltage is injected in discrete steps, $f(\Delta\omega)$

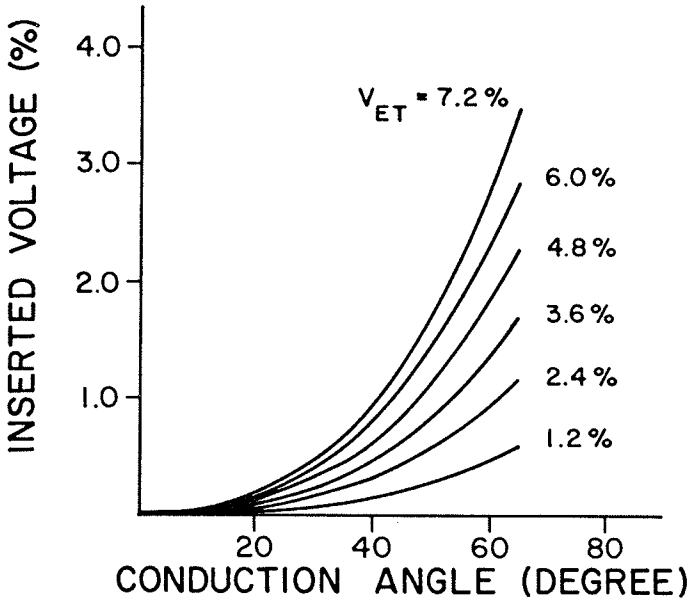

Figure 4.5: Injected quadrature voltage in boosting mode of operation

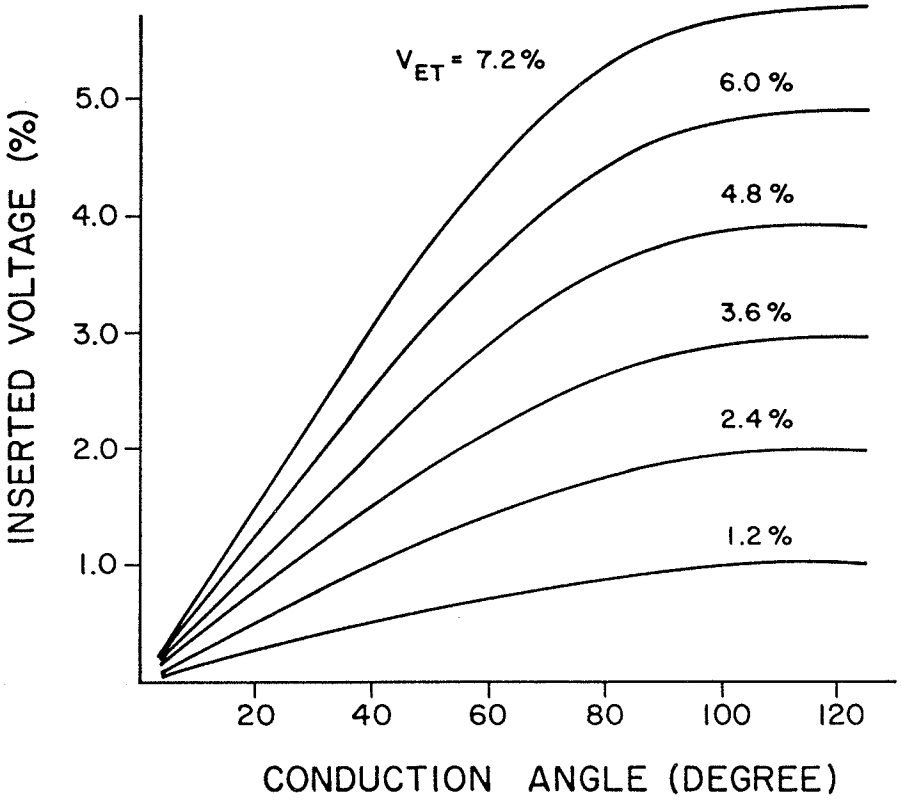

Figure 4.6: Injected quadrature voltage in bucking mode of operation

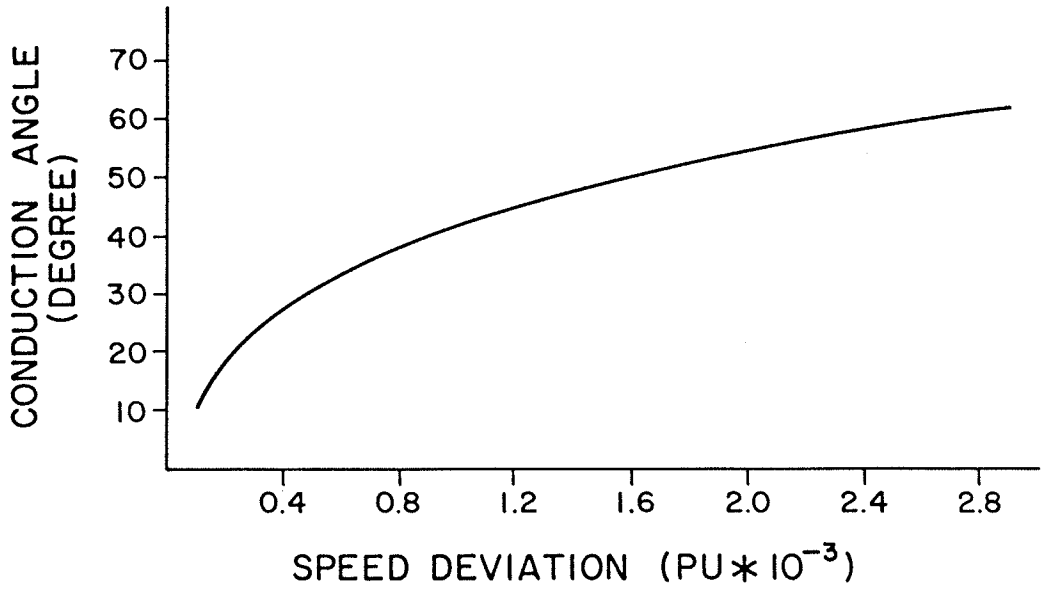

Figure 4.7: Function $f(\Delta\omega)$ for boosting mode of operation

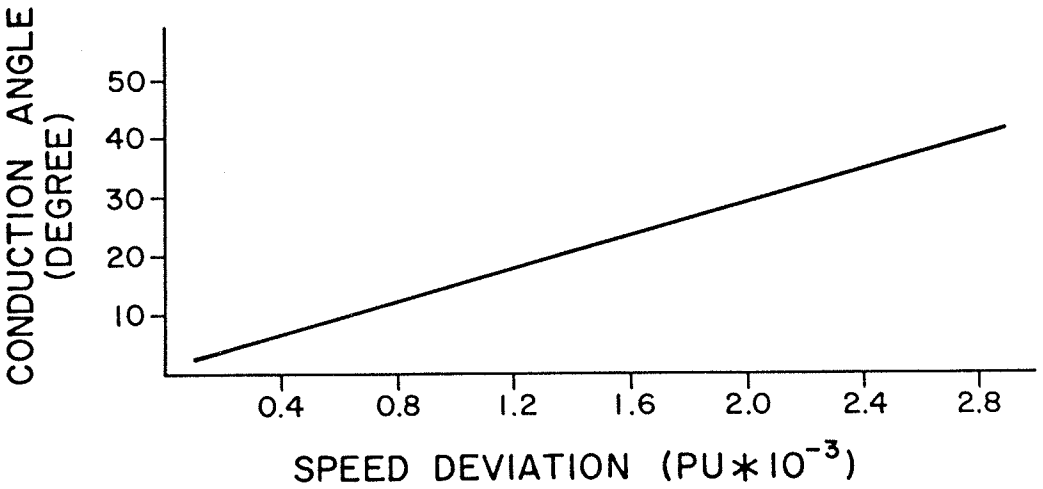

Figure 4.8: Function $f(\Delta\omega)$ for bucking mode of operation

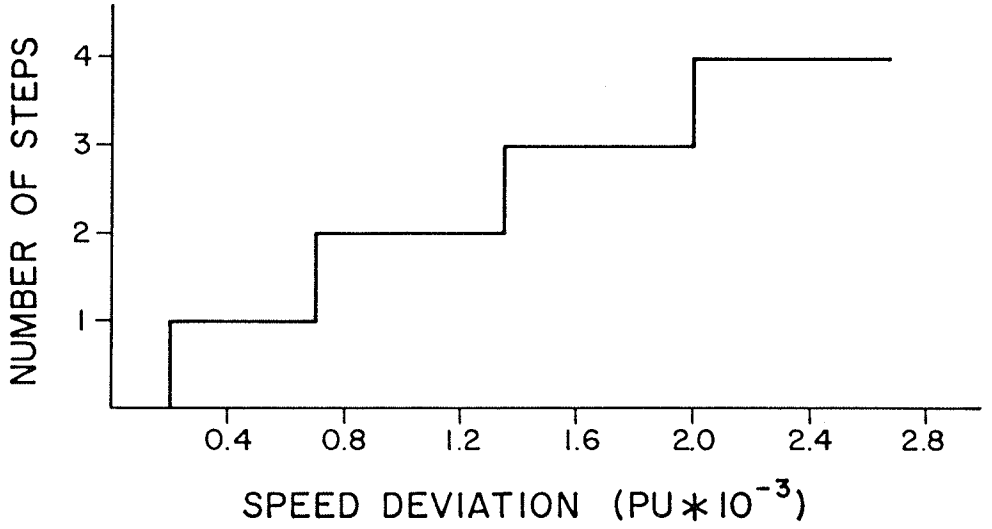

Figure 4.9: Function $f(\Delta\omega)$ for discrete step voltage insertion

represents the number of steps as a function of speed deviation. Fig.4.9 illustrates $f(\Delta\omega)$ when the quadrature voltage is injected in four equal steps, each step 0.6% of the system phase voltage and the controller gain is adjusted at g=9.0.

The performance of the proposed control system for damping SSO, will be examined by digital computer studies in Chapters 5 and 6.

4.4.1 Speed Measurement

The positive damping effect of a static phase-shifter for mitigating the shaft torsional oscillations of a turbine-generator unit is significantly affected by the phase and the gain of the control system. Therefore, the time constant of the speed transducer, as a result of the method used for the speed measurement, has a decisive impact upon the decrement factors of the torsional modes and the system stability.

In practical systems, the shaft speed deviation is obtained from a multi-toothed wheel. The instantaneous shaft speed is achieved by mounting the precision toothed wheel on the shaft, and detecting the teeth frequency by a magnetic pick-up [96]. An FM demodulator is used to extract the the torsional frequency from the toothed wheel frequency.

When the turbine-generator under consideration is equipped with the torsional monitoring system (TMS) [97,98], the output signals from TMS can be used to obtain the instantaneous speed deviations of the rotor.

4.5 CONCLUSIONS

Two practical schemes of the thyristor controlled static phase-shifters for injecting quadrature phase voltage in a power system are briefly explained. A control method for the static phase-shifters is suggested which can be utilized to provides positive damping for SSO.

Chapter V

SIMULATION OF SMALL SIGNAL OSCILLATIONS IN THE TIME DOMAIN

5.1 INTRODUCTION

In order to verify the analytical results of Chapter IV, a digital simulation study is performed on the first IEEE benchmark model, and the effect of the dynamically controlled phase-shifters on the unstable modes of oscillations of the turbine-generator is examined. The BPA's ElectroMagnetic Transients Program (EMTP) is used for the digital computer simulation of the: turbine-generator, transmission line, transformers, thyristor valves and control circuitry.

The two available control methods for the static phase-shifters, i.e., the point-on-wave and the discrete step are compared and their damping effects on the three unstable shaft torsional modes of the first IEEE benchmark system are presented. The results of the simulation studies indicate that injection of a fraction of the system voltage, in quadrature phase, can effectively damp all the unstable torsional modes. As compared with the point-on-wave controll method, the discrete step control method was found to be more effective for damping SSO.

5.2 DIGITAL TIME SIMULATION STUDIES

The analytical methods for the study of the dynamics of a power system are based on the simplified mathematical representation of the system components. Depending upon the operating nature of the component under consideration, the degree of simplifications which is required to obtain the linear mathematical model, varies in a wide range. Representation of those components which utilize static switches, by linearized mathematical equations, requires considerable simplifications of the real equations. It is a general practice that for small signal studies, these components and their controllers are represented by linear transfer functions which completely neglect the switching phenomenon of the thyristor valves. Therefore, the accuracy of the results obtained from analytical studies are significantly dependent upon the assumptions made to deduce the simplified equations of the system. Furthermore, in the case of a complicated systems, it would be difficult to estimate the effect of a particular assumption on the system response.

In order to overcome the foregoing difficulties and to verify the accuracy of the analytical approaches, it is desirable to compare the analytical results with those obtainable from other computational tools, e.g., digital time simulation methods. The underlying principle of the digital computer simulation techniques for the analysis of the dynamics of a power system is to solve the nonlinear differen-

tial equations of the system, using a step-by-step numerical integration technique.

The ElectroMagnetic Transients Program (EMTP) developed by the Bonneville Power Administration (BPA), including the Transient Analysis of Control Systems (TACS) is a well known package for the study of the generator-network problems. The detailed investigations of power system dynamics, by the EMTP, and comparison of the results with the field tests, establishes the validity of performance prediction of the power systems by using the EMTP [99]. The EMTP has also been proven as an accurate method of analysis for the problems associated with the subsynchronous oscillations phenomenon.

In the EMTP the power system model includes the typical components. The TACS consists of the digital model of individual components found in control circuits. Therefore, a system can be represented realistically and the flexibility of the program facilitates the design and optimization of the required system parameters. Furthermore, the EMTP has the capability to calculate and plot all the required system behaviour indices.

In spite of the appealing features of the digital simulation techniques for the analysis of power systems, they can not provide a deeper understanding of the physical phenomenon involved. Thus, the simulation methods are to be con-

sidered as the complement of analytical techniques and not as a substitute for them.

The EMTP-mode 28 [19] is used for the simulation studies reported in this chapter. The TACS dimensions of the original package is insufficient to handle the size of the control system required for the static phase-shifters used in this study, therefore, considerable effort was made to redimension the TACS section to accommodate the control system.

5.3 DIGITAL MODEL OF TURBINE-GENERATOR

The type-50 dynamic synchronous machine component of the EMTP-28 is utilized for the digital simulation of the IEEE benchmark turbine-generator. The shaft mechanical system is simulated as six lumped masses, to which adjacent masses are connected by spring constants. The masses represent the: high-pressure turbine (HP), intermediate-pressure turbine (IP), two low-pressure turbines (LPA,LPB), generator rotor (G) and exciter (EXC). The type-50 machine model has the capability for the spring-mass representation up to 10 masses. The generator electrical system is represented by d-q axes equations, with the field and one damper winding on the d-axis and two damper windings on the q-axis.

The digital model of the turbine-generator is obtained under the following assumptions.

1. The effect of the mechanical damping of the shaft system is neglected.
2. The dynamics of the governor system is neglected.
3. The field voltage is constant and corresponds to the rated terminal voltage.

5.4 DIGITAL MODEL OF TRANSMISSION SYSTEM

The transmission system consists of a 276 mile line, a step-up transformer, a series capacitor and a three-phase static phase-shifter. The line is divided in two sections of 246 and 30 miles by the series capacitor. The transmission line is represented by lumped, series R-L elements for each section.

The generator step-up transformer is modeled as a three-phase star-delta transformer. The excitation and the boosting transformers are simulated as single-phase transformers.

The point-on-wave controlled phase-shifter (Fig.4.1) and the discrete step controlled phase-shifter (Fig.4.2) are used for the digital computer studies, and their performances are compared. The point-on-wave controlled phase-shifter can be used to damp the torsional oscillations, by utilizing only the boosting or the bucking mode of operation. However, injection of only the boosting or the bucking quadrature phase voltage is not effective in damping SSO, as compared with the boost-buck method [100]. Therefore, the results of

the studies based on injection of only the boosting or the bucking quadrature phase voltage are not reported in this Chapter and this method will not be discussed further.

For the digital computer studies, the thyristor switches of the phase-shifters are represented by a detailed model of each thyristor valve and its snubber circuit.

5.5 DIGITAL MODEL OF THE CONTROL SYSTEM

The block diagrams of the control system, for one phase of the static phase-shifters used in this study, are shown in Fig.4.3, Fig.4.4 and Appendix E. The TACS provides the digital simulation of individual components of the control circuitry. There are no limitations to the number of components and their interconnections. The input signals for the control system are obtained from the EMTP, and the output signals from the TACS are interfaced with the EMTP. In this study the transfer functions of the high-pass filter and the compensater are those given in Chapter 4, Eqn.4.1 and Eqn.4.2 respectively. Functions $F(\Delta\omega)$ for the point-on-wave controlled and the discrete step controlled phase-shifters are graphically shown in Fig.4.7, Fig.4.8 and Fig.4.9.

5.6 SIMULATION RESULTS

Fig.5.1 shows the decrement factors of the unstable torsional modes of the IEEE benchmark, obtained from the eigenvalue analysis and the digital simulation study. Fig.5.1 shows the results, when the static phase-shifter is out of service and the generator delivers less than 1.3% of the rated MVA. The decrement factors which are obtained from the eigenvalue analysis are the real parts of the eigenvalues corresponding to the unstable shaft torsional oscillations. The decrement factors from the digital simulation study are the exponential rate of increase in the system variables, which are obtained by observing the system time responses. Fig.5.1 shows that the results from both methods are in good agreement. Furthermore, the results favorably agree with those reported in [54], which have been obtained from a hybrid computer simulation study.

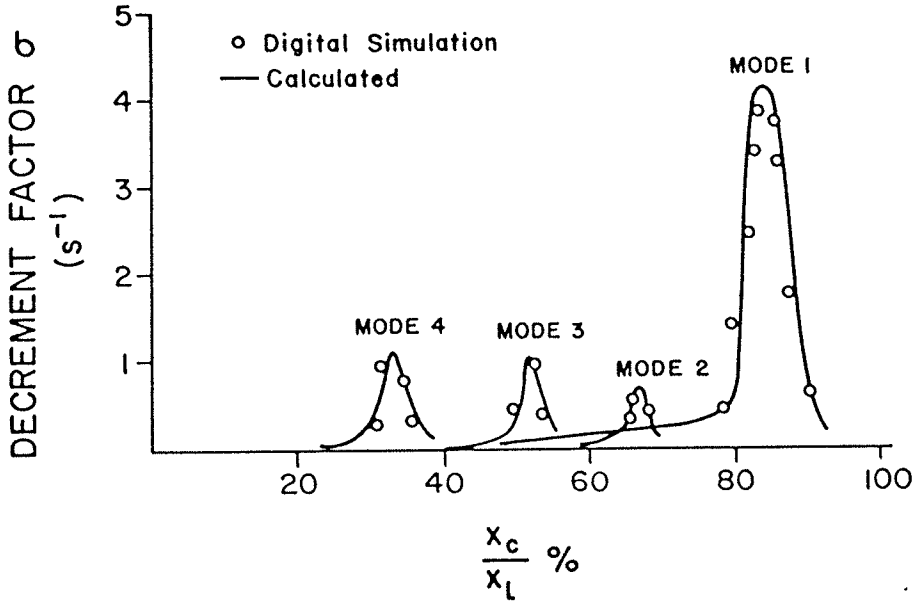

Figure 5.1: Decrement factors of unstable modes of the first IEEE benchmark model

5.6.1 Mode 1 of Torsional Oscillations

The system is initially delivering 80% of the rated MVA at 0.90 lagging power factor, and the series compensation is set at 90% of the line reactance. At time t=0.25 s, the compensation level is reduced to 80%, which causes the first mode of oscillations at f=15.7 Hz. Fig.5.2 illustrates the system response to the disturbance. In this case as well as in the subsequent studies, the following variables are plotted:

1. T_{HP-IP} the torque transmitted from HP to IP,
2. T_{IP-LPA} the torque transmitted from IP to LPA,
3. $T_{LPA-LPB}$ the torque transmitted from LPA to LPB,
4. T_{LPB-G} the torque transmitted from LPB to G,
5. T_{G-EXC} the torque transmitted from G to EXC,
6. T_{ELE} the air-gap torque,
7. $\Delta\dot{\delta}_{HP}$, $\Delta\dot{\delta}_{IP}$, $\Delta\dot{\delta}_{LPA}$, $\Delta\dot{\delta}_{LPB}$, $\Delta\dot{\delta}_{G}$, $\Delta\dot{\delta}_{EXC}$, changes in the speed of HP, IP, LPA, LPB, G and EXC masses, respectively, and
8. V_q the injected quadrature phase voltage.

Fig.5.3 shows the system response to the same disturbance, when the torsional oscillations are counteracted by using the point-on-wave controlled static phase-shifter. The injected quadrature phase voltage for the boosting and the bucking modes of operation is 6% of the system phase voltage. In Fig.5.3, V_q is the instantaneous injected voltage

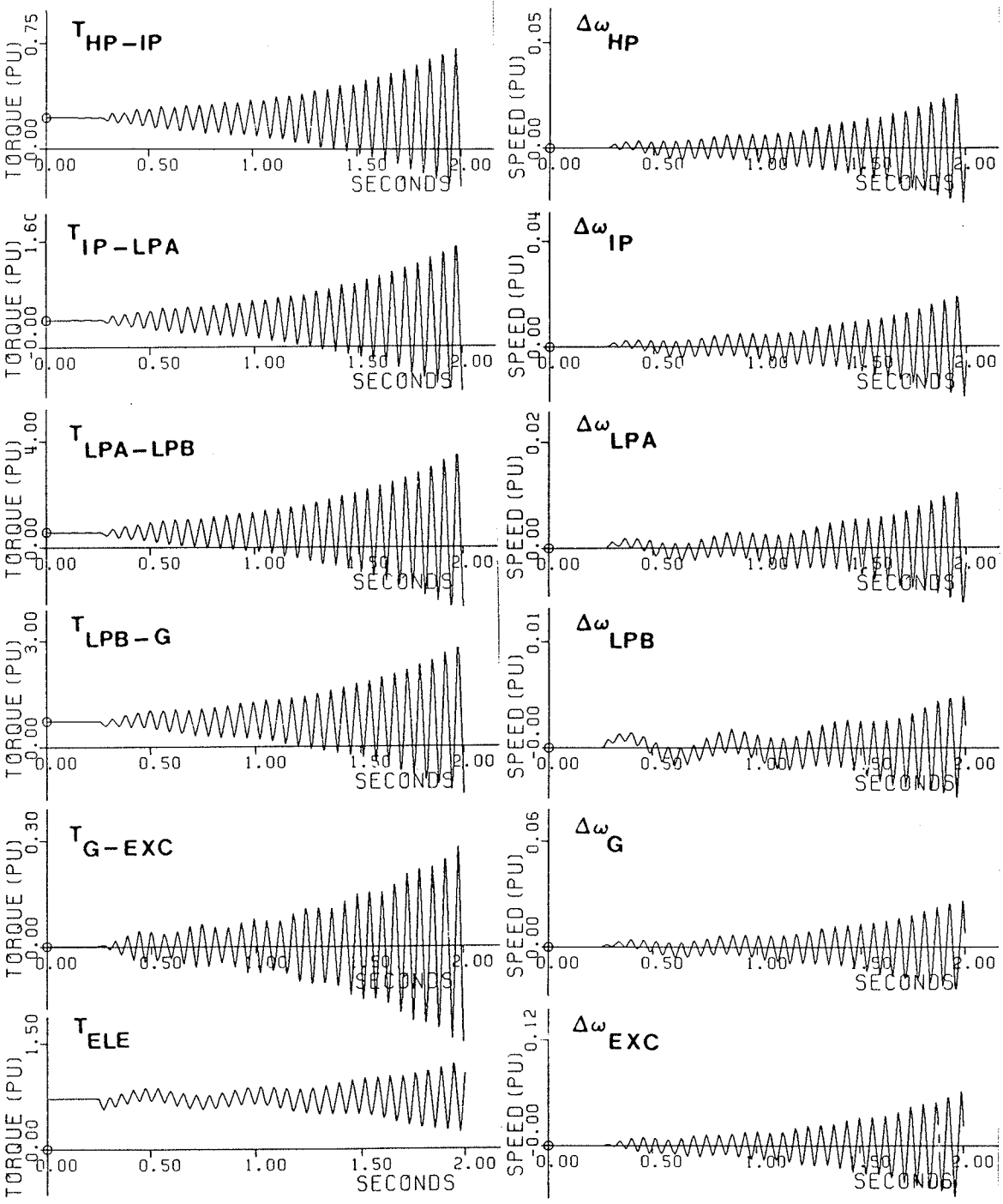

Figure 5.2: Shaft torsional oscillations at mode one, f=15.7 Hz, phase-shifter out of service

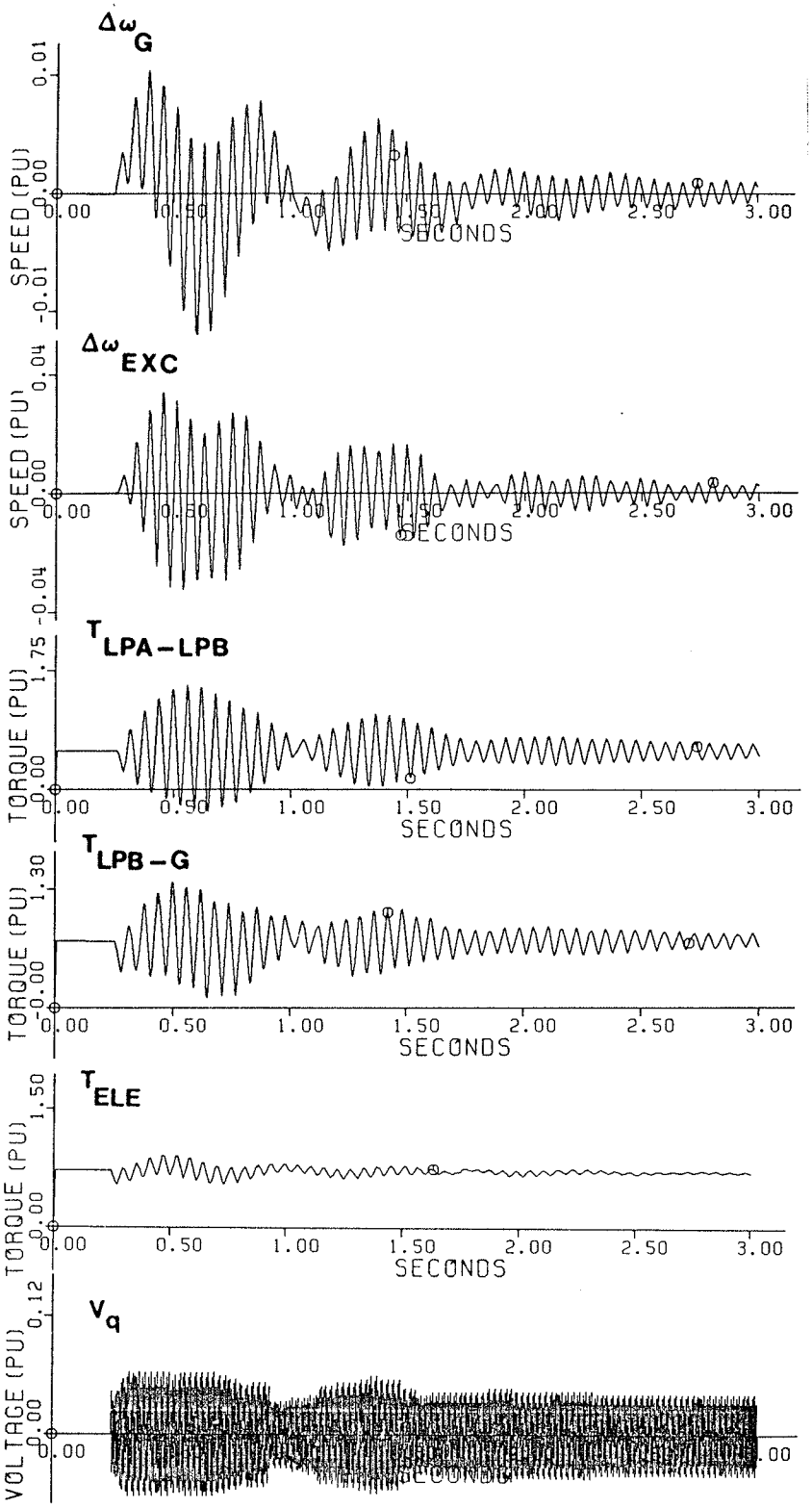

Figure 5.3: Damping mode one by injecting 6% system phase voltage using point-on-wave control method

in perunit, based on the peak magnitude of the system phase voltage. Fig.5.4 shows the system behaviour as a result of the same disturbance when the discrete step voltage injection method is used to suppress the oscillations. The quadrature phase voltage is injected in four discrete steps, each step 0.6% of the system phase voltage. For the results of the discrete step voltage injection, V_q is the rms magnitude of the injected voltage in perunit, based on the system rms phase voltage. Positive and negative values of V_q represent boosting and bucking voltage injection respectively.

As compared with Fig.5.3, Fig.5.4 indicates that with a smaller magnitude of the quadrature phase voltage, the discrete step method provides higher magnitude of positive damping for the torsional oscillations. The lower level of positive damping provided by the point-on-wave method is a result of the repetitive switchings of the thyristor valves at the peak of the injected quadrature phase voltage. The switching operation of the thyristor valves is equivalent to a series of disturbances in the system.

Fig.5.5 and Fig.5.6 show the damping effect of the discrete step voltage injection on the same disturbance, when the voltage is injected in 3 steps of 0.8%, and 2 steps of 1.2%, respectively. Comparison of Figs.5.4-6 indicates that the injection of the same magnitude of voltage in smaller steps is more effective for mitigating the torsional oscillations.

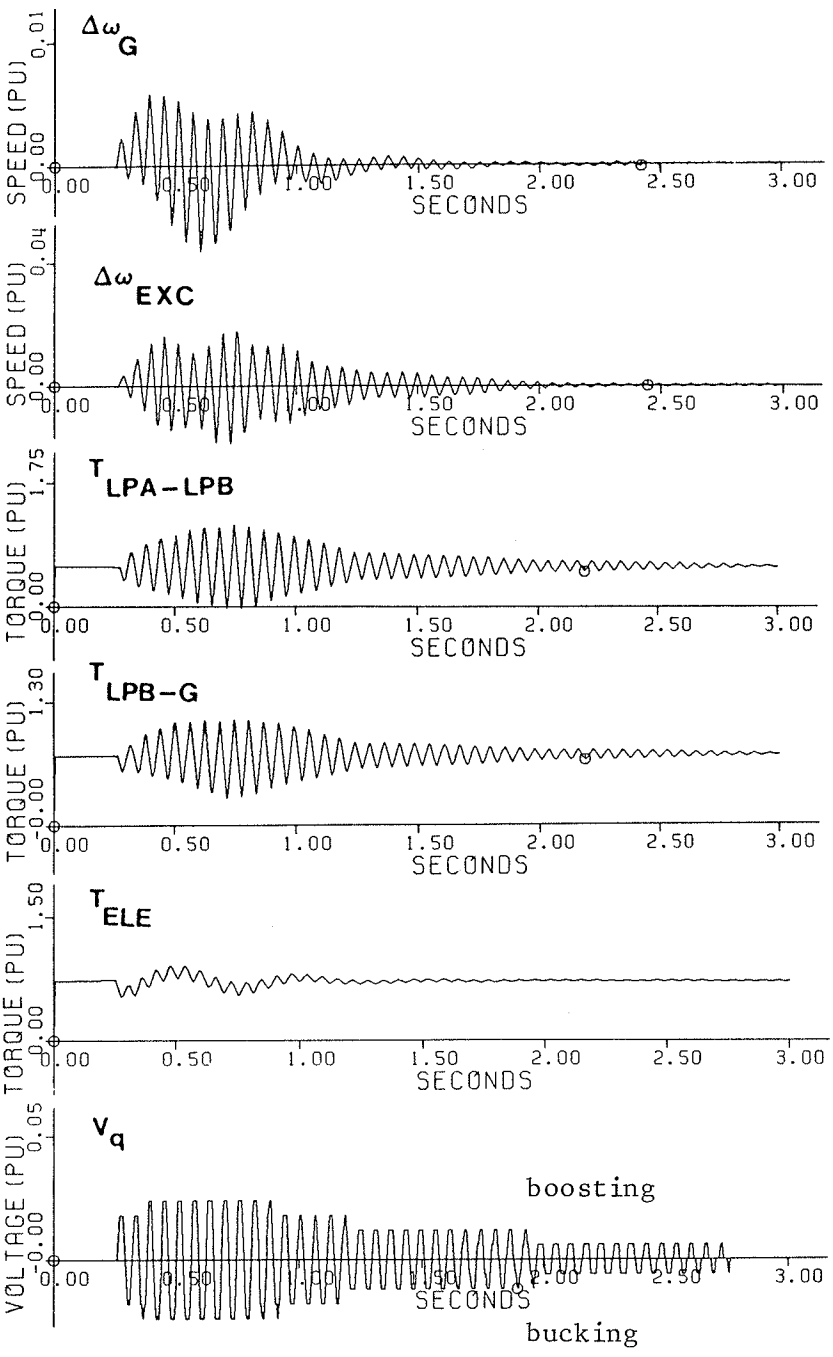

Figure 5.4: Damping mode one by injecting 2.4% system phase voltage in 4 discrete steps of 0.6%

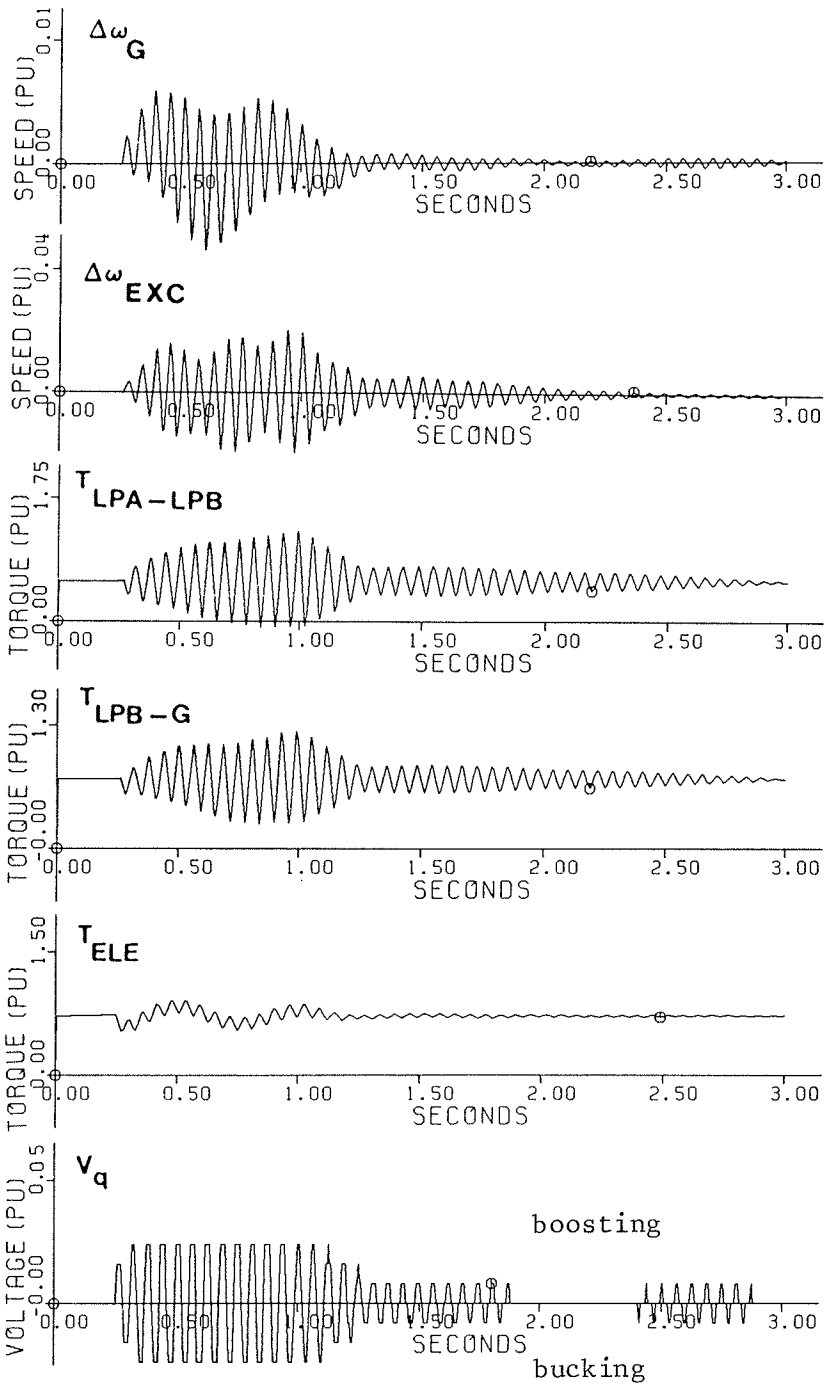

Figure 5.5: Damping mode one by injecting 2.4% system phase voltage in 3 discrete steps of 0.8%

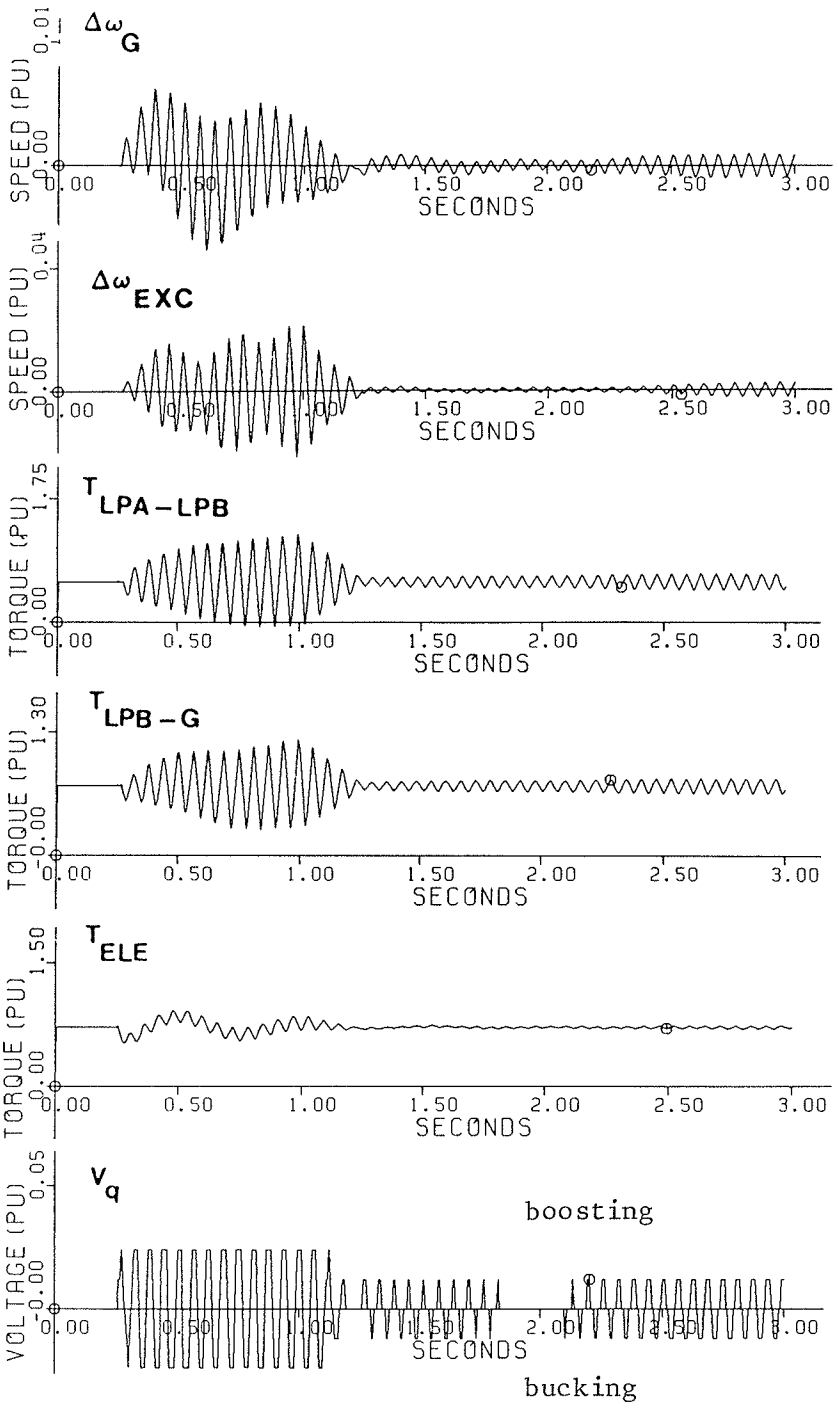

Figure 5.6: Damping mode one by injecting 2.4% system phase voltage in 2 discrete steps of 1.2%

As compared with Fig.5.3, Fig.5.4-6 show that the injection of 2.4% quadrature voltage in discrete steps is more effective in damping the first mode of oscillations of the first IEEE benchmark, than injection of 6% quadrature phase voltage by using the point-on-wave control method. The results of several computer runs at different operating points, and compensation levels in the range of 75-85%, indicate that injection of 2.4% voltage, in 0.6% steps can mitigate the first mode of oscillation of the IEEE benchmark.

5.6.2 Mode 3 of Torsional Oscillations

The shaft torsional oscillations at f=25.5 Hz is the third unstable mode of oscillations for the IEEE benchmark model. The mode three is stimulated at compensation levels around 50% of the line reactance. Fig.5.7 shows the shaft torsional behaviour when the compensation level is reduced from 60% to 50% at time t=0.25 s. The system is initially operat theing at 80% of the rated MVA at lagging power factor 0.90. Fig.5.7 shows that the shaft torques start to build up, as a result of the disturbance, but with a slower rate of growth as compared with the mode one.

Fig.5.8 shows the shaft torsional response to the same disturbance when the quadrature phase voltage is injected in the system, using the point-on-wave method. The magnitude of the injected quadrature phase voltage is 6% of the system phase voltage. Fig.5.9 shows the shaft response to

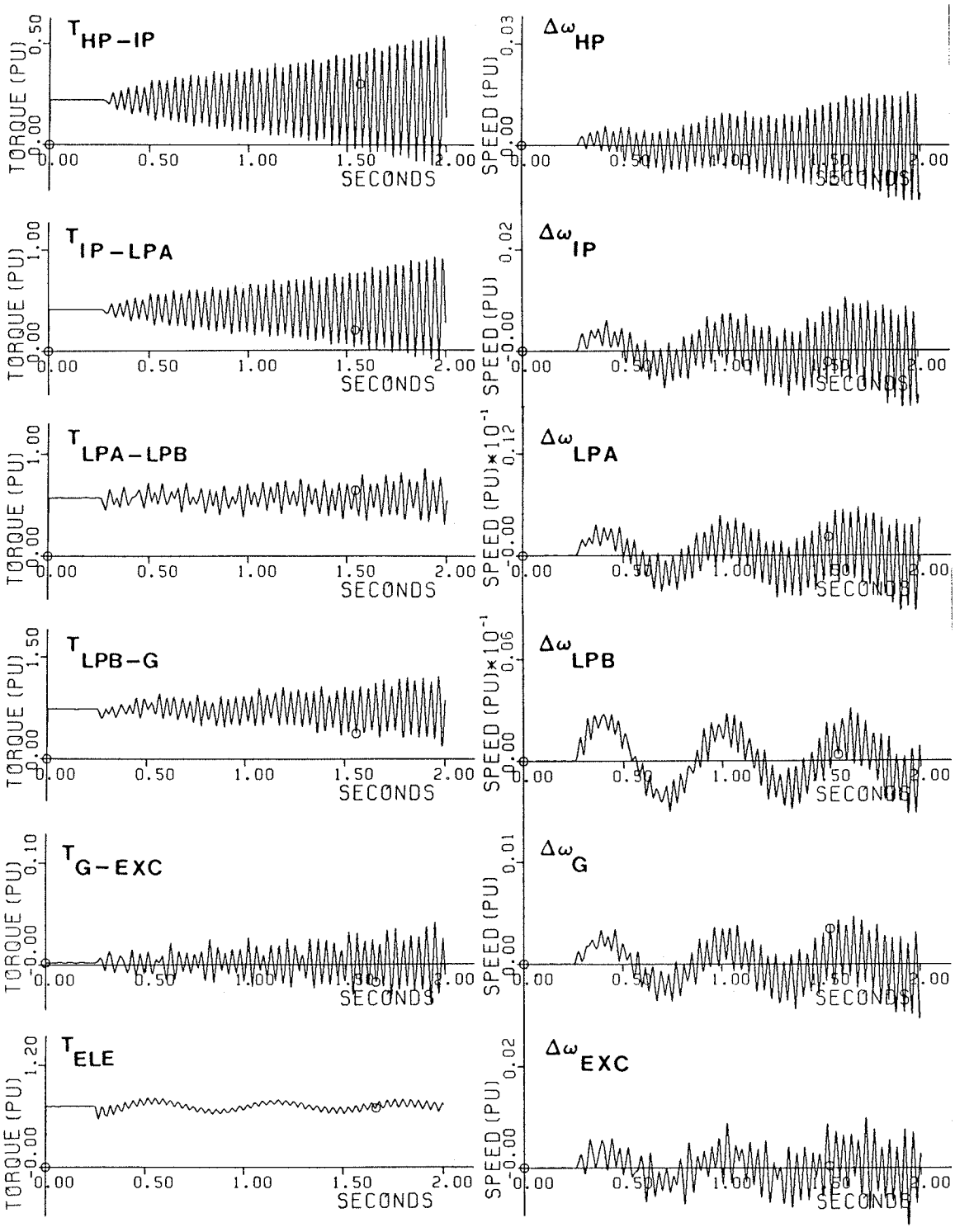

Figure 5.7: Shaft torsional oscillations at mode three, f=25.5 Hz, phase-shifter out of service

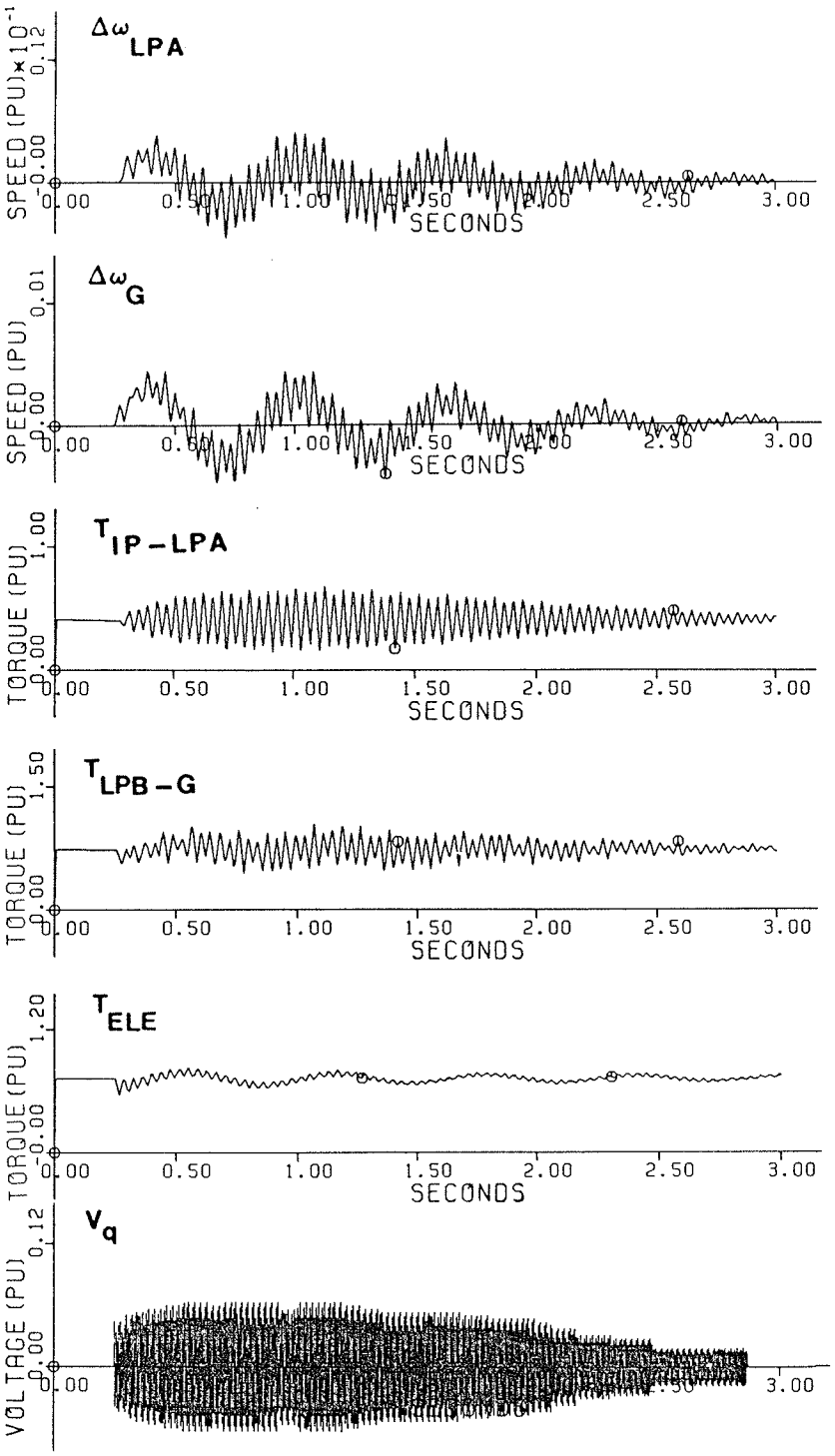

Figure 5.8: Damping mode three by injecting 6% system system phase voltage using point-on-wave control method

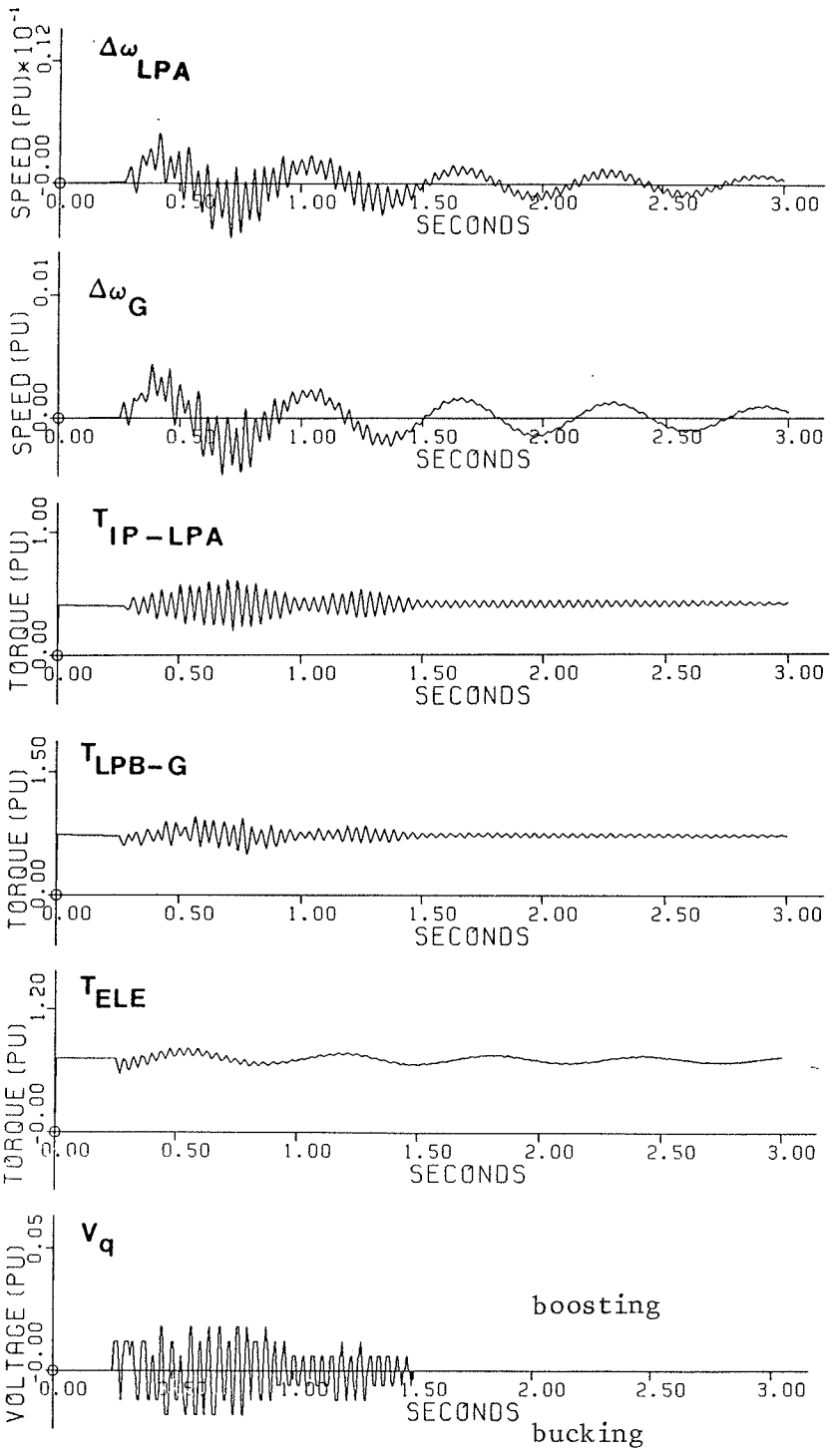

Figure 5.9: Damping mode three by injecting 1.8% system phase voltage in 3 discrete steps of 0.6%

the same disturbance when 2.4% quadrature phase voltage, in equal steps of 0.6% is injected in the system. As compared to Fig.5.8, Fig.5.9 shows that the discrete step voltage injection method provides the required damping with a smaller magnitude of the injected voltage (1.8%). The simulation results at different operating points and compensation levels in the range of 45-55%, reveal that the injection of 2.4% quadrature phase voltage in 4 steps of 0.6% can effectively damp the third mode of torsional oscillations of the IEEE benchmark.

5.6.3 Mode 4 of Torsional Oscillations

The mode four of the torsional oscillations of the IEEE benchmark (f=32.3 Hz) is stimulated at a series compensation level around 30% of the line reactance. Fig.5.10 illustrates the shaft response of the turbine-generator unit to a sudden drop in the compensation level from 40% to 30%, at time t=0.25 s. Initially, the generator delivers 80% of the rated MVA at the lagging power factor 0.90. Fig.5.11 shows the damping effect of the point-on-wave controlled quadrature phase voltage injection on the shaft oscillations for the same disturbance. The magnitude of the injected quadrature phase voltage during the boosting and bucking modes of operation is 6% of the system phase voltage. Fig.5.12 shows the shaft response to the same disturbance, when 1.2% of the system phase voltage is injected in two steps of %6.

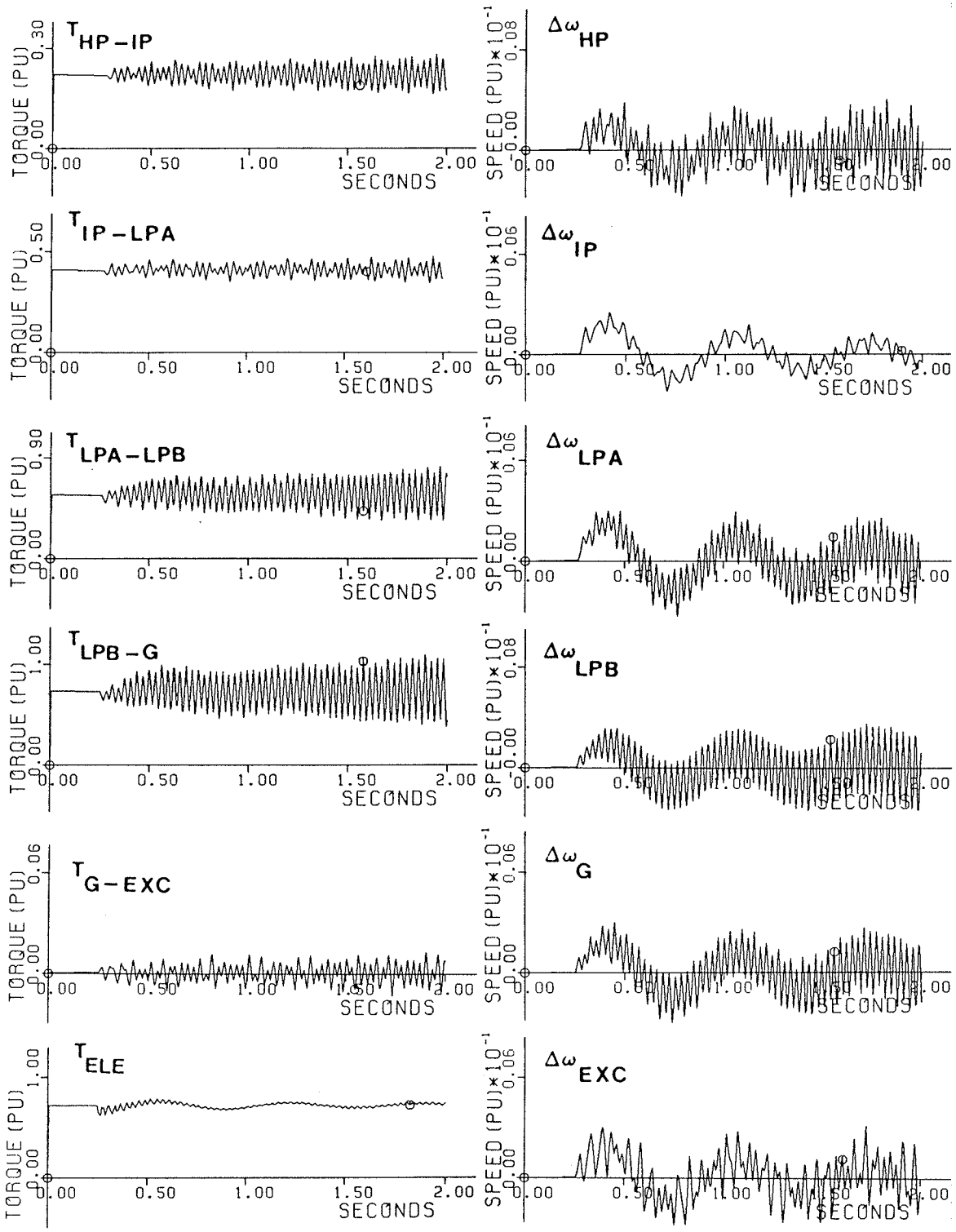

Figure 5.10: Shaft torsional oscillations at mode four, f=32.3 Hz, phase-shifter out of service

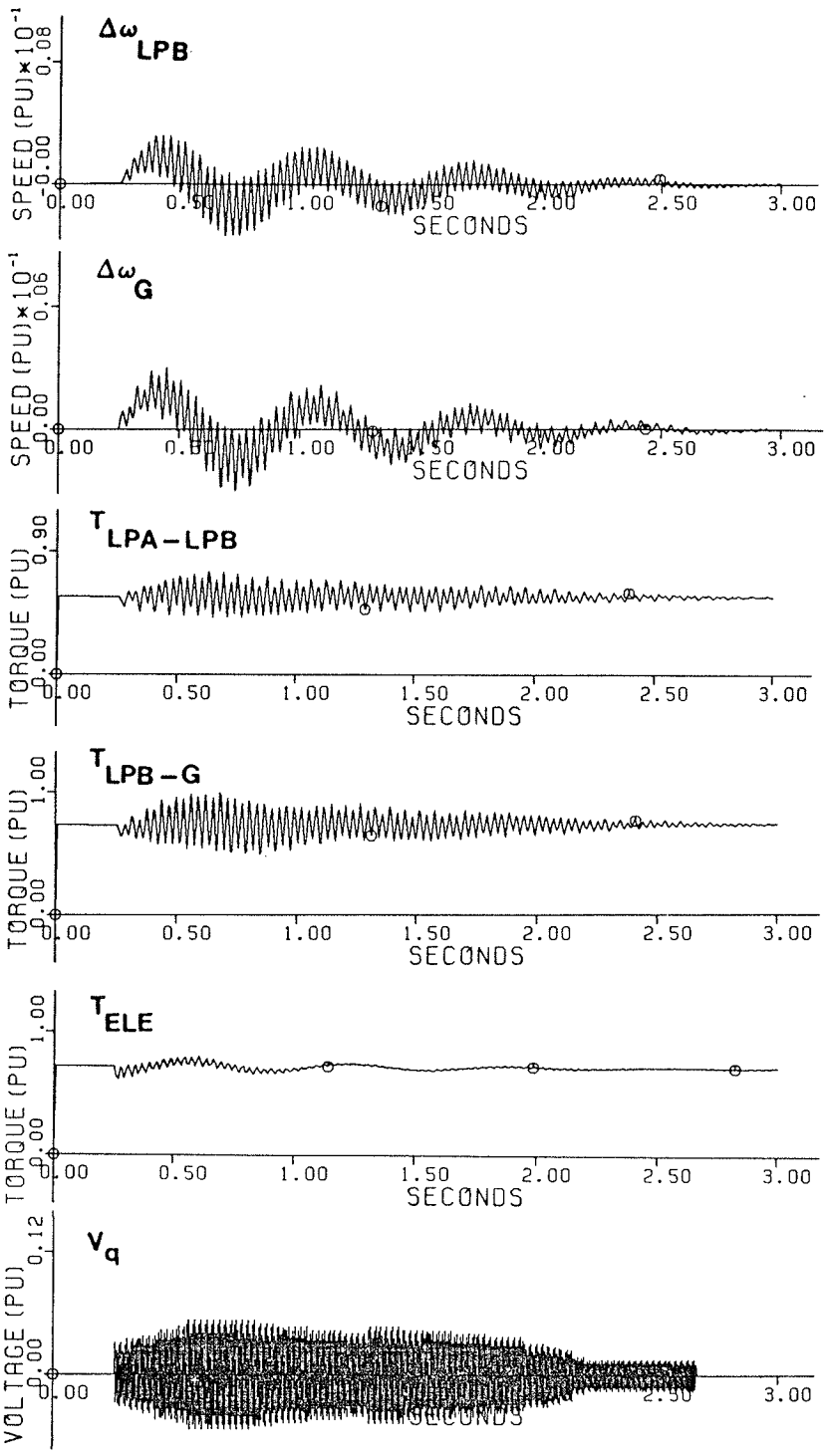

Figure 5.11: Damping mode four by injecting 6% system phase voltage using point-on-wave control method

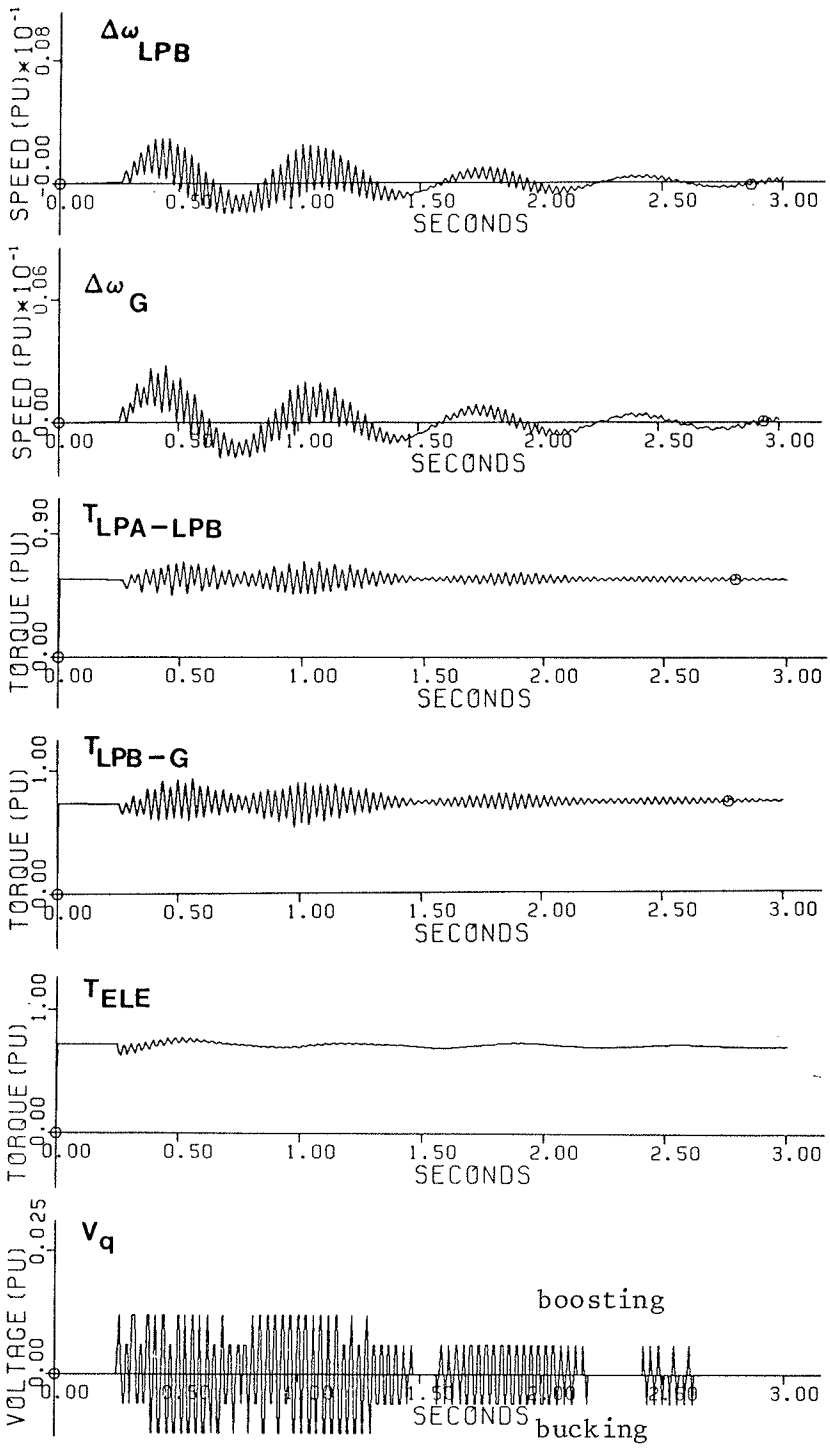

Figure 5.12: Damping mode four by injecting 1.2% system phase voltage in 2 discrete steps of 0.6%

The simulation studies were repeated at different operating points and series compensation levels in the range of 25-35%. The results show that injection of 1.8%, of the system voltage, in three steps of 0.6% can damp the mode four of the torsional oscillations of the IEEE benchmark.

5.7 CONCLUSIONS

A detailed digital time simulation study was conducted on the first IEEE benchmark model, in order to demonstrate the feasibility of the static phase-shifters for damping the torsional oscillations of the benchmark turbine-generator. The simulation results indicate that injection of 2.4% of the system phase voltage, in four steps of 0.6%, can suppress the unstable torsional modes of the IEEE benchmark modell. The same damping effect can be obtained by using the point-on-wave control method, but the magnitude of the injected voltage should be increased to 6% of the system phase voltage.

Chapter VI

DAMPING TRANSIENT SHAFT TORQUES USING A STATIC PHASE-SHIFTER

6.1 INTRODUCTION

In this chapter the shaft torsional stresses of turbine-generator, as a result of large disturbances in power system, are discussed. The effect of a three-phase fault, fault clearing, and its successive automatic fast reclosure (successful and unsuccessful) on the mechanical shaft torques are explained. The technical feasibility of a dynamically controlled static phase-shifter for damping the transient torques of large turbine-generator units is examined.

The system studied consists of two parallel transmission lines connecting the first IEEE SSO benchmark turbine-generator to an infinite bus. The BPA's EMTP is used for the digital time simulation studies of the shaft transient torque phenomenon.

The results obtained from the digital computer studies indicate that by use of a static phase-shifter, substantial positive damping for the shaft transient torques is obtained, which reduces the risk of shaft damage as a result of fatigue process.

6.2 BACKGROUND

As a result of switchings in a power system, the shaft sections of turbine-generators are subjected to transient torsional torques, caused by unidirectional and pulsating forces. These incidents may result in severe shaft fatigue or even catastrophic shaft failure. During the last decade, the effect of severe stresses on the turbine-generator shafts has received considerable attention [101,102] and several different aspects of the problem have been studied in considerable detail.

For many years the design criteria required that only the stator winding of turbine-generators had to withstand the stresses due to terminal three-phase short circuits. However, the results of extensive studies reveal that the shaft sections are affected more than the stator winding, as a result of being exposed to oscillatory torques due to some switching operations [103]. Severe electrical disturbances which may result in the loss of life of the turbine-generator shaft systems, in order of importance are the:

1. transient subsynchronous oscillations [104],
2. out-of-phase synchronization [105,106],
3. automatic triple-pole fast reclosing [103,107], and
4. three-phase short circuit and its subsequent fault clearing [108].

As a result of large disturbances in series capacitor compensated networks, due to the sustained feedback from the electrical system which maintaines the shaft torsional oscillations; the oscillatory stresses are amplified and may result even in catastrophic shaft failure. As compared with other electrical disturbances, the subsynchronous oscillations result in higher peak torsional torques and without proper countermeasure(s) can grow far above the shaft endurance limit. The principle approach to counteract the subsynchronous transient torques is to bypass the series capacitor and prevent the electrical system from contributing in torsional oscillations [40].

Due to the net positive damping of the electromechanical system, the turbine-generator shaft transient stresses with the exception of subsynchronous transient torques are decaying phenomena. The time required for the peak torsional torques to decay to the half of their peak values, is between 4 to 12 seconds, which depends upon the parameters of the system, operating point, the instant at which the incident occurs and the type of incident [108]. However as a result of the low magnitude of the system damping, with each disturbance the shaft system is exposed to a large number of alternating mechanical peak torques. Although mechanical stresses are usually lower than the shaft endurance limit, they can not be treated as isolated incidents, but the accumulative effect of all the stresses on the fatigue process

of the shaft system, determines the loss of life of the unit under consideration. Therefore, it is necessary to limit the magnitudes of the peak torques and reduce the number of the cycles during which the shaft system may encounter torsional stresses.

6.3 SHAFT MECHANICAL TORQUES DUE TO ELECTRICAL DISTURBANCES

Due to an electrical disturbance in a power system three components of electrical torques may be generated, which are: unidirectional torques, system frequency torques and double frequency torques. When the shaft system of a turbine-generator is torsionally excited, the shaft sections are subjected to pulsating torques with different amplitudes and shapes. The torsional response of each shaft section to an exciting torque is different, which results in different mechanical stress levels corresponding to different excitation torques. The investigation results indicate that the sensitivity of a turbine-generator shaft is highest for the unidirectional torques, then the system frequency torques, and finally the double frequency torques [108].

The high sensitivity of the shaft sections to the unidirectional torques is the reason for the high stress levels in the shaft sections, due to the symmetrical electrical disturbances. Those electrical disturbances which result in double frequency electrical torque components, do not con-

stitute a major danger regarding the shaft fatigue process [109]. However, the double frequency electrical torque may result in fractures in the turbine blades, as the consequence of resonance between the supersynchronous mechanical natural frequencies and the double frequency electrical torque component [9].

The peak magnitude of the mechanical shaft torques as a result of a fault and its subsequent fault clearing depends upon the following factors:

1. type of the fault,
2. location and impedance of the fault,
3. the system parameters,
4. the system configuration,
5. the system prefault operating point,
6. the fault clearing and reclosing time intervals, and
7. the short circuit capability of the system.

The most severe fault for a generator is a close-in three-phase fault at the generator high voltage bus. As a result of such a short circuit, the voltage drops to zero and the generator is not able to deliver power to the network. During the fault interval, the dc and system frequency currents excite the shaft mechanical torques. Depending upon the system transient stability criteria, the time elapsed before the fault removal, is in the order of 3-10 cycles (60 Hz system). During the short circuit interval, the generator

rotor accelerates, thus, the rotor phase angle increases relative to that of the network. The increase in the rotor phase angle depends upon the mechanical input power which is determined by the prefault operating point, and the time elapsed before the fault is cleared. In order to maintain the system stability and avoid high torsional torques, the clearing time of the three-phase faults should be less than 90 ms [108].

If the generator is connected to the network by a multi-line transmission system, with the fault on one of the lines, at the instant of short circuit clearing, the return of the voltage at increased load angle is equivalent to a malsynchronization, which is followed by severe mechanical stresses. In the case of a single tied generator, the fault clearance does not result in additional shaft stresses, but the generator rotor angle increases by the time that the generator terminals are open.

In the systems which are equipped with automatic fast reclosing switches, the reclosure of the faulty line has the most significant effect on the transient shaft torques. The reclosure interval is selected based on the system transient stability criteria, and for 60 Hz systems is in the range of 15-40 cycles [107]. A triple-pole unsuccessful reclosure of a multi-line system, subjects the turbine-generator shaft system to the three-phase short circuit stresses, which are followed by additional fault clearing torsional torques. De-

pending upon the time intervals between the first fault clearance, reclosure, and the second fault clearance, the peak magnitude of the mechanical stresses can increase above the permissible values. Under favourable timing conditions, the shaft torques due to different incidents counteract each other and the resultant component may have a small magnitude. A triple-pole successful reclosure corresponds to a sudden applied load which is equivalent to a sudden electrical torque. Depending upon the switching time intervals, the peak mechanical stresses vary in a wide range.

A successful triple-pole reclosure of a single tied generator is equivalent to an out-of-phase synchronization with a high magnitude of phase difference between the generator rotor and the network, which causes severe shaft stresses. In the case of a single tied generator, the load angle increases after the fault occurance, during the fault clearing and reclosing time intervals, therefore, the peak mechanical torques are expected to be higher than those of a multi-line system. However under favourable switching sequence, the shaft stresses can be limited to smaller values. Furthermore, reclosure time interval has a deterministic effect on the stability of a single tied generator.

From the foregoing discussion one can conclude that the proper timing of the switching operations can prevent the occurance of high mechanical stresses and reduce the fatigue process in the turbine-generator shaft sections. However, due to the variation of the parameters of turbine-generators

in a system and the tolerance of the circuit brakers, precise timing of brakers is not considered as a practical method to reduce the transient shaft torques to a desired level. Therefore, countermeasures should be implemented to prevent the shaft loss of life, due to severe disturbnaces.

A thyristor-controlled phase-shifter, based on the the same control principle as described in Chapter IV, can be implemented to mitigate the shaft mechanical stresses during power system disturbances. To verify the effectiveness of a static phase-shifter for damping shaft stresses, due to three-phase faults, fault clearing and automatic reclosure, a digital time simulation study is carried out, as explained in the following sections.

6.4 DESCRIPTION OF SYSTEM STUDIED

The power system considered for this study consists of a multi-mass turbine-generator unit, connected to an infinite bus through two parallel transmission lines, Fig.6.1. The turbine-generator and the step-up transformer are those of the first IEEE benchmark model as explained in Chapter 3, Section 3.2. Torsional damping effect of the point-on-wave controlled phase-shifter, (Fig.4.1), and the discrete step controlled phase-shifter, (Fig.4.2), for different electrical disturbances are compared. When the quadrature phase voltage is injected based on the point-on-wave control method, the magnitude of the injected voltage is 16% of the sys-

tem phase voltage. In the case of the discrete step control method, the voltage is injected in four discrete steps of 1.75% of the system phase voltage. The data for the boosting and the excitation transformers is given in Appendix B. The transmission lines are presented with lumped, series R-L parameters, Fig.6.1. Point A on the transmission system indicates the location of a three-phase fault with the impedance 0.01 perunit.

For the transient torque studies, the magnetic saturation of the generator and the transformers are included in the digital computer model of the system. The opening action of the brakers are represented by opening at the zero crossing of the line currents. The generator field voltage is assumed to be constant, corresponding to the rated terminal voltage. The applied mechanical power to turbines are assumed to be constant at their steady-state operating point values. The effect of the mechanical damping of the rotating masses are neglected.

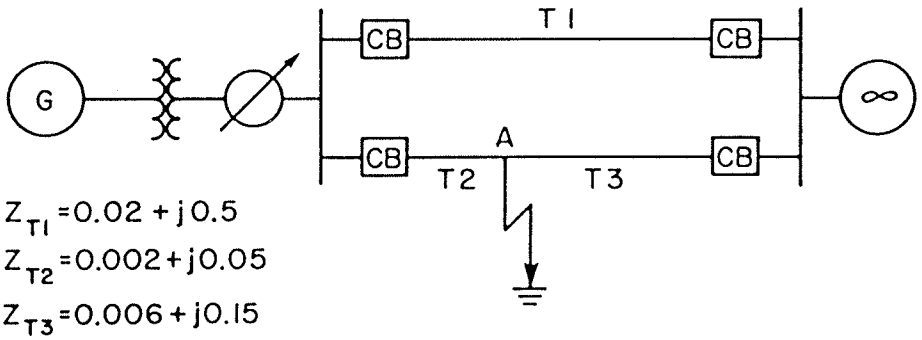

Figure 6.1: Single line diagram of the system for transient studies

6.5 DIGITAL TIME SIMULATION RESULTS

6.5.1 Double Line Configuration, Successful Reclosure

In Section 6.5, a three-phase fault, a three-phase fault clearing, and a triple-pole automatic reclosure, are referred as: a fault, a fault clearing, and a reclosure, respectively.

6.5.1.1 Case 1

Initially, the machine is delivering the rated MVA at 0.90 lagging power factor, through the two parallel lines, Fig.6.1. At time t=0.10 s, the system is subjected to a fault at point A, followed by a three cycle clearing of the faulty line. Fig.6.2 depicts the system response to the disturbance. The following system variables are plotted:

1. $T_{LPA-LPB}$ the torque transmitted from LPA to LPB,
2. T_{LPB-G} the torque transmitted from LPB to the generator rotor,
3. T_{ELE} the air-gap torque,
4. P the power delivered to the transmission system, and
5. V_q the injected quadrature phase voltage.

Fig.6.2 shows that as a result of the fault and its subsequent line tripping, different torsional modes are excited.

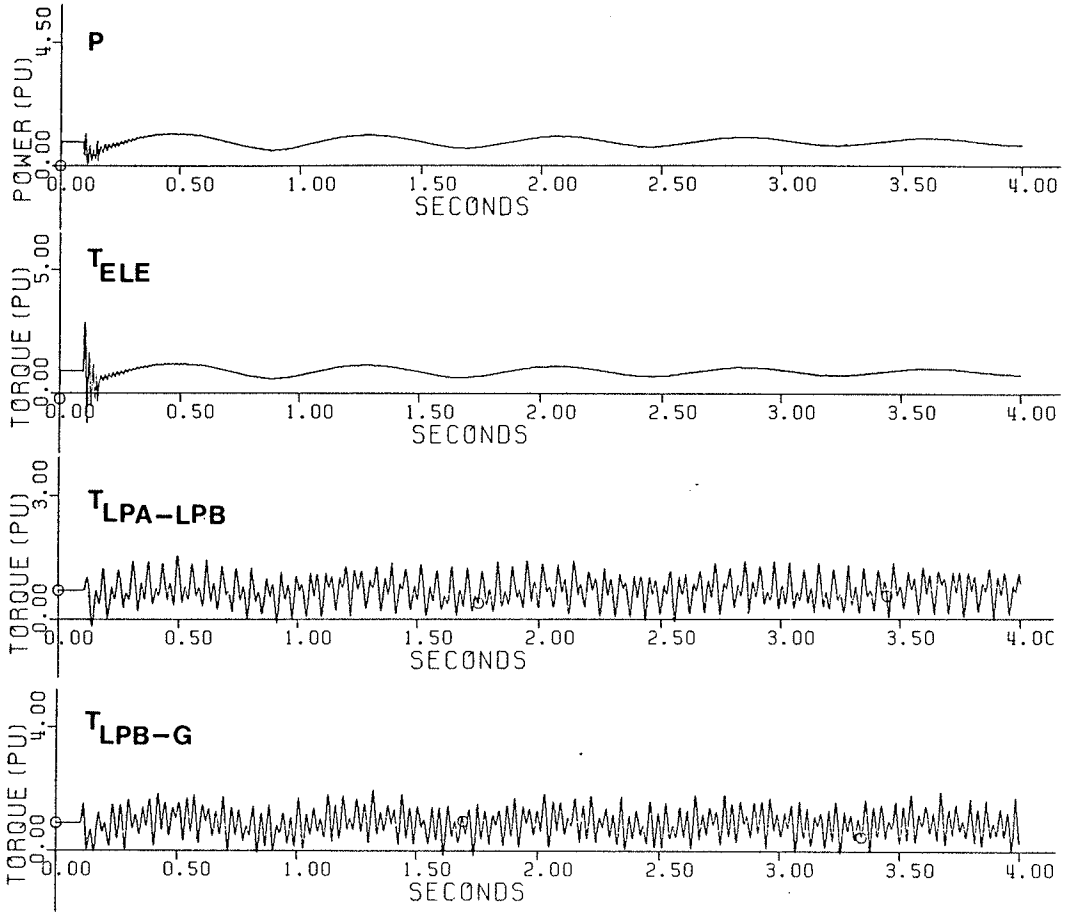

Figure 6.2: System transient response to a three-phase fault followed by three cycle fault clearing, phase-shifter out of service

Fig.6.3(a) shows the mechanical shaft stresses for the same disturbance , when the point-on-wave controlled phase-shifter is used to mitigate the excited torsional stresses. Fig.6.3(b) shows the system response when the shaft oscillations are counteracted by the discrete step quadrature phase voltage injection. As compared with Fig.6.3(a), Fig.6.3(b) shows that the injection of quadrature phase voltage, in discrete steps, is more effective in damping transient shaft torques than the point-on-wave control method.

6.5.1.2 Case 2

Fig.6.4 depicts the system variables when the fault and the line tripping is followed by an additional 15 cycle successful reclosing. As compared with Fig.6.2, Fig.6.4 reveals that as a result of the reclosing action, the peak mechanical stresses are considerably increased. Fig.6.5 shows the shaft torsional behaviour as a result of the: fault, fault clearing, and successful reclosing, with the sequence 3-15 cycles, when the point-on-wave and the discrete step voltage injection methods are used as the countermeasures. As compared with Fig.6.5(a), Fig.6.5(b) shows that the injection of a smaller voltage, in discrete steps, results in shorter life-time of the torsional torques, and the shaft system is subjected to less number of peak torques. Also, the maximum stress level is less in Fig.6.5(b), as compared with Fig.6.5(a).

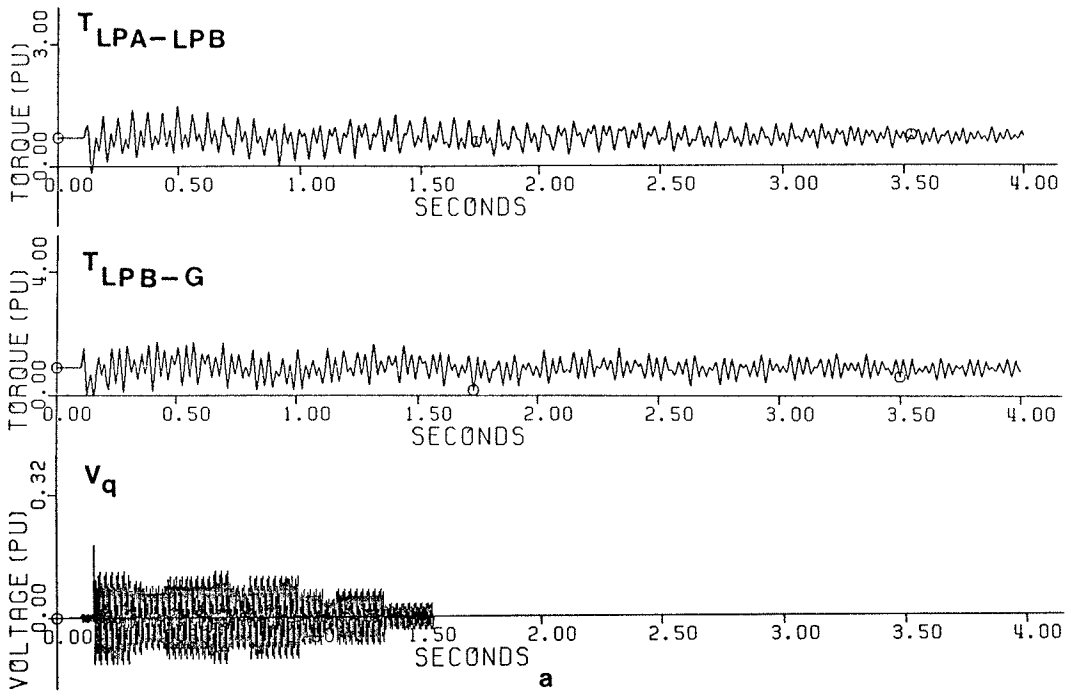

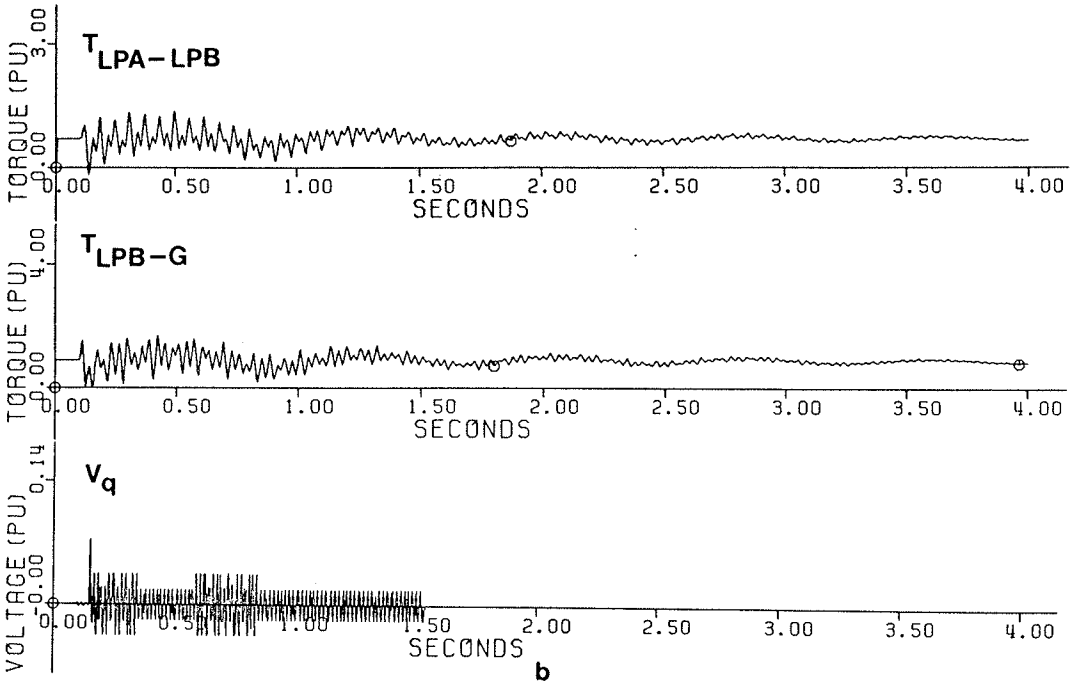

Figure 6.3: System transient response to a three-phase fault followed by three cycle fault clearing, phase-shifter in service
a - point-on-wave control method
b - discrete step control method

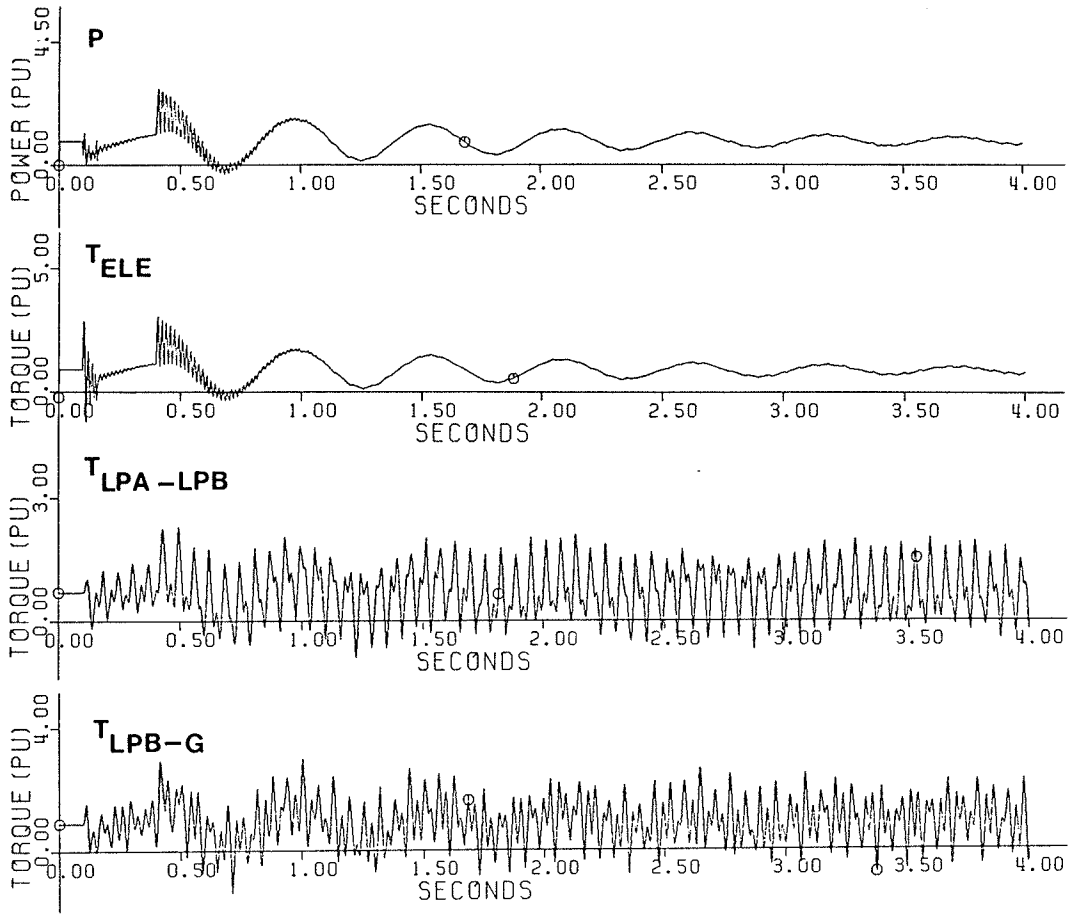

Figure 6.4: System transient response to a successful reclosure with the sequence 3-15 cycles, phase-shifter out of service

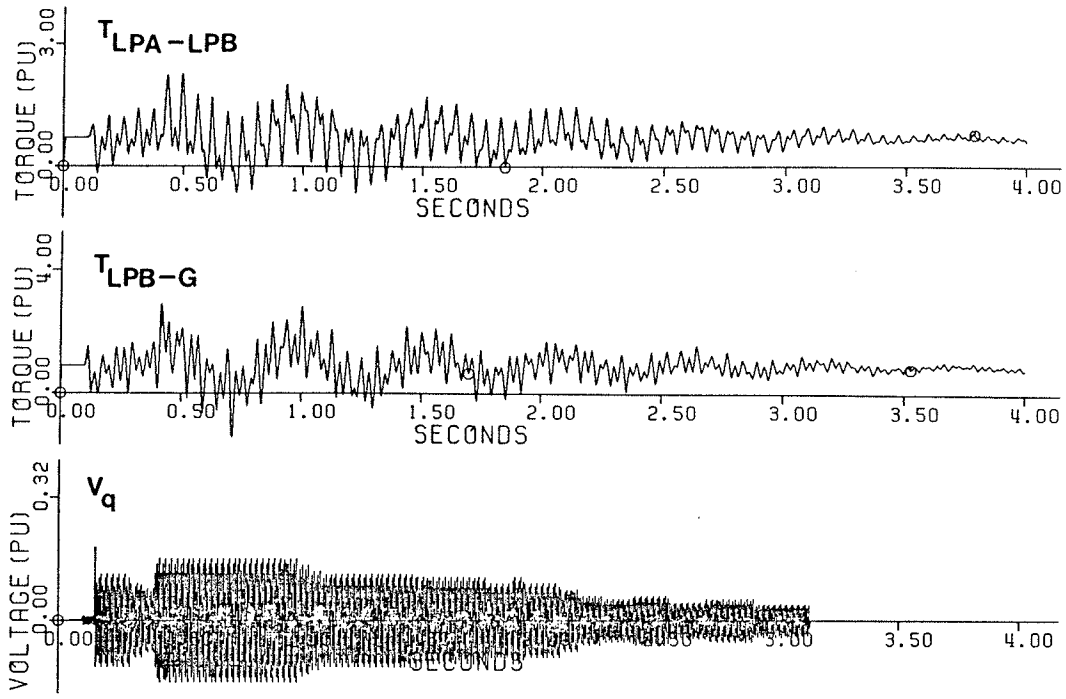

a

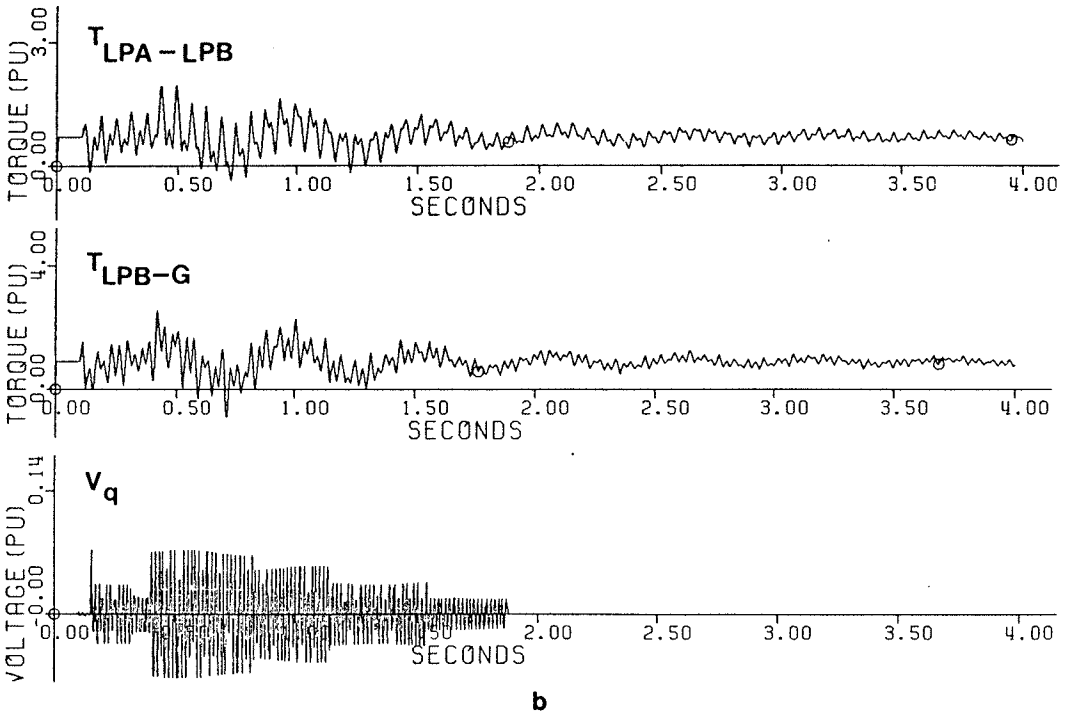

b

Figure 6.5: System transient response to a successful reclosure with the sequence 3-15 cycles, phase-shifter in service
a - point-on-wave control method
b - discrete step control method

6.5.1.3 Case 3

At each operating point the influence of the reclosing action on the shaft stresses depends upon the instant of reclosing. Fig.6.6 shows the system behaviour to a fault at t=0.10 s, followed by a fault clearing and a successful reclosing, with the sequence 3-30 cycles. As compared with Fig.6.4, Fig.6.6 indicates that the shaft torques are reduced to a lower level. This is due to the change in the reclosing sequence from 3-15 to 3-30 cycles. Fig.6.7 illustrate the damping effect of the static phase-shifters, on the torsional torques, due to the 3-30 cycles reclosing operation. As compared with Fig.6.5(b), Fig.6.7(b) indicates that when the voltage is injected in discrete steps, increasing the reclosure sequence from 3-15 to 3-30 cycles, results in a noticeable reduction in the maximum stress levels. This is due to the additional time given to the phase-shifter to damp the torques, as a result of the fault removal.

6.5.1.4 Case 4

It should be noted that increasing the reclosing interval does not necessarily result in lower shaft torsional torques. For example, as shown in Fig.6.8, increasing the reclosure sequence from 3-30 to 3-30.5 cycles results in higher shaft torsional torques. Fig.6.9 shows the damping effect of the point-on-wave and the discrete step quadrature

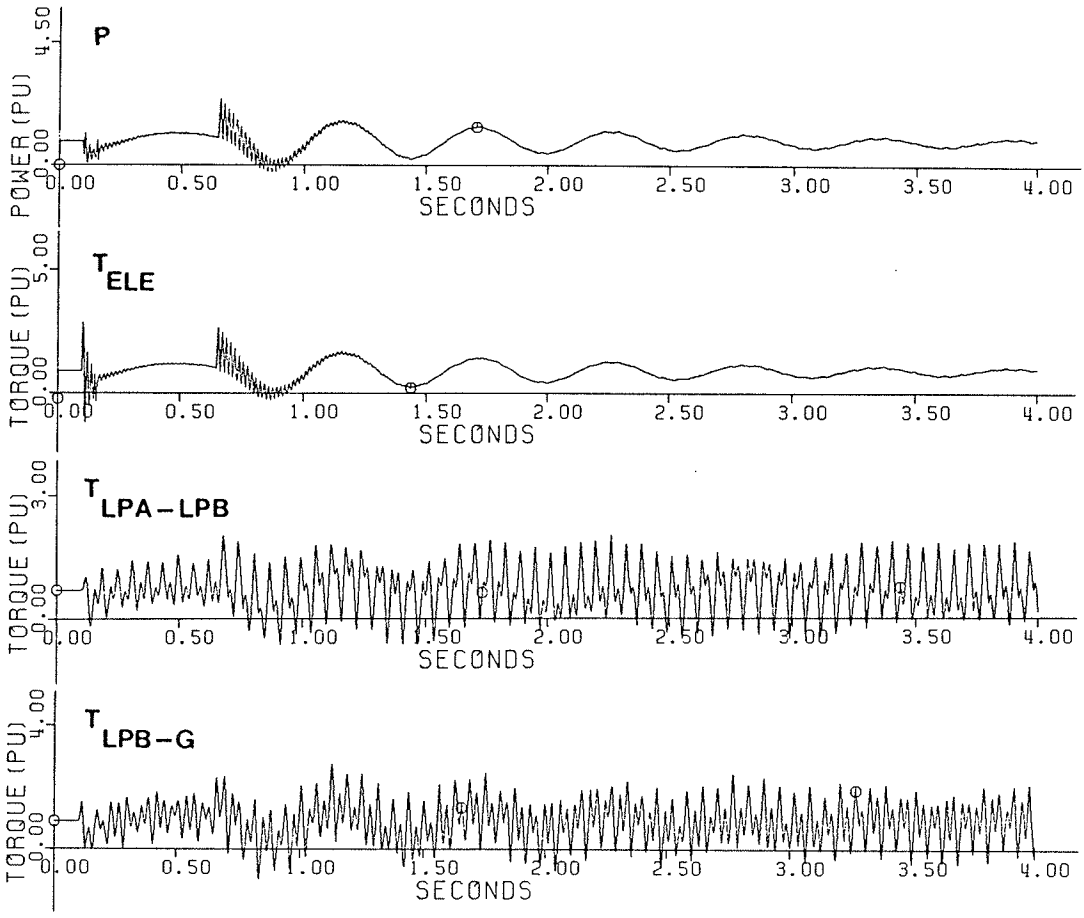

Figure 6.6: System transient response to a successful reclosure with the sequence 3-30 cycles, phase shifter out of service

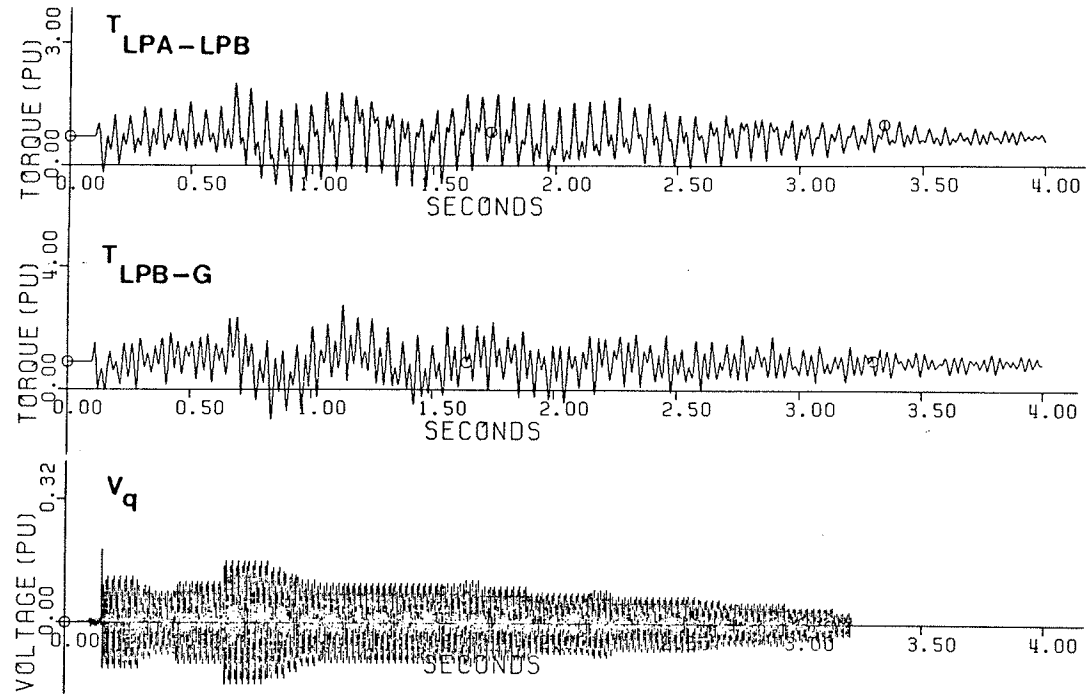

a

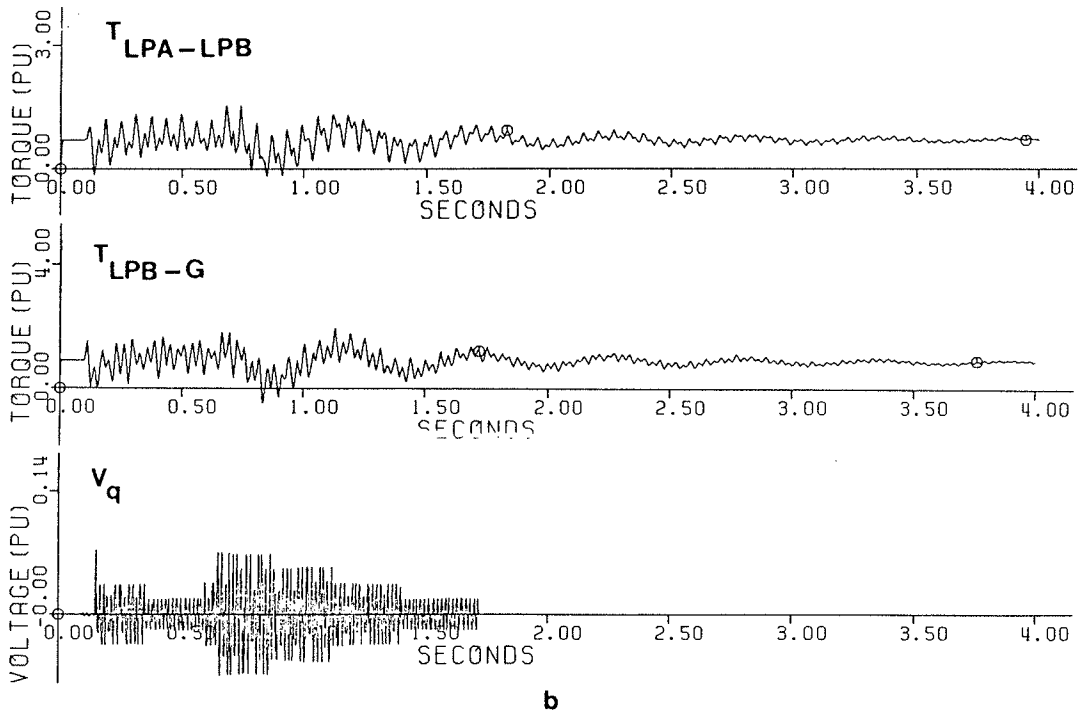

b

Figure 6.7: System transient response to a successful reclosure with the sequence 3-30 cycles, phase-shifter in service
a - point-on-wave control method
b - discrete step control method

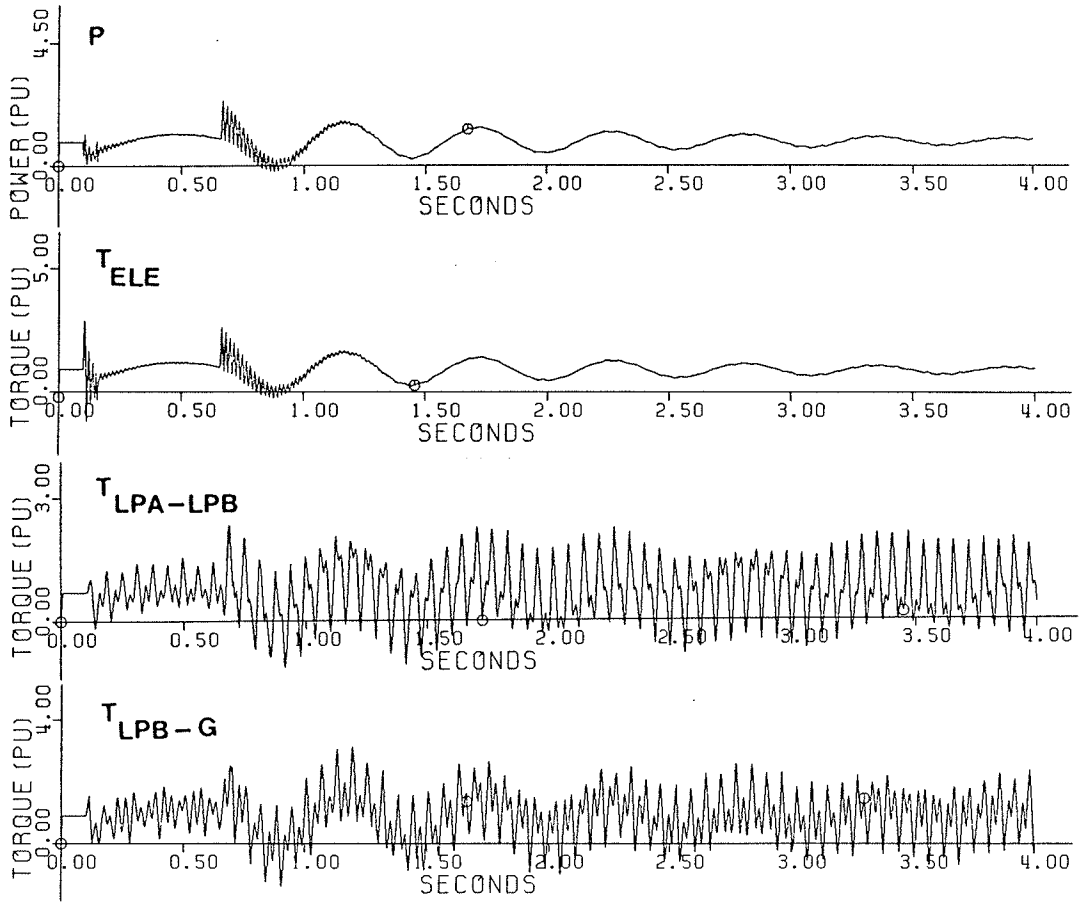

Figure 6.8: System transient response to a successful reclosure with the sequence 3-30.5 cycles, phase shifter out of service

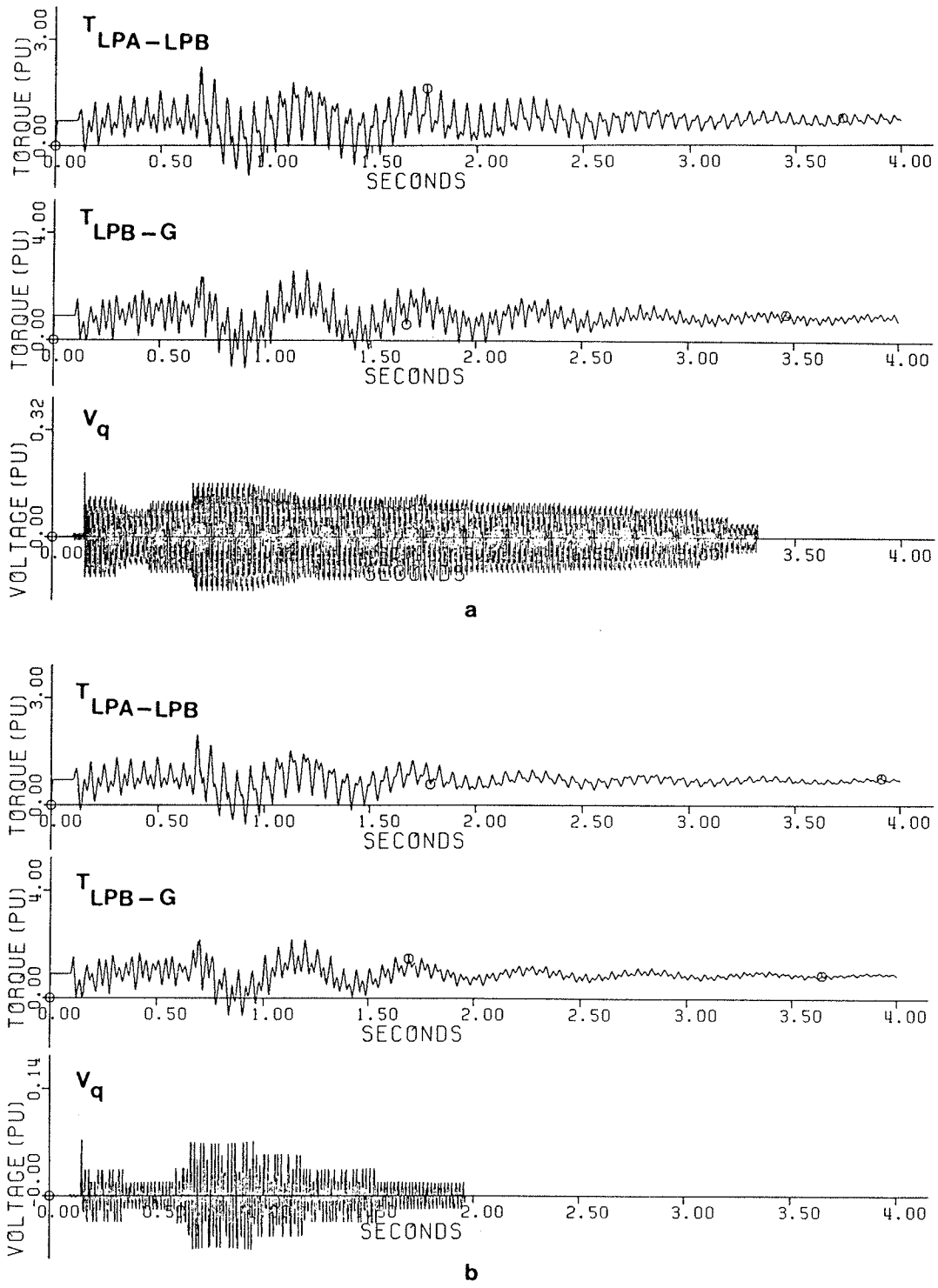

Figure 6.9: System transient response to a successful reclosure with the sequence 3-30.5 cycles, phase-shifter in service
a - point-on-wave control method
b - discrete step control method

phase voltage injection on the shaft oscillations, as a result of the 3-30.5 cycle reclosing operation.

6.5.2 Double Line Configuration, Unsuccessful Reclosure

The unsuccessful reclosure of a three-phase fault and its successive line tripping leads to severe shaft torsional stresses, and as a result considerable fatigue. From the generator terminal point of view, a three-phase unsuccessful reclosure is equivalent to a three-phase fault which is followed by a three-phase line tripping. At a constant operating point, the peak mechanical stresses due to an unsuccessful reclosure, depend upon the reclosing sequence.

6.5.2.1 Case 5

Fig.6.10 shows the response of the system of Fig.6.1 to a three-phase unsuccessful reclosing with the sequence 3-15-3 cycles. Initially, the generator is delivering the rated MVA at 0.90 lagging power factor, through the two parallel lines. At time t=0.10 s, a three-phase fault occurs at point A, which is followed by a three cycle fault clearance. After 15 additional cycles the line is reclosed. Due to the fault existance, after three more cycles the fault is cleared again. After the second fault clearance, the generator is permanently connected to the infinite bus through line T1.

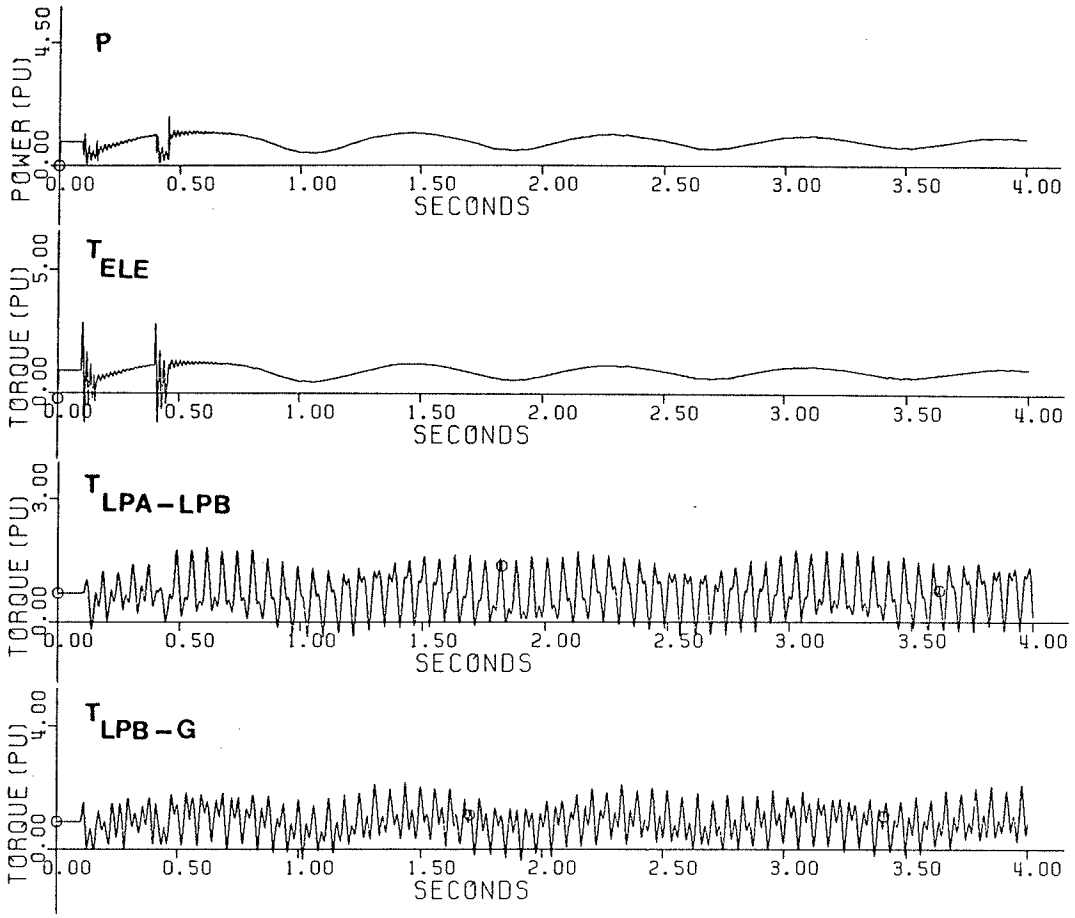

Figure 6.10: System transient response to an unsuccessful reclosure with the sequence 3-15-3 cycles, phase-shifter out of service

As compared with Fig.6.4, Fig.6.10 indicates that the peak mechanical torques, as a result of the 3-15-3 cycle unsuccessful reclosure, are less than those due to the 3-15 cycle successful reclosure. This is due to the fact that the unsuccessful reclosure is performed under a favourable timing sequence. Fig.6.11 shows the effect of the phase-shifters on the shaft oscillations, as a result of the 3-15-3 cycle unsuccessful reclosure. As compared with Fig.6.11(a), Fig.6.11(b) reveals that the discrete step voltage injection is more effective in damping the torsional stresses, due to the triple-pole unsuccessful reclosure.

6.5.2.2 Case 6

Fig.6.12 shows the system response to a 3-30.5-3 cycle unsuccessful reclosure. As compared with Fig.6.10, Fig.6.12 indicates higher stresses, which are the results of increasing the reclosure interval from 15 to 30.5 cycles. Fig.6.13 shows the shaft response to the 3-30.5-3 cycle unsuccessful reclosure, when the oscillations are counteracted by the point-on-wave and the discrete step voltage injection.

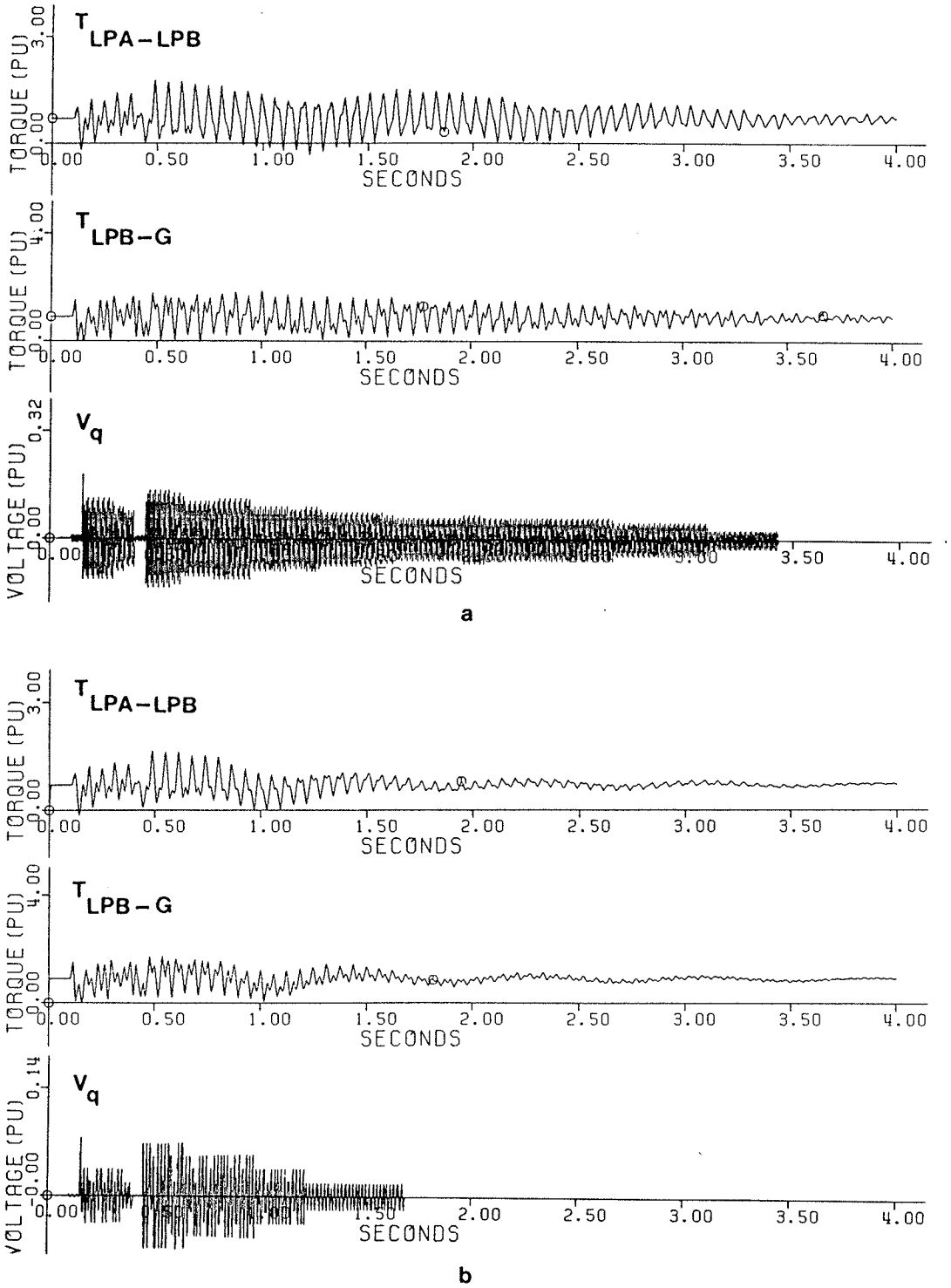

Figure 6.11: System transient response to an unsuccessful reclosure with the sequence 3-15-3 cycles, phase-shifter in service
a - point-on-wave control method
b - discrete step control method

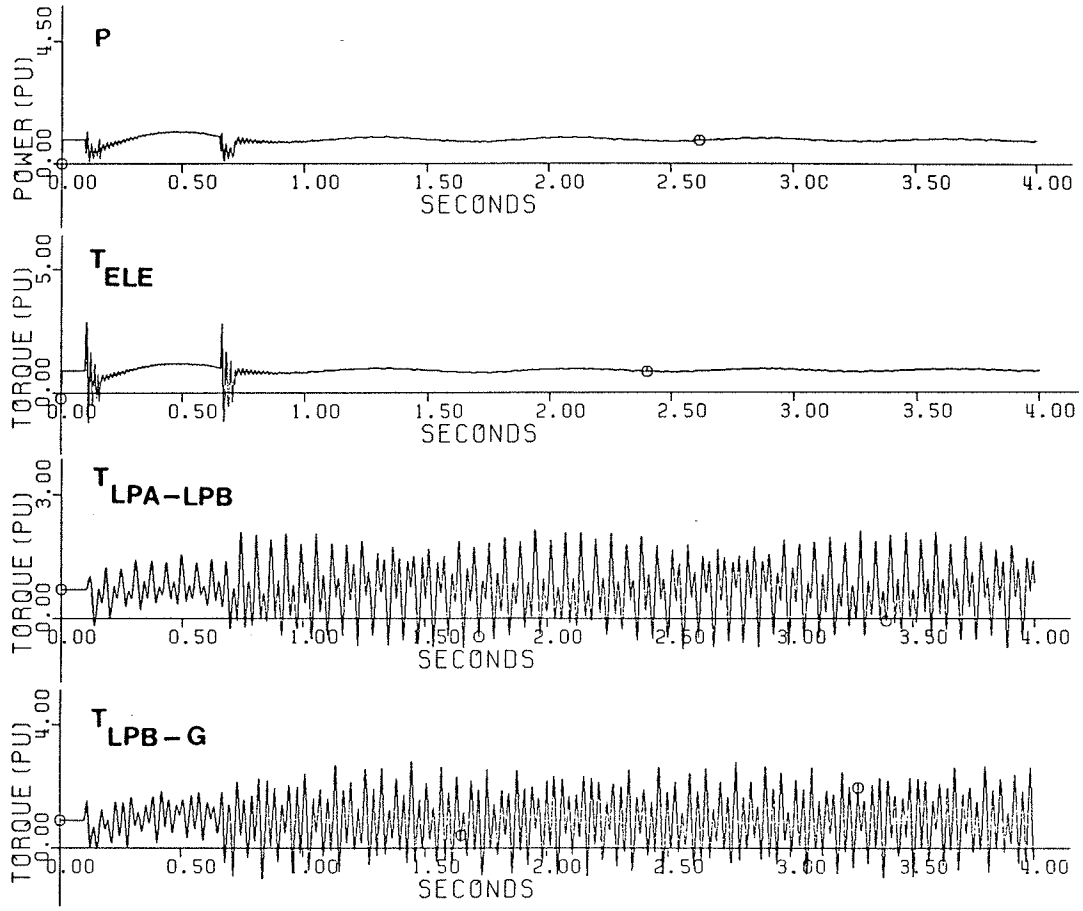

Figure 6.12: System transient response to an unsuccessful reclosure with the sequence 3-30.5-3 cycles, phase-shifter out of service

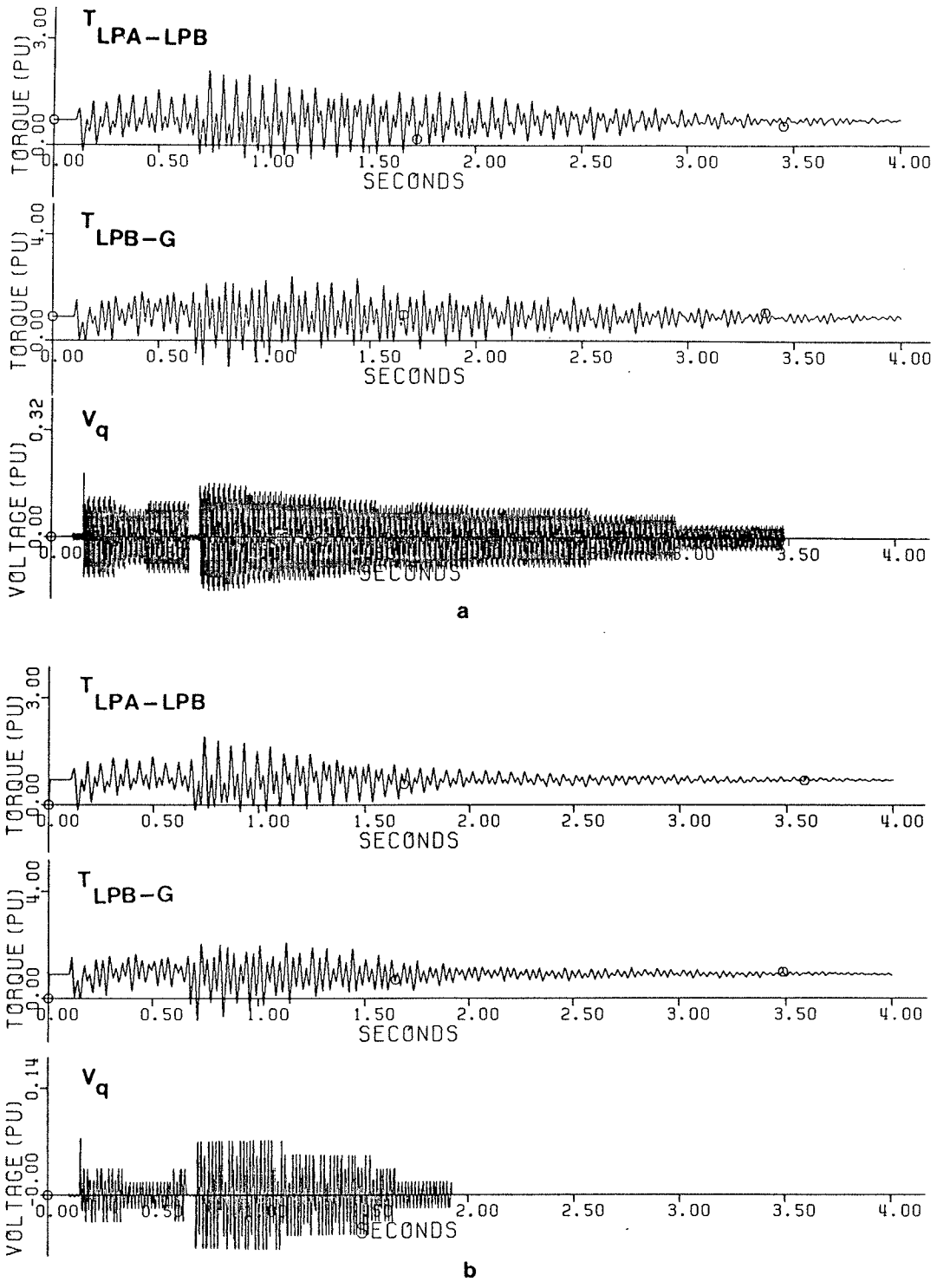

Figure 6.13: System transient response to an unsuccessful reclosure with the sequence 3-30.5-3 cycles, phase-shifter in service
a - point-on-wave control method
b - discrete step control method

6.5.3 Single Line Configuration

For a single tied turbine-generator, a three-phase fault and its subsequent fault clearing and reclosure, not only has a significant influence on the system stability, but also has a decisive impact upon the torsional stresses. When the generator is capable to deliver some amount of power during the disturbance interval, the unit acceleration is relatively less and the sudden torques at the instant of fault clearing and line reclosing are smaller. For a single tied generator a three-phase fault reduces the power transfer to a negligible value and the fault clearance reduces the power transfer to zero. This sequence of disturbances is equivalent to a complete load rejection.

During the time interval between the fault occurance and reclosure, the generator rotor accelerates and the pole axis advances ahead of the system voltage phasors. Consequently, reclosing action is equivalent to a malsynchronization, which results in severe torsional stresses. An unsuccessful reclosure results in further acceleration of the unit and the generator instability. A successful reclosure may also lead in the generator instability, depending upon the operating point prior to the fault occurance.

6.5.3.1 Case 7

Fig.6.14 shows the system response to a 3-15 cycle successful reclosure when line T1 is out of service. Initially, the generator is delivering 480 MVA at 0.90 lagging power factor, through the single line T2-T3. In spite of less power transfer, as compared with Fig.6.4 which depicts the shaft response for the same disturbance when the two parallel lines are in service, Fig.6.14 indicates higher peak torques. The amount of power transfer prior to the fault for Fig.6.14 is 432 MW and for Fig.6.4 is 803 MW.

Fig.6.15 shows the damping effect of the quadrature phase voltage injection on the shaft torques, due to a the 3-15 cycle successful reclosure, using the point-on-wave and the discrete step control methods, respectively. Fig.6.15 indicates that during the reclosing time interval (15 cycles), both methods of voltage injection have no damping effect on the shaft oscillations, therefore, the peak torques at the reclosing instant can not be effectively reduced. This is the result of the fact that after the fault removal, power transfer from the generator reduces to zero and the phase-shifter is not able to affect the amount of power transfer from the generator. As compared with Fig.6.15(a), Fig.6.15(b) shows that after the successful reclosing, the discrete step voltage injection is more effective in damping the shaft stresses.

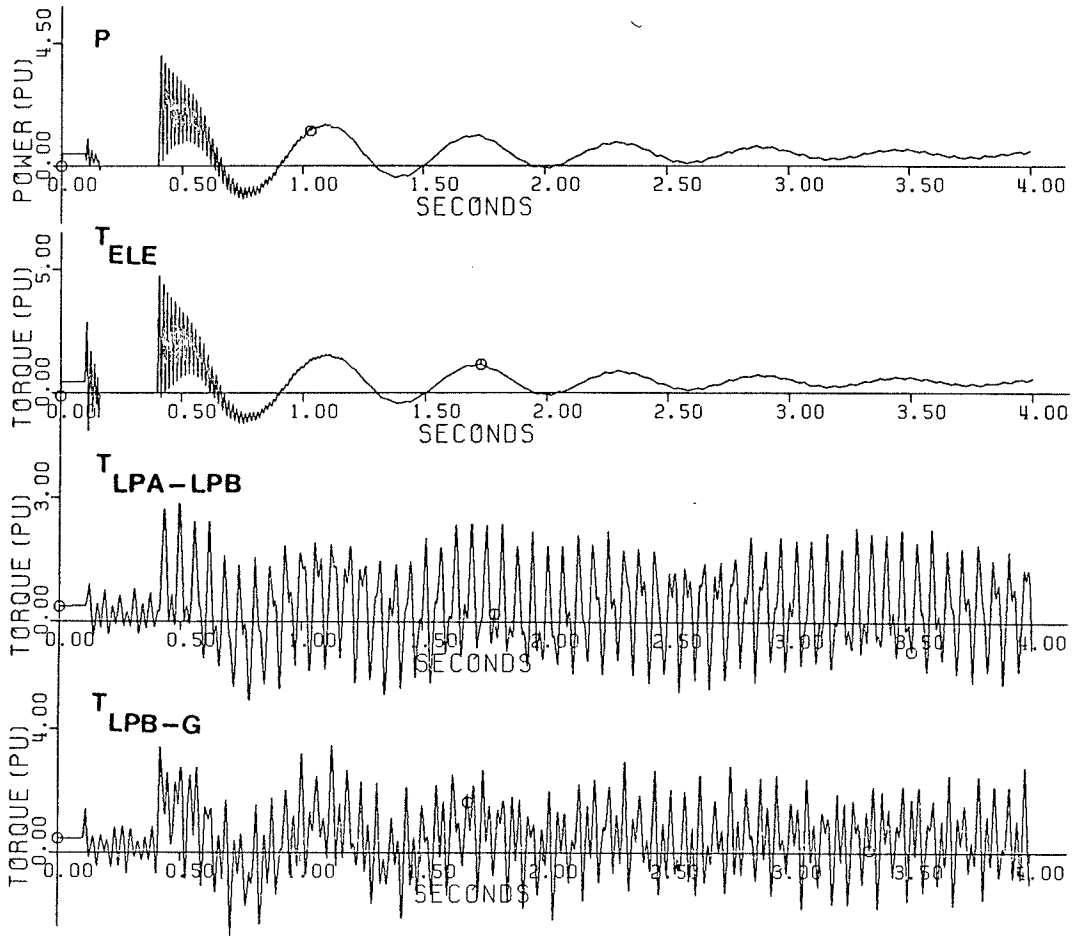

Figure 6.14: System transient response to a successful reclosure with the sequence 3-15 cycles, phase-shifter out of service, MVA=480, pf=0.90

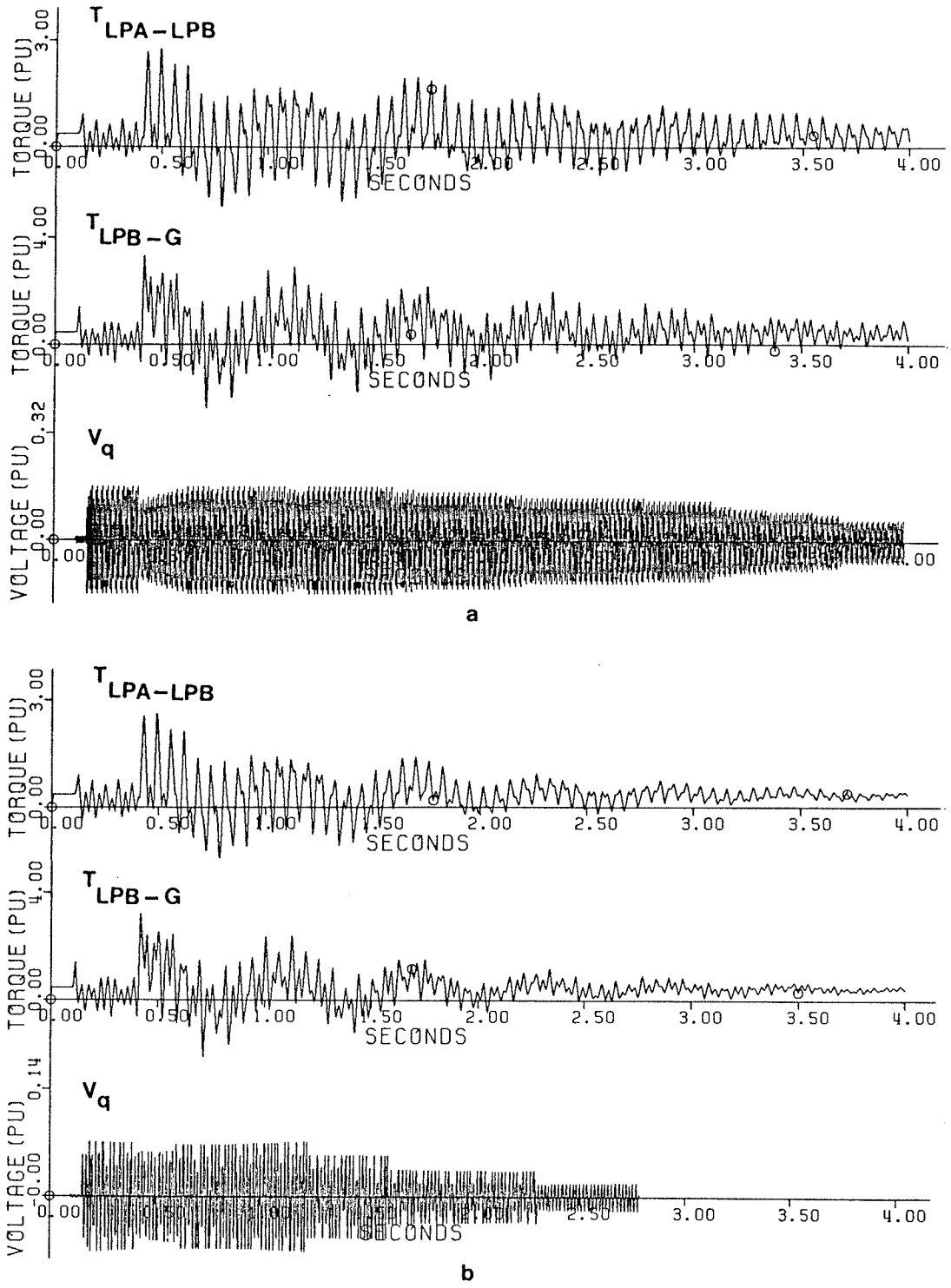

Figure 6.15: System transient response to a successful reclosure with the sequence 3-15 cycles, phase-shifter in service, MVA=480, pf=0.90
a - point-on-wave control method
b - discrete step control method

6.5.3.2 Case 8

The magnitude of power transfer prior to a fault occurance for a single tied system has a decisive effect on the shaft peak torques and the generator stability. For the same disturbance, higher peak torques occur when the amount of power transfer is higher. Fig.6.16 shows the system response to a 3-15 cycle successful reclosing, when the generator is delivering 595 MVA at 0.90 lagging power factor (535 MW). As compared with Fig.6.14, Fig.6.16 indicates that when the power is increased from 432 MW to 535 MW, the magnitudes of the shaft stresses increase. Fig.6.17 shows the shaft response when the transient mechanical stresses are counteracted by the quadrature phase voltage injection methods. The simulation results indicate that when the generator delivers more than 590 MW to the infinite bus through the single line T2-T3, the 3-15 cycle successful reclosure results in the loss of synchronism. Also a 3-30 cycle successful reclosure results in the loss of synchronism, unless the the power transfer prior to the fault is less than 23% of the rated MVA.

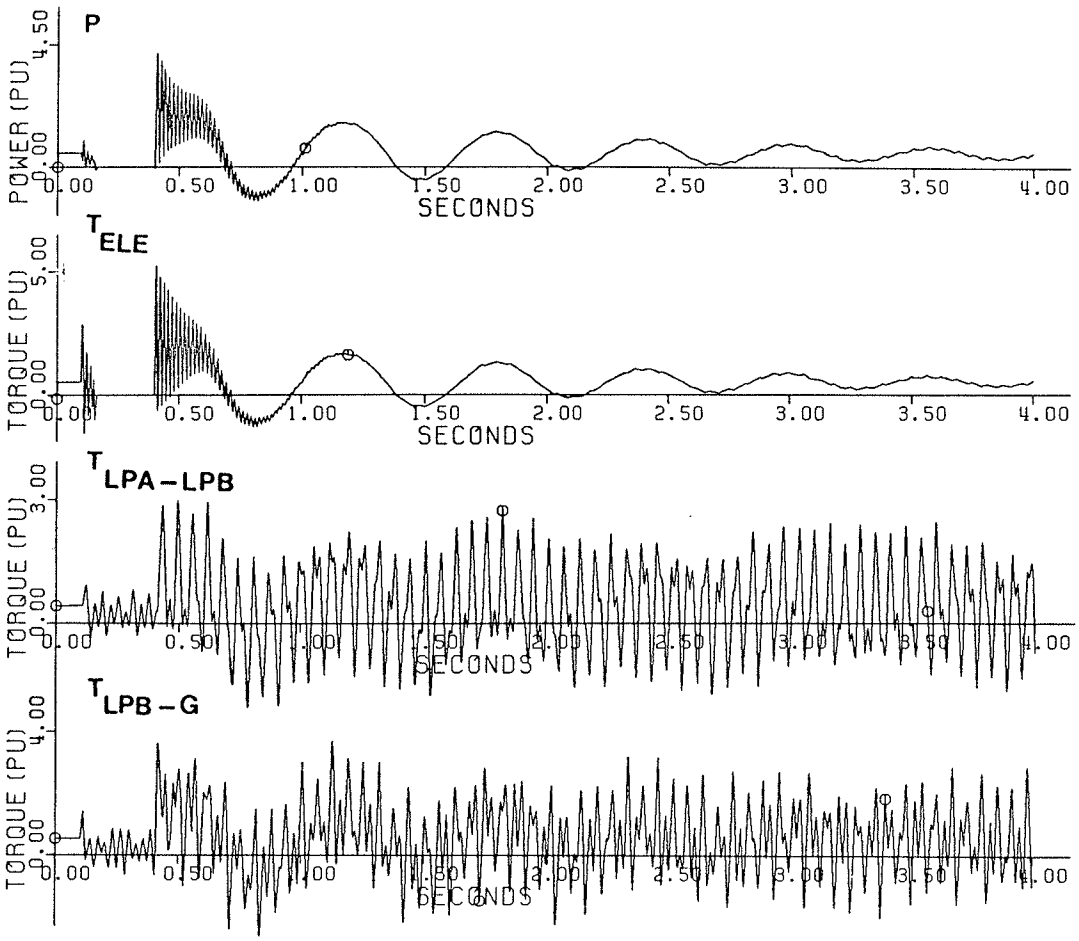

Figure 6.16: System transient response to a successful reclosure with the sequence 3-15 cycles, phase-shifter out of service, MVA=595, pf=0.90

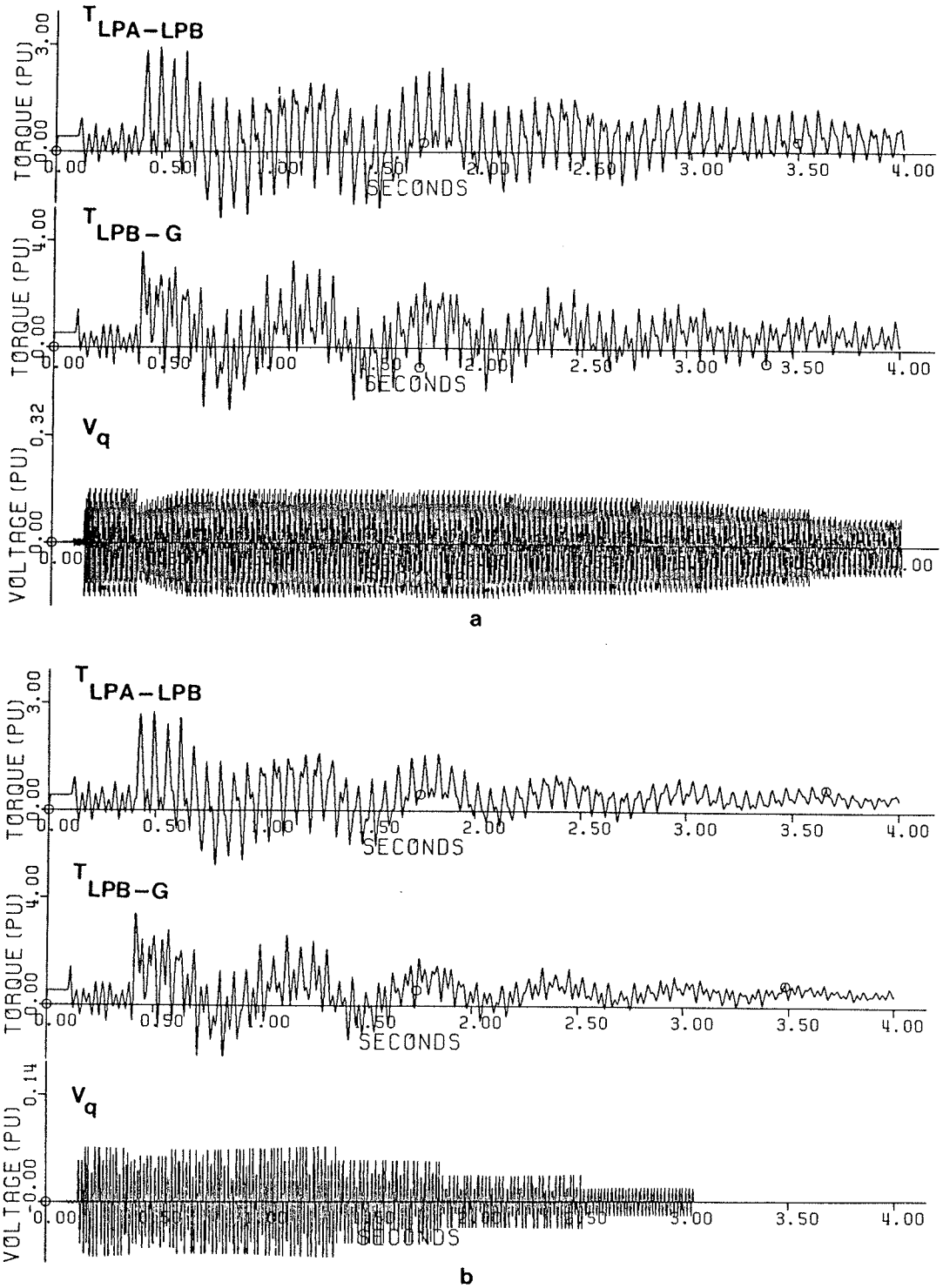

Figure 6.17: System transient response to a successful reclosure with the sequence 3-15 cycles, phase-shifter in service, MVA=595, pf=0.90
a - point-on-wave control method
b - discrete step control method

6.6 EFFECT ON LIFE-TIME AND PEAK MAGNITUDE OF TORSIONAL TORQUES

The accumulative fatigue process of the shaft segments of a turbine-generator is a function of the:

1. peak magnitude of the mechanical stresses,and
2. time interval that the shaft is subjected to the oscillatory torques.

Therefore, the peak magnitude and the duration of the oscillatory stresses can be used as the comparison indices to illustrate the positive damping effect of a dynamically controlled phase-shifter on a turbine-generator shaft transient torques. Here, the shaft peak torque is defined as the maximum torque encountered after the last switching incident, and the half life-time of an oscillatory shaft torque is defined as the time required for the oscillatory torque to decay to half of its maximum peak-to-peak value.

For the cases studied in Section 6.5, Fig.6.18 shows the peak torque as a result of the electrical disturbances, for the shaft segments between the low-pressure turbine A (LPA) and the low-pressure turbine B (LPB), and LPB and the generator rotor (G). Fig.6.18 indicates that the positive damping effect of the point-on-wave quadrature phase voltage injection method on the peak torques is minor, especially in the case of a single tied generator. However, the discrete step quadrature voltage injection method can considerably reduce the peak stresses.

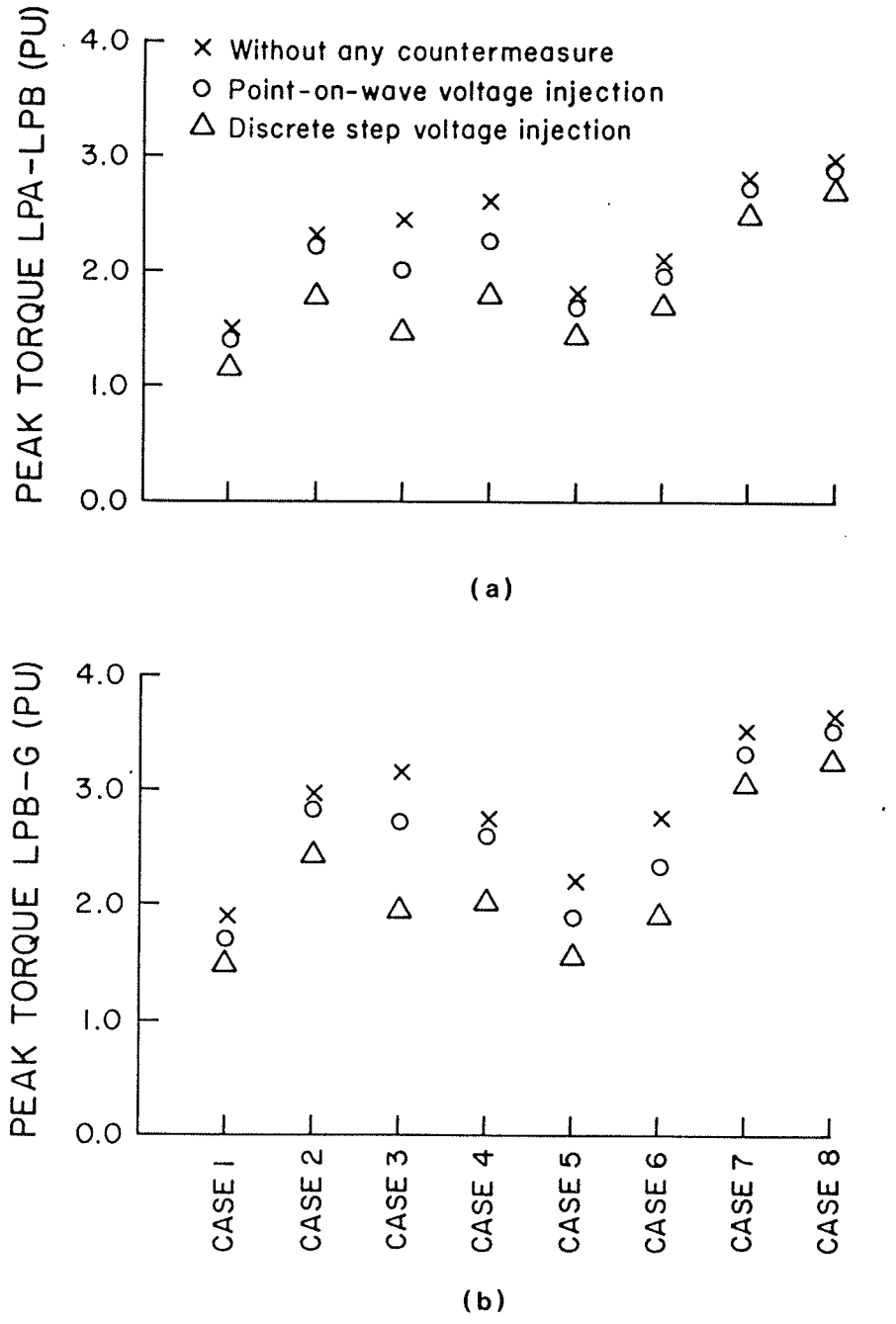

Figure 6.18: Shaft peak torque for the cases 1-8
a - shaft section between LPA and LPB
b - shaft section between LPB and G

For the cases studied in Section 6.5, Fig.6.19 illustrates the effect of the quadrature phase voltage injection method on the life-time of the torsional stresses of the shaft segments LPA-LPB and LPB-G. Due to the high cost of computer simulation, in the studies presented in Section 6.5, the shaft response to the electrical disturbances was not obtained beyond four seconds. During this time interval, with no countermeasure, the shaft transient torques experience virtually no decay, therefore, in Fig.6.19 the half life-times of the free torsional oscillations are assumed to be 12 s. Fig.6.19 shows that as a result of the quadrature phase voltage injection, the life-times of the oscillatory torques are considerably reduced, especially for the case of discrete step voltage injection. Due to the high decay rate of the torsional stresses when a static phase-shifter is in service, the shaft segments are subjected to a less number of peak torques, which results in a considerable save in the life-time of the turbine-generator unit.

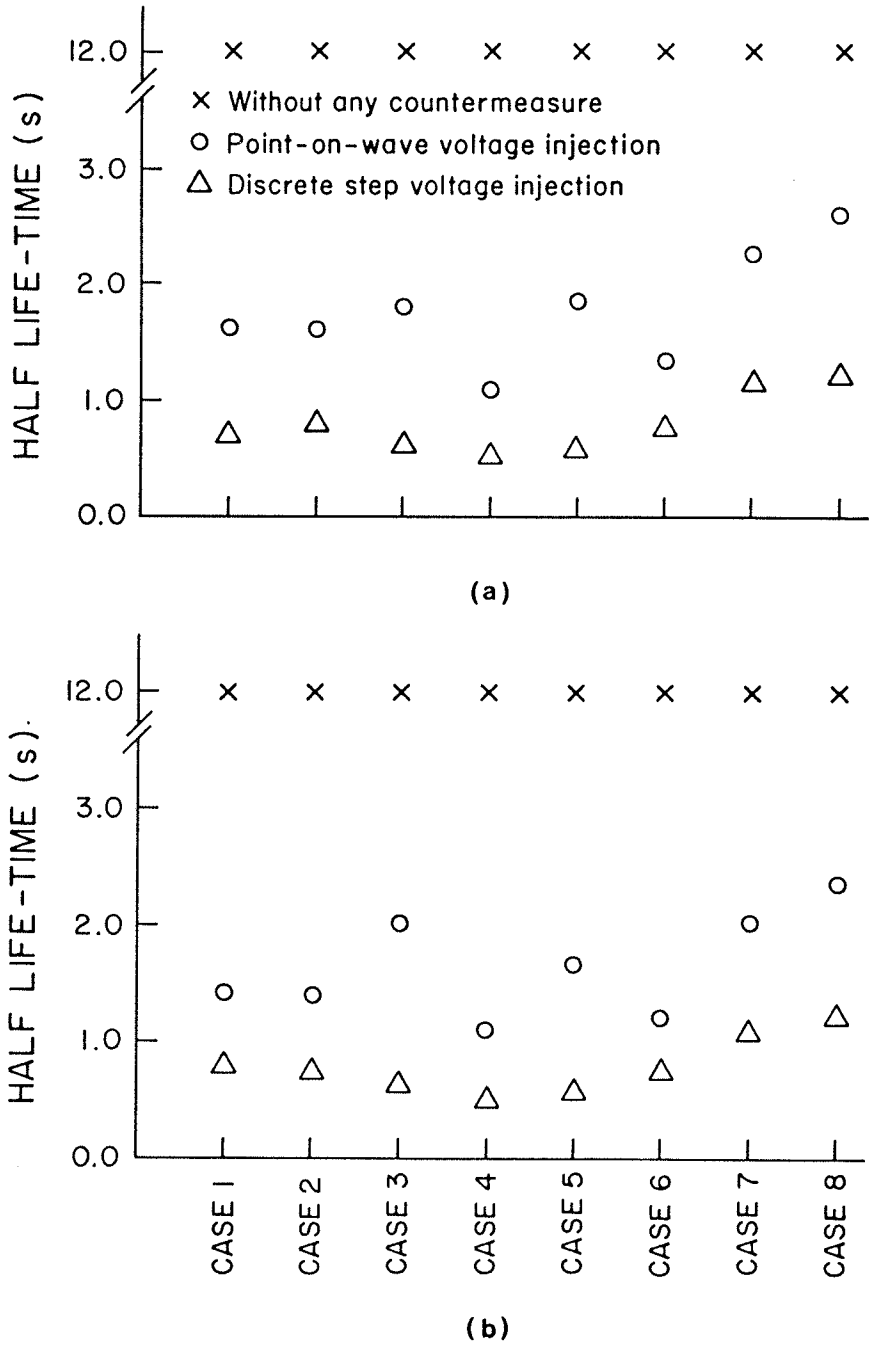

Figure 6.19: Half life-time of shaft torsional torques
a - shaft section between LPA and LPB
b - shaft section between LPB and G

6.7 CONCLUSIONS

The technical feasibility of a static phase-shifter for mitigating the transient torques of turbine-generators is examined. The supplementary damping is achieved based on active power modulation, using the shaft speed deviation as the control signal. The effect of switching time intervals and operating point on the shaft stresses are studied, using the BPA's EMTP. Emphasis is placed on the severe electrical disturbances, e.g., three-phase fault, three-phase fault clearing, and fast automatic reclosing (successful and unsuccessful).

The digital simulation results indicate that:

1. Injection of 7% of the system phase voltage, in quadrature phase, in four discrete steps of 1.75%, is more effective in damping the shaft transient torques, as compared with the injection of 16% quadrature phase voltage, based on the point-on-wave control method.
2. The point-on-wave control method does not have a noticeable effect on the peak transient shaft torques.
3. Damping effect of a static phase-shifter on the mechanical stresses is more pronounced for a multi-line system as compared with a single tied generator.

Chapter VII

CONCLUSIONS AND SUGGESTIONS FOR FURTHER STUDIES

The main objective of the thesis has been to investigate the technical feasibility of the static phase-shifters for:

1. suppressing the torsional torques of the steam turbine-generator shafts as a result of small signal perturbations and large disturbances in power systems, and
2. establishing a basis for further investigations in order to examine the thyristor-controlled phase-shifters for the stability enhancement of power systems.

7.1 GENERAL CONCLUSIONS

Based on the results from the analytical and the digital time simulation studies, the following conclusions are deduced:

1. A thyristor-controlled phase-shifter can be used as an effective countermeasure for the shaft torsional oscillations of a steam turbine-generator, in a series compensated power systems.

2. Phase-shifting by means of a point-on-wave controlled phase-shifter results in the voltage harmonics in the system, which necessitates the application of harmonic filters. A discrete step controlled phase-shifter, however, reduces the magnitude of the injected harmonics to a negligible value, and eliminates the need for filters.
3. A static phase-shifter can be used to alleviate the fatigue phenomenon of the shaft segments of turbine-generator assemblies, by reducing the duration and the peak torque of the shaft mechanical stresses, as a result of large disturbances.
4. As compared with the point-on-wave controlled phase shifting method, the discrete step control method is more effective for:
    (i) damping the shaft torsional oscillations during small signal perturbations, and
    (ii) reducing the peak torques and the duration of the transient torques.
5. In the studies presented, the effect of mechanical damping of the rotating masses were neglected. The mechanical damping has a significant effect on the shaft oscillation under heavy load conditions, especially during large disturbances. Thus, the results are pessimistic.
6. The successful performance of a static phase-shifter, for suppressing torsional and transient torques, re-

quires fast speed measurement techniques, using either precision-toothed wheels or auxiliary signals from a torsional monitoring system.

7.2 DISCUSSION OF THE RESULTS

For the system studied, the following observations are made:

1. Insertion of 2.4% of the system phase voltage in quadrature phase, in four discrete steps of 0.6%, can suppress the shaft torsional oscillations, as a result of small signal perturbations. The same positive damping effect can be achieved by injecting 6% of the system phase voltage in quadrature phase, using the point-on-wave control method. As compared with injecting 6% of the system phase voltage, the injection of 2.4% of the system phase voltage results in a negligible system voltage fluctuation from the steady-state value. This clearly reveals the technical advantage of a discrete step controlled phase-shifter over a point-on-wave controlled phase-shifter.
2. Injection of 7% of the system phase voltage in quadrature phase, in four discrete steps of 1.75% , during large disturbances:
   (i) reduces the half life-time of the shaft oscillatory stresses to about 0.75 s, which otherwise takes between 4 to 12 s, and
   (ii) reduces the peak torques to 77% of their val-

ues where no countermeasure is used.

3. Injection of 16% of the system phase voltage in quadrature phase, during large disturbances, using the point-on-wave control method:
   (i) reduces the half life-time of the oscillatory stresses to about 1.1 s, which otherwise takes between 4 to 12 s, and
   (ii) reduces the peak torques to around 91% of their values where no countermeasure is used.

7.3 MAJOR CONTRIBUTIONS

1. A novel approach for damping the shaft torsional oscillations of large turbine-generator units, during small signal perturbations and severe disturbances, based on quadrature phase voltage injection, by means of the static phase-shifters was suggested and examined.
2. An analytical formulation for the small signal perturbation analysis of power systems, based on "complex torque coefficient method" was developed. This analytical formulation was employed to investigate the stabilizing effect of a static phase-shifter on SSO. Furthermore, this method was used to optimize the phase and the gain of the control system of a static phase-shifter for damping SSO.

3. Detailed digital time simulation studies were conducted to verify the analytical results and to demonstrate the technical feasibility of the static phase-shifters for damping SSO.
4. Based on the digital computer studies, two practical configurations of static phase-shifters for damping turbine-generator mechanical stresses were compared, and their control algorithms were developed.

7.4 SUGGESTIONS FOR FURTHER STUDIES

1. Optimizing the cost effective parameters of a static phase-shifter, i.e., turns ratio of the excitation and the boosting transformers, the number and the rating of sub-converters.
2. Studying the effect of overvoltages and transient currents on the static phase-shifters, in order to establish the design criteria.
3. Investigating the interaction between the excitation system of generators and the static phase-shifters, especially when a supplementary damping for SSO is provided by the excitation control.
4. Studying the interaction between the governor system and the static phase-shifter, during large disturbances.
5. Investigating the possibility of the accelerating power as the control signal for a static phase-shifter. Utilization of the accelerating power, instead of

the shaft speed is advantageous when a phase-shifter is to be installed remote from a generating station.

6. Investigating the performance and the effect of the static phase-shifter on the transient torques, as a rsult of asymmetrical faults.
7. Investigating the possibility of using the static phase-shifters for damping the supersynchronous torsional oscillations of the steam turbine blades
8. Studying the damping effect of the static phase-shifters for suppressing the transient torques in series capacitor compensated systems.

REFERENCES

1. J.W.Botler, C. Concordia, "Analysis of Series Capacitors Application Problem", AIEE Trans., Vol.56, pp.975-988, 1937.

2. IEEE Committee Report, "A Bibliography for Study of Subsynchronous Resonance Between Rotating Machines and Power System", IEEE Trans., Vol. PAS-95, pp. 216-218, 1976.

3. IEEE Committee Report, "First Supplement to a Bibliography for Study of Subsynchronous Resonance Between Rotating Machines and Power System", IEEE Trans., Vol. PAS-98, pp. 1872-1875, 1979.

4. IEEE Subsynchronous Working Group, "Proposed Terms and Definitions for Subsynchronous Oscillations", IEEE Trans., Vol. PAS-99, pp. 506-511, 1980.

5. E.V.Larsen, H.S.Patel, and R.J.Piwko, "The Effect of HVDC System on Turbine-Generator Torsional Variation - Focus on Solution and Impact on System Planing", Proceedings of the American Power Conference, Vol. 43 pp. 594-597, 1981.

6. W.Watson, and M.E.Coultes, "Static Stabilizer Signal on Large Generators - Mechanical Problems", IEEE Trans., Vol. PAS-92, pp. 204-211, 1973.

7. G.Andersson, R.Atmuri, R.Rosengvist, and S.Torseng, "Influence of Hydro Units Generator-to-Turbine Ratio on Damping of Subsynchronous Oscillations", IEEE Trans., Vol. PAS-103, pp. 2352-2361, 1984.

8. R.Quay, and R.J.Placek, "Cyclic Fatigue of Turbine-Generator Shaft", IEEE PES Publication #76CH1066-0-PWR, pp. 12-21, 1976.

9. D.Lambrecht, and T.Kuling, "Torsional Performance of Turbine Generator Shafts Specially Under Resonant Excitation", IEEE Trans., Vol. PAS-101, pp. 3689-3702, 1982.

10. C.Concordia, "System Planning Consideration of Sub-Synchronous Resonance", IEEE PES Publication #76CH1066-0-PWR, pp.51-54, 1976.

11. S.Goldberge, and W.R.Schimus, "Subsynchronous Resonance and Torsional Stress in Turbine Generator Shaft", Paper C73 135-1 presented at PES Winter Meeting, 1973.

12. D.E.Walker, C.E.J.Bowler, R.L.Jackson, and D.A.Hodge, "Results of Subsynchronous Resonance Tests at Mohave", Paper T75 176-3, presented at PES Winter Meeting, 1975.

13. C.F.Wagner, "Self Excitation of Induction Motors With Series Capacitors", AIEE Trans., Vol. 60, pp. 1241-1247, 1941.

14. R.L.Witzke, and E.L.Michelson, "Technical Problems Associated With the Application of a Capacitor in Series With a Synchronous Condenser", AIEE Trans., Vol. 70, pp. 519-525, 1951.

15. L.A.Kilgore, L.C.Elliot, and E.R.Taylor, "The Prediction and Control of Self Excited Oscillations Due To Series Capacitors in Power SYstems", IEEE Trans., Vol. PAS-90, pp. 1305-1311, 1971.

16. O.Saito, H.Mukae, and K.Murotani, "Suppression of Self-Excited Oscillations in Series Compensated Transmission Lines", Paper C73180-5, presented at PES- Winter Meeting, 1973.

17. R.D.Dunlop, et al., "Turbine-Generator Shaft and Fatigue; Part II - Impact of System Disturbances and High-Speed Reclosers", IEEE Trans., Vol. PAS-98, pp.2308-2328, 1979.

18. IEEE Subsynchronous Resonance Task Force, "First Benchmark Model for Computer Simulation of Subsynchronous Resonance", IEEE Trans., Vol. PAS-96, pp. 1565-1572, 1977.

19. Electro-Magnetic Transient Program (EMTP) User's Manual, Mode 28, Sept. 1980.

20. L.Meirovitch, "ANALYTICAL METHODS IN VIBRATIONS", Macmillan, New York, 1967.

21. D.G.Ramey, and G.C.Kung, "Important Parameters in Considering Transient Torques on Turbine-Generator Shaft Systems", IEEE Trans., Vol. PAS-99, pp. 311-317, 1980.

22. D.M.Triezenberg, "Characteristic Frequencies and Mode Shapes For Turbogenerator Shaft Torsional Vibration", IEEE Trans., Vol. PAS-99, pp. 352-357, 1980.

23. C.Concordia, "SYNCHRONOUS MACHINES, THEORY AND PERFORMANCE", Wiley, New York, 1951.

24. B.Adkins, and R.G.Harley, "THE GENERAL THEORY OF ALTERNATING CURRENT MACHINES", Chapman and Hall, London, 1975.

25. IEEE Subsynchronous Resonance Working Group, "Proposed Terms and Definitions for Subsynchronous Resonance in Series Compensated Transmission Systems", IEEE Special Publication, 76CH1066-0-PWR, pp. 55-58, 1976.

26. H.A.Paterson, and P.C.Krauce, "A Direct and Quadrature Axis Presentation of a Parallel ac and dc Power System", IEEE Trans., Vol. PAS-85, pp. 210-225, 1966.

27. B.L.Agrawal, and R.G.Farmer, "Use of Frequency Scanning Technique for Subsynchronous Resonance Analysis", IEEE Trans., Vol. PAS-98, pp. 341-349, 1979.

28. M.El-Marsafaway, "Use of Frequency-Scan Techniques for Subsynchronous Resonance Analysis of a Practical Series-Capacitor Compensated ac Network", IEE Proc., Vol. 135, No.1, pp. 28-40, 1983.

29. L.A.Kilgore, D.C.Ramey, and M.C.Hall, "Simplified Transmission and Generation System Analysis Procedure for Subsynchronous Resonance Problems", IEEE Special Publication, 76CH1066-0-PWR, pp. 6-11, 1976.

30. I.M.Canay, "Subsynchronous Resonance - An Explanation of the Physical Relationship", Brown Boveri Review, Vol. 86, pp.348-357, Aug/Sept 1981.

31. I.M.Canay, "A Novel Approach to the Torsional Interaction and Electrical Damping of Synchronous Machine, Part I", IEEE Trans., Vol. PAS-101, pp. 3630-3638, 1982.

32. I.M.Canay, "A Novel Approach to the Torsional Interaction and Electrical Damping of the Synchronous Machine, Part II", IEEE Trans., Vol. PAS-101, pp. 3639-3647, 1982.

33. H.W.Dommel, "Digital Computer Solution of Electromagnetic Transients in Single- and Multi-Phase Networks", IEEE Trans., Vol. PAS-88, pp. 388-399, 1969.

34. G.Gross, and M.C.Hall, "Synchronous Machine and Torsional Dynamics Simulation in the Computation of Electro-Magnetic Transient", IEEE Trans., Vol. PAS-97, pp. 1074-1086, 1978.

35. H.K.Lauw, and W.S.Mayer, "Universal Machine Modeling for the Representation of Rotating Electric Machinery in an Electromagnetic Transient Program", IEEE Trans., Vol. PAS-101, pp. 1342-1351, 1982.

36. D.A.Woodford, A.M.Gole, and R.W.Menzies, "Digital Simulation of DC Links and AC Machines", IEEE Trans., Vol. PAS-102, pp. 1616-1623, 1983.

37. V.Brandwagin, and H.W.Dommel, "Interfacing Generator Models with an Electromagnetic Transient Program", IEEE PES Summer Meeting, Portland Oregon, 1976.

38. T.S.Ning, "Subsynchronous Overcurrent Relay for Generators Connected to Series Compensated Power Systems", IEEE Special Publication 76CH1066-0-PWR, pp. 51-54, 1976

39. A.L.Schwalb, "Navajo Project Subsynchronous Resonance Monitor and Relaying Equipment", IEEE Special Publication, 76CH1066-0-PWR, 1976.

40. IEEE Subsynchronous Resonance Working Group, "Series Capacitors Control and Settings as a Countermeasure to Subsynchronous Resonance", Paper 81WM009-0, IEEE Winter Meeting, 1980.

41. L.A.Kilgore, et al., "Solution to the Problem of Subsynchronous Resonance in Power Systems with Series Capacitors", Proceedings of The American Power Conference, Vol. 35, pp. 1120-1128, 1973.

42. R.H.Hartely, et al., "EHV Series Capacitor Applications Considering Subsynchronous Oscillations", CIGRE, Paper 31-06, 1974.

43. L.Ahlgren, N.Fahlen, and K.E.Johansson, "EHV Series Capacitors with Dual Gap and Non-Linear Resistors Provide Technical and Economical Advantages", Paper A79-049-3, IEEE PES Winter Meeting, 1979.

44. J.B.Tice, and C.J.Bowler, "Control of Phenomenon of Subsynchronous Resonance", Proceedings of The American Power Conference, Vol. 37, 1975.

45. T.M.Morong, C.H.Holley, C.E.J.Bowler, and J.B.Tice, "Design and Test of the Navajo Plant Subsynchronous Resonance Protective Filters", CIGRE, Paper 31-06, 1976.

46. D.J.N.Limebeer, R.G.Harley, and M.A.Lohoud, "Suppressing Subsynchronous Resonance with Static Filters", IEE Proc. Vol.128, Pt.C, No.1, pp. 33-44, 1981.

47. J.M.Undrill, and F.P. DeMello, "Subsynchronous Oscillations, Part:II Shaft System Dynamic Interaction", IEEE Trans., Vol. PAS-95, pp. 1456-1463, 1976.

48. R.G.Farmer, A.L.Schwalb, and E.Katz, "Navajo Project Report on Subsynchronous Analysis and Solution", IEEE Trans., Vol. PAS-96 pp. 1226-1232, 1977.

49. C.E.J.Bowler, D.H.Baker, N.A.Mincer, and P.R.Vandiveer, "Operation and Test of the Navajo SSR Protective Equipment", IEEE Trans., Vol. PAS-97, pp.1030-1035, 1978.

50. L.A.Kilgore, D.G.Ramey, and W.H.South, "Dynamic Filter and Other Solutions to Subsynchronous Resonance Problem", Proceedings of the American Power Conference, Vol. 37, pp. 923-929, 1975.

51. T.H.Putman, and D.G.Ramey, "Theory of Modulated Reactance Solution for Subsynchronous Resonance", IEEE Trans., Vol. PAS-101, pp. 1527-1535, 1982.

52. IEEE Subsynchronous Resonance Working Group, "Countermeasures to Subsynchronous Resonance Problem", IEEE Trans., Vol. PAS-99, pp. 1810-1818, 1980.

53. T.H.Putman, and D.G.Ramey, "A modulated Inductance Stabilizer for Power Systems Subjected to Subsynchronous Resonance", Proceedings of the International Symposium on Controlled Reactive Compensation, Montreal, Canada, pp.269-289, 1979.

54. O.Wasynczuk, "Damping Subsynchronous Resonance Using Reactive Power Control ", IEEE Trans., Vol. PAS-100, pp. 1096-1104, 1981.

55. D.G.Ramey, R.A.Whyte, J.W.Dorney, and F.H.Kroening, "Application of Dynamic Stabilizer to Solve an SSR Problem", Proceedings of the American Power Conference, Vol. 43, pp. 605-609, 1981.

56. D.G.Ramey, D.S.Kimmel, J.W.Dorrey, and F.H.Kroening, "Dynamic Stabilizer Verification Tests at the San Juan Station", IEEE Trans., Vol. PAS.100, pp. 5011-5019, 1981.

57. O.Wasynczuk, "Damping Shaft Torsional Oscillations Using a Dynamically Controlled Resistor Bank", IEEE Trans., Vol. PAS-100. pp. 3340-3349 1981.

58. Y.Ichihara, et al., "Laboratory Tests and Feasibility Study of two Countermeasures to Subsynchronous Resonance", IEEE Trans., Vol. PAS-102 pp. 300-310, 1983.

59. H.A.Paterson, N.Mohn, and R.W.Boom, "Supperconductive Energy Storage Inductor-Converter Unit for Power Systems", IEEE Trans., Vol. PAS-94 pp. 1337-1348, 1975.

60. O.Wasynczuk, "Damping Shaft Torsional Oscillations with Application to High-Speed Reclosure", IEEE Trans., Vol. PAS-100, pp. 1089-1095, 1981.

61. O.Wasynczuk, "Damping Subsynchronous Resonance Using Energy Storage", IEEE Trans., Vol. PAS-101, pp. 905-914, 1982.

62. H.Hingorani, et al., "Analysis of Subsynchronous Resonance Interactions Involving HVDC Transmission Systems", IEEE Proceedings of Overvoltage and Compensation on Integrated AC-DC Systems, Winnipeg, Manitoba, Canada, pp. 7-14, 1980.

63. M.Bahrman, E.V.Larsen, R.J.Piwko, and H.S.Patel, "Experience with HVDC-Turbine-Generator Torsional at Square Butte ", IEEE Trans., Vol. PAS-99, pp. 966-975, 1980.

64. S.Svensson, and K.Mortensen, "Damping Subsynchronous Oscillations by an HVDC Link. An HVDC Simulator Study", IEEE Trans., Vol. PAS-100, pp. 1431-1439, 1981.

65. K.Mortensen, E.V.Larsen, and R.J.Piwko, "Field Test and Analysis of Torsional Interaction Between the Cool Creek Turbine-Generator and the CU HVDC System", IEEE Trans., Vol. PAS-100, pp. 336-344, 1981.

66. R.J.Piwko, and E.V.Larsen, "HVDC Control for Damping of Subsynchronous Oscillations", IEEE PES Transmission and Distribution Conference, Paper 81TD660-0, 1981.

67. Electric Power Research Institute, "HVDC Control for Damping of Subsynchronous Oscillations", EPRI EL-2708, Project 1425-1, Final Report, 1982.

68. N.G.Hingorani, "A New Scheme for Subsynchronous Resonance Damping of Torsional Oscillations and Transient Torques, Part I", IEEE Trans., Vol. PAS-100, pp.1852-1855, 1981.

69. R.A.Hadin, K.B.Stump, and N.G.Hingorani, "A New Scheme for Subsynchronous Resonance Damping of Torsional Oscillations and Transient Torques, Part II", IEEE Trans., Vol. PAS-100, pp. 1856-1863, 1981.

70. C.Concordia, and F.P.DeMello, "Concept of Synchronous Machine Stability as Affected by Excitation Control", IEEE Trans., Vol. PAS-88, pp. 316-329, 1969.

71. K.E.Bollinger, R.Winsor, and A.Campbell, "Frequency Response Method for Tuning Stabilizers To Damp Out Tie-Line Power Oscillations, Theory and Field Test Results", IEEE Trans., Vol. PAS-98, pp. 1509-1515, 1979.

72. S.T.Naumann, et al., "Underexcited Operation and Stability Test at the Powerton Station", Proceedings of the American Power Conference Vol. 45, pp. 1093-1096, 1979.

73. E.T.Oai, and M.M.Sartawi, "Concept of Field Excitation of Subsynchronous Resonance in Synchronous Machines", IEEE Trans., Vol. PAS-97, pp. 1637-1644, 1978.

74. R.A.Lawson, D.A.Swann, and G.F.Wright, "Minimization of Power System Stabilizer Torsional Interaction", IEEE Trans., Vol. PAS-97, pp. 183-190, 1978.

75. R.A.Larsen, and D.A.Swann, "Appling Power System Stabilizer, Part I: General Concept", IEEE Trans., Vol. PAS-100. pp. 3017-3024, 1981.

76. E.V.Larsen, and D.A.Swann, "Appling Power System Stabilizer, Part II: Performance Objective And Tuning Concept", IEEE Trans., Vol. PAS-100, pp. 3025-3033, 1981.

77. E.V.Larsen, and D.A.Swann, "Applying Power System Stabilizers, Part III: Practical Considerations", IEEE Trans., Vol. PAS-100, pp. 3034-3046.

78. V.M.Raina, W.J.Wilson, and J.H.Anderson, "The Control of Rotor Torsional Oscillations Excited by Supplementary Exciter Stabilization" , Paper A76-457-2, IEEE PES Winter Meeting, Oregon, 1976.

79. O.Saito, H.Mukae, and K.Morotani, "Suppression of Self-Excitation Oscillations in Series Compensated Transmission Lines by Excitation Control of Synchronous Machines", IEEE Trans., Vol. PAS-94, pp. 1777-1788, 1975.

80. A.Yan, M.D.Wvong, and Y.Yu, "Excitation Control of Torsional Oscillations", IEEE PES Summer Meeting, Paper A79505-9, 1979.

81. A.Yan, and Y.Yu, "Multimode Stabilization of Torsional Oscillations Using Output Feedback Excitation Control", IEEE Trans., Vol. PAS-101 pp. 1245-1253, 1982.

82. A.E.Hammad, and M.Sadek", Application of a Thyristor Controlled VAR Compensater For Damping Subsynchronous OSCillations in Power Systems", IEEE Trans., Vol. PAS-103, pp. 198-212, 1984.

83. A.A.Fouad, and K.T.Khu, "Subsynchronous Resonance Zones in IEEE Benchmark Power System", IEEE Trans., Vol.PAS-97, pp. 744-751, 1978.

84. M.R.Iravani, and R.M.Mathur, "Application of Static Phase-Shifters for Damping Turbine-Generator Torsional Torques", Proceedings of IEEE International Communications and Energy Conference, pp. 107-111, Oct. 1984.

85. M.R.Iravani, and R.M.Mathur, "Damping Subsynchronous Oscillations in Power Systems Using a Static Phase-shifter", Submitted for PES Winter Meeting, New York, Feb. 1985.

86. J.Dobsa, "Transformer for In-phase, Phase-angle and Quadrature Phase Regulation", Brown Boveri Review, Vol.8, pp. 376-383, 1972.

87. D.O'Kelly, and G.Musgrave, "An Appraisal of Transformer Tap Changing Technique", IEE Conference Publication, No.123, pp. 112-117, 1973.

88. J.Arrillaga, and R.M.Duke, "A Static Alternative to the Transformer On-Load Tap-Changer", IEEE Trans., Vol. PAS-99, pp. 86-91, 1980.

89. H.Stemmler, and G.Guth, "The Thyristor Controlled Static Phase-Shifter - A New Toll for Power System flow Control in AC Transmission System", Brown Boveri Review, Vol.69, pp. 73-78, 1982.

90. D.O'Kelly, and G.Musgrave, "Improvement of Power System Transient by Phase-Shift Insertion", IEE Proc., Vol.120, pp. 247-252, 1973.

91. R.M.Mathur, and R.S.Basati, "A Thyristor Controlled Static Phase-Shifter for AC Power Transmission", IEEE Trans., Vol. PAS-100, pp. 2650-2655, 1981.

92. C.P.Arnold, R.M.Duke, and J.Arrillaga, "Transient Stability Improvement Using Thyristor Controlled Quadrature Voltage Injection", IEEE Trans., Vol. PAS-100, pp. 1382-1388, 1981.

93. R.Baker, G.Guth, W.Egli, and P.Eglin, "Control Algorithm for a Static Phase Shifting Transformer to Enhance Transient and Dynamic Stability of Large Power Systems", IEEE Trans., Vol. PAS-101, pp. 3532-3542, 1982.

94. J.Arrillaga, and R.M.Duke, "Thyristor Controlled Quadrature Boosting ' IEE Proc., Vol.126, pp. 493-498, 1979.

95. N.Mohan, "Continuous Alternating Voltage Regulation Using a Thyristor Bridge", Proc. IEE, Vol. 126, pp. 1002-1004, 1979.

96. J.D.Hurley, and W.H.South, "Torsional Monitor Equipment For Turbine-Generator Units", Proceedings of the American Power Conference, Vol.41, pp. 1163-1169, 1979.

97. J.S.Joyce, and D.Lambrecht, "Monitoring The Fatigue Effect of Electrical Disturbances on Steam Turbine-Generators", Proceedings of the American Power Conference, Vol.41, pp. 1153-1162, 1979.

98. D.G.Ramey, et al., "Subsynchronous Resonance Tests and Torsional monitoring System Verification at the Cholla Station", IEEE Trans., Vol. PAS-99, pp.1900-1907, 1980.

99. T.Ino, R.M.Mathur, and M.R.Iravani, "Validation of Digital Simulation of DC links - Part II", Submitted for PES Winter Meeting, New York, Feb. 1985.

100. M.R.Iravani, and R.M.Mathur, "Damping Subsynchronous Oscillations Using a Thyristor-Controlled Phase-Shifter", 26th Midwest Symposium on Circuits and Systems, August 1983, Mexico.

101. IEEE Special Publication, "State-of-the-Art Symposium - Turbine-generator Shaft Torsionals", Publication No. 79TH0059-6-PWR, 1979.

102. N.E.Dowling, "Torsional Fatigue Life of Power Plant Equipment Rotating Shafts", U.S.Department of Energy, Contract No. AC05-80RA29353, Sept. 1982.

103. J.S.Joyce, T.Kuling, and D.Lambrecht, "Torsional Fatigue of Turbine-Generator Shafts Caused by Different Electrical System Faults and Switching Operations", IEEE Trans., Vol. PAS-97, pp. 1965-1977, 1978.

104. L.Ahlgren, K.E.Johanson, and A.Gadhammer, "Estimated Life Expenditure of Turbine-Generator Shafts at Network Faults and Risk of Subsynchronous Resonance in the Swedish 400kV System", IEEE Trans., Vol. PAS-97, pp. 2005-2018, 1978.

105. P.C.Krauce, et al., "Shaft Torques During Out-Of-Phase Synchronization", IEEE Trans., Vol. PAS-96, pp.1318-1323, 1977.

106. J.S.Misysche, and P.A.Rusche, "Shaft Torsional Stress Due to Asynchronous Faulty Synchronization", IEEE Trans., Vol. PAS-99, pp. 1864-1870, 1980.

107. C.E.J.Bowler, P.G.Brown, and D.N.Walker, "Evaluation of the Effect of Power Circuit Braker Reclosing on Turbine-Generator Shafts", IEEE Trans., Vol. PAS-99, pp. 1764-1779, 1980.

108. A.Abolins, et al., "Effect of Clearing Short Circuits and Automatic Reclosing on Torsional Stress and Life Expenditure of Turbine-Generator Shafts", IEEE Trans., Vol. PAS-95, pp. 14-25, 1976.

109. I.M.Canay, H.J.Roher, and K.E.Schnirel, "Effect of Electrical Disturbances, Grid Recovery and Generator Inertia on Maximization of Mechanical Torques in Large Turbogenerator Sets", IEEE Trans., Vol. PAS-99, pp.1357-1370, 1980.

Appendix A

The turbine-generator mechanical data of the first IEEE benchmark model for SSO studies [18].

MASS	SHAFT	INERTIA(s)	SPRING CONSTANT(pu)
HP		0.092897	
	HP-IP		19.303
IP		0.155580	
	IP-LPA		34.920
LPA		0.858570	
	LPA-LPB		52.038
LPB		0.884215	
	LPB-GEN		70.858
GEN		0.868495	
	GEN-EXC		2.822
EXC		0.034216	

MASS	HP	IP	LPA	LPB	GEN	EXC
FRACTIONAL INPUT MECHANICAL TORQUE	0.30	0.26	0.22	0.22	0.0	0.0

UNSTABLE MODE	TORSIONAL FREQUENCY(Hz)
1	15.71
2	20.21
3	25.55
4	32.28

Appendix B

Generator electrical data of the first IEEE benchmark model [18]:

Rated MVA = 892.4
Rated voltage = 26 kV

x_d = 1.790	pu	x_q'' = 0.200	pu
x_d' = 0.169	pu	r_a = 0.0	pu
x_d'' = 0.135	pu	T_{d0}' = 4.300	s
x_L = 0.130	pu	T_{d0}'' = 0.032	s
x_q = 1.710	pu	T_{q0}' = 0.850	s
x_q' = 0.228	pu	T_{q0}'' = 0.850	s

$$X_d(p) = x_d\,[(1+pT_d')(1+pT_d'')]/[(1+pT_{d0}')(1+pT_{d0}'')]$$

$$X_q(p) = x_q\,[(1+pT_q')(1+pT_q'')]/[(1+pT_{q0}')(1+pT_{q0}'')]$$

$$G(p) = (x_{md}/r_f)(1+pT_{kd})/(1+pT_{d0}'')$$

Step-up transformer data:

Rated MVA = 910
Rated voltage = 26/520 kV
x=0.14 pu
r=0.0035 pu

Transmission line data:

Section between sending end and series capacitor	Section between series capacitor and network
r=0.02 pu	r=0.00 pu
x=0.50 pu	x=0.06 pu

Boosting transformer data:

	MVA	kV	x(pu)	r(pu)
Point-on-wave method dynamic studies	21	20/20	0.05	0.01
point-on-wave method transient studies	60	50/50	0.07	0.01
Discrete step method dynamic studies	12	10/10	0.05	0.01
discrete step method transient studies	26	22/22	0.05	0.01

Excitation transformer data:

	MVA	kV	x(pu)	r(pu)
point-on-wave method dynamic studies	21	520/20	0.09	0.01
point-on-wave method transient studies	60	520/50	0.09	0.01
discrete step method dynamic studies	12	520/10	0.09	0.01
discrete step method transient studies	26	520/22	0.09	0.01

Appendix C

Fig.C.1 illustrates the general form of the system charateristic matrix for the eigenvalue study of Section 3.6. Nonzero elements of the system characteristic matrix are given in the following pages.

$$\underline{A} = \begin{vmatrix}
0 & 0 & 0 & 0 & 0 & 0 & * & 0 & 0 & 0 & 0 & 0 & 0 & 0 & 0 & 0 & 0 & 0 & 0 & 0 & 0 \\
0 & 0 & 0 & 0 & 0 & 0 & 0 & * & 0 & 0 & 0 & 0 & 0 & 0 & 0 & 0 & 0 & 0 & 0 & 0 & 0 \\
0 & 0 & 0 & 0 & 0 & 0 & 0 & 0 & * & 0 & 0 & 0 & 0 & 0 & 0 & 0 & 0 & 0 & 0 & 0 & 0 \\
0 & 0 & 0 & 0 & 0 & 0 & 0 & 0 & 0 & * & 0 & 0 & 0 & 0 & 0 & 0 & 0 & 0 & 0 & 0 & 0 \\
0 & 0 & 0 & 0 & 0 & 0 & 0 & 0 & 0 & 0 & * & 0 & 0 & 0 & 0 & 0 & 0 & 0 & 0 & 0 & 0 \\
0 & 0 & 0 & 0 & 0 & 0 & 0 & 0 & 0 & 0 & 0 & * & 0 & 0 & 0 & 0 & 0 & 0 & 0 & 0 & 0 \\
* & * & 0 & 0 & 0 & 0 & 0 & 0 & 0 & 0 & 0 & 0 & 0 & 0 & 0 & 0 & 0 & 0 & 0 & 0 & 0 \\
* & * & * & 0 & 0 & 0 & 0 & 0 & 0 & 0 & 0 & 0 & 0 & 0 & 0 & 0 & 0 & 0 & 0 & 0 & 0 \\
0 & * & * & * & 0 & 0 & 0 & 0 & 0 & 0 & 0 & 0 & 0 & 0 & 0 & 0 & 0 & 0 & 0 & 0 & 0 \\
0 & 0 & * & * & * & 0 & 0 & 0 & 0 & 0 & 0 & 0 & 0 & 0 & 0 & 0 & 0 & 0 & 0 & 0 & 0 \\
0 & 0 & 0 & * & * & * & 0 & 0 & 0 & 0 & 0 & 0 & * & * & * & * & * & * & 0 & 0 & 0 \\
0 & 0 & 0 & 0 & * & * & 0 & 0 & 0 & 0 & 0 & 0 & 0 & 0 & 0 & 0 & 0 & 0 & 0 & 0 & 0 \\
0 & 0 & 0 & 0 & * & 0 & 0 & 0 & 0 & 0 & * & 0 & * & * & * & * & * & * & * & 0 & * \\
0 & 0 & 0 & 0 & * & 0 & 0 & 0 & 0 & 0 & * & 0 & * & * & * & * & * & * & * & 0 & * \\
0 & 0 & 0 & 0 & * & 0 & 0 & 0 & 0 & 0 & * & 0 & * & * & * & * & * & * & * & 0 & * \\
0 & 0 & 0 & 0 & * & 0 & 0 & 0 & 0 & 0 & * & 0 & * & * & * & * & * & * & 0 & * & * \\
0 & 0 & 0 & 0 & * & 0 & 0 & 0 & 0 & 0 & * & 0 & * & * & * & * & * & * & 0 & * & * \\
0 & 0 & 0 & 0 & * & 0 & 0 & 0 & 0 & 0 & * & 0 & * & * & * & * & * & * & 0 & * & * \\
0 & 0 & 0 & 0 & 0 & 0 & 0 & 0 & 0 & 0 & * & 0 & * & 0 & 0 & 0 & 0 & 0 & 0 & * & 0 \\
0 & 0 & 0 & 0 & 0 & 0 & 0 & 0 & 0 & 0 & * & 0 & * & 0 & 0 & 0 & 0 & 0 & * & 0 & 0 \\
0 & 0 & 0 & 0 & 0 & 0 & 0 & 0 & 0 & 0 & * & 0 & 0 & 0 & 0 & 0 & 0 & 0 & 0 & 0 & * \\
\end{vmatrix}$$

Figure C.1: System charateristic matrix
* - nonzero element
0 - zero element

In matrices $\underline{M}$ and $\underline{K}$, subscripts 1 to 6 correspond to masses from high-pressure turbine to exciter, respectively (generator rotor is defined as mass number 5).

$$\underline{M} = \text{diag} \left[M_1 \; M_2 \; M_3 \; M_4 \; M_5 \; M_6 \right]$$

$$\underline{K} = \begin{vmatrix} K_{1,1} & -K_{1,2} & 0 & 0 & 0 & 0 \\ -K_{1,2} & K_{2,2} & -K_{2,3} & 0 & 0 & 0 \\ 0 & -K_{2,3} & K_{3,3} & -K_{3,4} & 0 & 0 \\ 0 & 0 & -K_{3,4} & K_{4,4} & -K_{4,5} & 0 \\ 0 & 0 & 0 & -K_{4,5} & K_{5,5} & -K_{5,6} \\ 0 & 0 & 0 & 0 & -K_{5,6} & K_{6,6} \end{vmatrix}$$

$$K_{i,i} = K_{i,i+1} + K_{i-1,i}$$

$$\underline{L} = \begin{vmatrix} -L_d & L_{md} & L_{md} & 0 & 0 & 0 \\ -L_{md} & L_f & L_{md} & 0 & 0 & 0 \\ -L_{md} & L_{md} & L_{kd} & 0 & 0 & 0 \\ 0 & 0 & 0 & -L_q & L_{mq} & L_{mq} \\ 0 & 0 & 0 & -L_{mq} & L_{kq} & L_{mq} \\ 0 & 0 & 0 & -L_{mq} & L_{mq} & L_g \end{vmatrix}$$

$$\underline{L}^{-1} = \begin{vmatrix} L_{11} & L_{12} & L_{13} & 0 & 0 & 0 \\ L_{21} & L_{22} & L_{23} & 0 & 0 & 0 \\ L_{31} & L_{32} & L_{33} & 0 & 0 & 0 \\ 0 & 0 & 0 & L_{44} & L_{45} & L_{46} \\ 0 & 0 & 0 & L_{54} & L_{55} & L_{56} \\ 0 & 0 & 0 & L_{64} & L_{65} & L_{66} \end{vmatrix}$$

$a_{1,7} = a_{2,8} = a_{3,9} = a_{4,10} = a_{5,11} = a_{6,12} = 1.0$

$a_{7,1} = -k_{1,1}/M_1$, $a_{7,2} = k_{1,2}/M_1$, $a_{8,1} = k_{1,2}/M_2$

$a_{8,2} = -k_{2,2}/M_2$, $a_{8,3} = k_{2,3}/M_2$, $a_{9,2} = k_{2,3}/M_3$

$a_{9,3} = k_{3,3}/M_3$, $a_{9,4} = k_{3,4}/M_3$, $a_{10,3} = k_{3,4}/M_4$

$a_{10,4} = -k_{4,4}/M_4$, $a_{10,5} = k_{4,5}/M_4$, $a_{11,4} = k_{4,5}/M5$

$a_{11,5} = -k_{5,5}/M_5$, $a_{11,6} = k_{5,6}/M_5$

$a_{11,13} = (i_{qo}L_q - i_{qo}L_d) / M_5$, $a_{11,14} = L_{md}i_{q0} / M_5$

$a_{11,15} = L_{md}i_{q0} / M_5$, $a_{11,16} = (1_q i_{d0} - L_d i_{q0} + L_{md}i_{d0}) / M_5$

$a_{11,17} = -L_{md}i_{d0} / M_5$, $a_{11,18} = - L_{md}i_{d0} / M_5$

$a_{12,5} = K_{5,6} / M_6$, $a_{12,6} = -K_{6,6} / M_6$

$a_{13,5} = v_{Nqo}L_{11}$

$a_{13,11} = x_t i_{q0}L_{11} + L_q L_{11} i_{q0} - L_{mq}L_{11}i_{kq0} - L_{mq}L_{11}i_{q0}$

$a_{13,13} = (r_a + r_t + x_t)\ L_{11}$, $a_{13,14} = r_f L_{12}$

$a_{13,15} = r_{kd}L_{13}$, $a_{13,16} = (L_q L_{11} - x_t L_{11})\ \dot{\delta}_{G0}$

$a_{13,17} = -L_{mq}L_{11}$, $a_{13,18} = -L_{mq}L_{11}$

$a_{13,19} = L_{11}$, $a_{13,21} = v_{q0}L_{11}$, $a_{14,5} = v_{nq0}L_{21}$

$a_{14,11} = x_t i_{q0}L_{21} + L_q L_{21} i_{q0} - L_{mq}L_{21}i_{kq0} - L_{mq}L_{21}i_{go}$

$a_{14,13} = (r_a + r_t + x_t)\ L_{21}$, $a_{14,14} = r_q L_{22}$

$a_{14,15} = r_{kd}L_{23}$, $a_{14,16} = (L_q L_{21} - x_t L_{21})\ \dot{\delta}_{Go}$

$a_{14,17} = -L_{mq}L_{21}\dot{\delta}_{go}$, $a_{14,18} = -L_{mq}L_{21}\dot{\delta}_{Go}$

$a_{14,19} = L_{21}$, $a_{14,21} = v_{qo}L_{21}$, $a_{15,5} = v_{Nq0}L_{31}$

$a_{15,11} = x_t i_{q0}L_{11} + L_q i_{q0}L_{31} - L_{mq}i_{kq0}L_{31} - L_{mq}L_{31}i_{q0}$

$a_{15,13} = (r_a + r_t + x_t)\ L_{31}$, $a_{15,14} = r_f L_{32}$

$a_{15,15} = r_{kd}L_{33}$, $a_{15,16} = (L_q L_{31} - x_t L_{31})\ \dot{\delta}_{Go}$

$a_{15,17} = -L_{mq}L_{31}\dot{\delta}_{Go}$, $a_{15,18} = -L_{mq}L_{31}\dot{\delta}_{Go}$

$a_{15,19} = L_{31}$, $a_{15,21} = v_{q0} L_{11}$

$a_{16,5} = -v_{Nd0} L_{44}$, $a_{16,13} = (x_t L_{44} - L_d L_{44})\ \dot{\delta}_{Go}$

$a_{16,11} = x_t i_{d0} L_{44} - L_d i_{d0} L_{44} + L_d i_{f0} L_{45} + L_d i_{kd0} L_{46}$

$a_{16,14} = L_d L_{45} \dot{\delta}_{Go}$, $a_{16,15} = L_d L_{46} \dot{\delta}_{Go}$

$a_{16,16} = (r_a + x_t + r_t)\ L_{44}$, $a_{16,17} = r_{kq} L_{45}$

$a_{16,18} = r_g L_{46}$, $a_{16,20} = L_{44}$, $a_{16,21} = -v_{d0} L_{44}$

$a_{17,5} = -v_{Nd0} L_{44}$, $a_{17,13} = (x_t L_{44} - L_d L_{54})\ \dot{\delta}_{Go}$

$a_{17,11} = x_t i_{d0} L_{44} - L_d L_{54} i_{d0} + L_{md} L_{55} i_{f0} + L_{md} L_{56} i_{kd0}$

$a_{17,14} = L_{md} L_{55} \dot{\delta}_{Go}$, $a_{17,15} = L_{md} L_{56} \dot{\delta}_{Go}$

$a_{17,16} = r_a L_{54} + (r_t + x_t)\ L_{55}$, $a_{17,17} = r_{kg} L_{55}$

$a_{17,18} = r_g L_{56}$, $a_{17,20} = L_{55}$, $a_{17,21} = -v_{d0} L_{44}$

$a_{18,5} = -v_{Nd0} L_{66}$, $a_{18,14} = L_{md} L_{65} \dot{\delta}_{Go}$

$a_{18,11} = x_t i_{q0} L_{66} + L_{md} L_{65} i_{f0} + L_{md} L_{65} i_{kd0} - L_d L_{64} i_{d0}$

$a_{18,13} = (x_t L_{66} - L_d L_{64})\ \dot{\delta}_{Go}$, $a_{18,15} = L_{md} L_{66} \dot{\delta}_{Go}$

$a_{18,16} = r_q L_{64} + (r_t + x_t)\ L_{66}$, $a_{18,17} = r_q L_{65}$

$a_{18,18} = r_g L_{66}$, $a_{18,20} = L_{66}$, $a_{18,21} = -v_{d0} L_{66}$

$a_{19,11} = v_{cq0}$, $a_{19,13} = x_c$, $a_{19,20} = \dot{\delta}_{Go}$

$a_{20,11} = -v_{cd0}$, $a_{20,13} = x_c$, $a_{20,19} = -\dot{\delta}_{Go}$

$a_{21,11} = g/T$, $a_{21,21} = -1 / T$

Appendix D

The Principle of Operation of Static Phase-Shifters

D.1. Point-on-Wave Controlled Phase-shifter

A point-on-wave controlled phase-shifter has two modes of operation: boosting mode, and bucking mode. The boosting mode of operation is referred to the case when a leading quadrature phase voltage is injected into the system, by the proper firing of thyristor switches S1 and S2, Fig.D.1. The bucking mode of operation is the case when a lagging quadrature phase voltage is injected into the system, by the proper firing of thyristor switches S3 and S2.

The boosting mode of operation for the static phase-shifter of Fig.D.1(a) is described with reference to Fig.D.1(b). In Fig.D.1(b), V_A is the system line-to-ground voltage, V_q is the quadrature phase voltage, i is the line current, and V_T is the injected voltage. When V_A is positive, thyristor 3 is forward biased and can be switched on during the positive half-cycle of the line current. During that period of time when thyristor 3 is conducting, thyristor 4 is reverse-biased. Thyristor 1 is forward biased when V_q is positive. Therefore, when V_q is positive, thyristor 1 can be turned on and a commutation from thyristor 3 to thy-

ristor 1 takes place. When thyristor 1 is conducting and v_q changes polarity, thyristor 3 is forward biased. Hence, provision of a gate pulse can turn on thyristor 3, and a commutation from thyristor 1 to thyristor 3 takes place. The operation of the phase-shifter during the negative half-cycle of the line current is the same as described for the positive half-cycle, and the commutation takes place between thyrsitors 2 and 4. A complete commutation cycle for the boosting mode of operation is shown below.

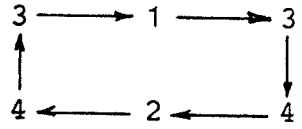

Fig.D.1(c) shows the waveforms for the bucking mode of operation. The principle of operation for the bucking mode is similar to the boosting mode. The commutation sequence for thyristors 3, 4, 5, and 6, during the bucking mode of operation is shown below.

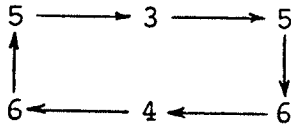

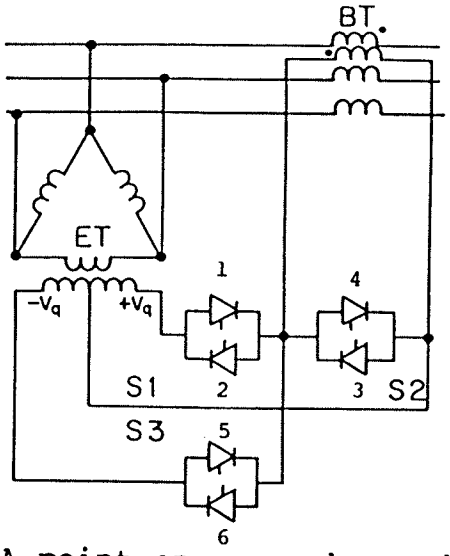

(a) - A point-on-wave phase-shifter

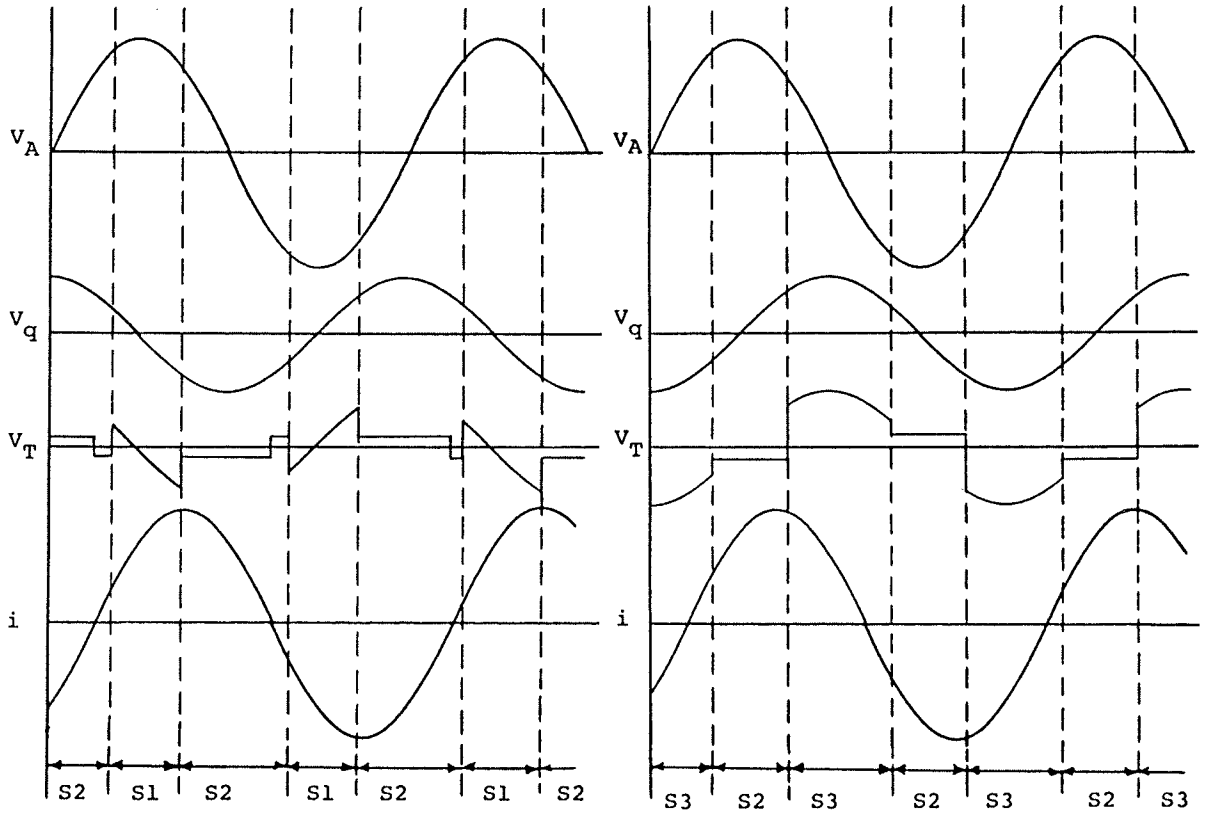

(b) - Boosting mode of operation (c) - Bucking mode of operation

Figure D.1: Waveforms of a point-on-wave phase-shifter

D.2. Discrete Step Controlled Phase-Shifters

The output voltage from a discrete step controlled phase-shifter, (Fig.4.2), is adjusted by controlling the operating modes of the thyristor bridges. Each thyristor bridge has three modes of operation: (1) the output voltage is in-phase with the input voltage, (2) the output voltage is in phase opposition with the input voltage, and (3) the output voltage is zero and the bridge is used as a current path. The modes of operation of a thyristor bridge are shown in Fig.D.2. In Fig.D.2, V_T is the output voltage of the bridge, V_A is the bridge input voltage, and i is the current which is determined by the power system. Fig.D.2(b) shows the output voltage waveform and the corresponding conducting thyristors, when the bridge output voltage is in-phase with the input voltage. Fig.D.2(c) shows the output voltage waveform and the corresponding conducting thyristors, when the output voltage is in phase opposition with the input voltage. The bridge operates as a current path, with zero output voltage, when either switches S1-S4 or S2-S3 conduct.

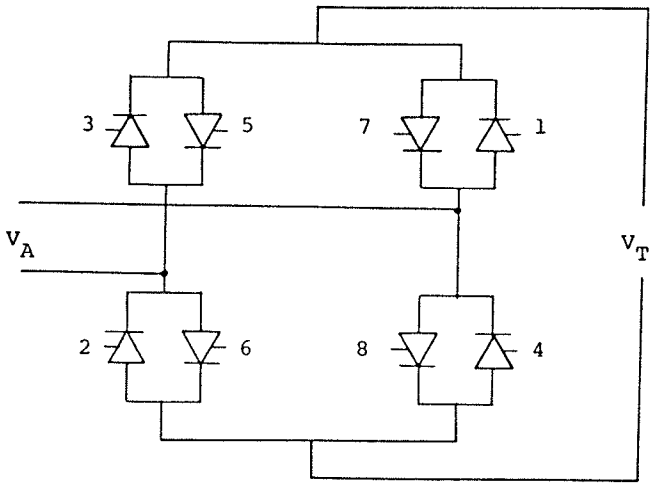

(a) - A thyristor bridge

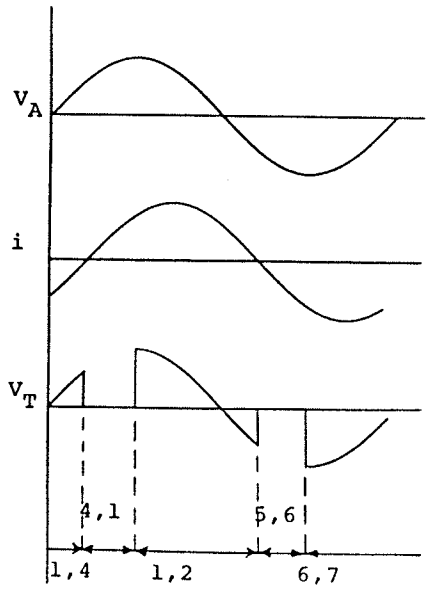

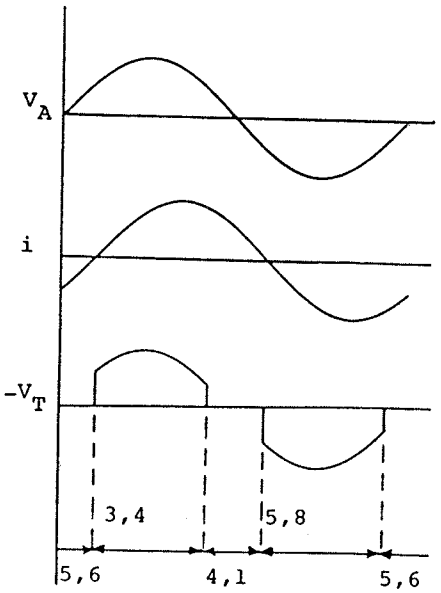

(b) - Operation at mode (1) | (c) - Operation at mode (2)

Figure D.2: Waveforms of a thyristor bridge